PHENOTYPIC AND MOLECULAR CHARACTERIZATION OF RIBOSOMAL PROTEIN OF THE SMALL SUBUNIT 6 PHOSPHORYLATION IN *Arabidopsis thaliana*

A Dissertation Presented for the
Doctor of Philosophy
Degree
The University of Tennessee, Knoxville

Anwesha Dasgupta
August 2023

Copyright © 2023 by Anwesha Dasgupta.

All rights reserved.

DEDICATION

To my beloved Baba and Ma, this thesis is dedicated to you with boundless love and gratitude. Throughout my academic journey, you have been my constant source of encouragement, unwavering support, and understanding. Your belief in me, even during moments of self-doubt, has given me the strength to persevere and overcome challenges. Your sacrifices and hard work have laid the foundation for my pursuit of knowledge. Your unwavering faith in my abilities from halfway across the world has fueled my determination to reach this milestone. This thesis is dedicated to both of you as a small token of my gratitude for the immeasurable impact you have had on my life.

ACKNOWLEDGEMENTS

I would like to take this opportunity to express my heartfelt gratitude to the incredible individuals who have contributed to my academic journey and the completion of this PhD thesis. Your unwavering support, guidance, and encouragement have been instrumental in shaping my growth as a researcher and as an individual.

First and foremost, I extend my deepest appreciation to my advisor, Dr. Albrecht von Arnim, for his mentorship and belief in my abilities. His insightful feedback, critical insights, and dedication to my academic success have been pivotal in shaping the direction of this research. His passion for knowledge has been an inspiration, shaping the trajectory of this thesis and my intellectual growth.

I am immensely thankful to my esteemed committee members, Dr. Barry Bruce, Dr. Daniel Roberts, Dr. Tessa Burch-Smith, and Dr. Elizabeth Fozo, for their valuable contributions, thoughtful insights, candid feedback, and thorough evaluations. Their expertise and constructive criticism have significantly improved the quality of this work and have contributed to my development as a scientist. I would like to thank Dr. Andreas Nebenfuhr for all his help and guidance with microscopy throughout these years. To my former lab members, Dr. Ansul Lokdarshi, Dr. Ramya Enganti, Dr. SungKi Cho, Mark Edens, and Ola Noras, thank you for your invaluable contributions and supportive spirit during this time. Your camaraderie and support have made my time in the lab truly memorable. To the undergraduate students, particularly Lindsey Tucker and John Torreverde, who have been a part of this research, I extend my gratitude for your dedication and enthusiasm. Your eagerness to learn and contribute has been a source of inspiration.

Special thanks go to the current lab members Ricardo Urquidi-Camacho, Abigail Burke, and Colton Goodman for creating a positive and supportive research environment.

As an international student, several people in Knoxville have been like family to me. I would like to acknowledge Dr. Ranjan Ganguly and Dr. Nivedita Ganguly for their constant love and support. Here, I would also like to thank Dr. Barry Bruce and Dr. Roz Miltenberger for their invaluable mentorship and constant concern for my well-being. I would like to offer my heartfelt thanks to my aunt Agomoni Mukherjee, whose unwavering love and encouragement in this country have been a constant source of strength throughout my academic journey. To my dear friends Nicholas, Anjali, Jyotirmoy, Mark, Chandrima, Amrita, Arani, Samik, Aveek, Amartya, Ricardo, Samantha, Maddie, Vidya, and Jayashree, you have been my pillars of strength, offering a listening ear, a helping hand, and countless words of encouragement. Your belief in my potential has given me the confidence to push the boundaries of my research. Thank you for being my pillars of support and for believing in me, even during moments of self-doubt. Nicholas, your love, friendship, support, and encouragement have been invaluable to my success. Your insightful conversations and shared passion for learning have left a lasting impression and made this journey unforgettable. To all my aunts, uncles, and cousins, your constant cheerleading and company have brought joy to my days and laughter to my heart, making this journey more joyful. I am profoundly grateful to my grandparents for their love, wisdom, and constant encouragement towards excellence. To my brother Arka, thank you for always being there for me. Your belief in my abilities and unwavering support have been a source of motivation. Lastly, to my parents, words cannot express the depth of my appreciation for everything you have done for me. Your endless sacrifices, unconditional

love, and unwavering faith in my potential have been the driving force behind my accomplishments.

This thesis would not have been possible without each and every one of you. Your love, support, and belief in me have been the driving force behind my success. As I conclude this chapter of my academic journey, I carry with me the profound impact you have had on my life. To all those mentioned and even those not named, your presence and support have been instrumental in my success. I am truly humbled and blessed to have each one of you in my life.

ABSTRACT

The TOR kinase pathway is responsible for mediating the phosphorylation of eS6, a ribosomal protein unique to eukaryotes. The implications of this dynamic phosphorylation event in response to environmental stimuli are still a matter of debate and not fully comprehended despite extensive research conducted over more than five decades. Studies have revealed that eS6-P is implicated in the regulation of cell size, translation, and ribosome biogenesis in mammals and yeast. However, the extent to which it plays a similar role in plants is yet to be determined.

To address the role of eS6 phosphorylation in plants, the experimental approach was to generate multiple combinations of phospho-mutant versions of eS6 with the motivation of generating transgenic lines in a genetic background mutated for both paralogs of the eS6 genes (RPS6) in Arabidopsis, to have a system to investigate the function of eS6 phosphorylation. I analyzed these lines for several generations and identified the ones that were completely devoid of endogenous eS6, harboring either phospho-enabled eS6 or phospho-deficient eS6. Their phenotypes were characterized at the level of translation, photosynthesis, plant growth and development. Our data showed that eS6-P is not essential for the basic functions of eS6 as a ribosomal protein or for bulk translation but has subtle functional consequences at the level of cell-cycle and ribosome biogenesis. However, its primary biochemical readout remains a subject for future work.

eS6 phosphorylation is dynamically regulated in response to various external stimuli including abiotic stresses. Abiotic stress also triggers massive translational inhibition. I studied autophagic turnover in *rps6a* single mutant, phospho-deficient eS6A, and phospho-enabled eS6A complemented double mutants, after hypoxia treatment. The

MDC vesicle staining pattern varied between seedlings that were phospho-defective and those that were phospho-enabled, suggesting a potential role of eS6-P in the response. Nonetheless, the results were complicated by factors such as high background staining, a distinct phenotype in *rps6a*, and the confounding effects of sucrose present in the medium during hypoxia.

The work presented here advances our understanding of the physiological and molecular implications of eS6 protein and its phosphorylation, with its modest but clear effect on early plant development.

TABLE OF CONTENTS

LIST OF FIGURES

CHAPTER 1: INTRODUCTION

1.1 RIBOSOME, AND ITS LAYERS

Protein synthesis has garnered significant attention in the scientific community over the past fifty years, however, the intricate three-dimensional composition of the ribosome remained elusive for much of this time. The initial comprehension of the bacterial ribosome's form and its dissimilar ribosomal subunits was established through the reconstruction of negatively stained electron microscopy (EM) images (Vasiliev, 1974). Nevertheless, the development of precise atomic models only occurred following the emergence of X-ray crystallographic structures of the complete 70S ribosome, as well as the individual 30S and 50S subunits (Ban *et al.*, 1998, Ban *et al.*, 1999, Ban *et al.*, 2000, Cate *et al.*, 1999, Clemons *et al.*, 1999). The first eukaryotic crystal structure of the ribosome was from *Saccharomyces cerevisiae*, at 4.2 Å and subsequently at 3.0 Å resolution, providing insight into the differences in protein synthesis and its regulation between eukaryotes and prokaryotes (Ben-Shem *et al.*, 2011, Ben-Shem *et al.*, 2010).

The eukaryotic ribosome is a complex structure consisting of four ribosomal RNAs and nearly 80 distinct types of ribosomal proteins (RPs) that are uniquely categorized as prokaryotic (p), eukaryotic (e), or universal (u), based on their roles in either the small (S) or large (L) subunit. These ribosomal proteins are numbered based on decreasing molecular weight. Despite the fact that the ribosome's fundamental function in template-directed peptide chain elongation is conserved, its size varies significantly across the three domains of life, ranging from 2.3 MDa to over 4 MDa (Melnikov *et al.*, 2012). In cryo-EM analysis of ribosomes in insects and mammals, particular attention is given to the rRNA expansion segments located on the outer periphery of the ribosomes. These segments are involved in

the formation of dynamic interactions between RP-rRNA and rRNA-rRNA. Additionally, the positioning and interactions of ribosomal proteins in eukaryotic ribosomes are also highlighted. (Anger *et al.*, 2013). Recent studies have suggested that intrinsic ribosome components can be modulated and varied to carefully control cellular proteome expression (Anger *et al.*, 2013, Simsek & Barna, 2017, Yusupova & Yusupov, 2014).

The central functional core of the ribosome, consisting of the areas of attachment for tRNA molecules, displays an impressive degree of consistency across eukaryotic organisms. However, the peripheral shell of the ribosome, which is unique to eukaryotes, exhibits a certain degree of variability depending on the particular domain of life. Prior to the recent past, the sole extant model of a plant ribosome in the process of translation was derived from wheat, and this model indicated that the ribosome in question bore greater similarity to those of yeast and humans (Armache *et al.*, 2010). However, recent studies of the tobacco 80S and tomato 80S ribosomes, both belonging to the Solanaceae family, have shown a high degree of similarity but also some distinctive differences between species (Cottilli *et al.*, 2022, Smirnova *et al.*, 2023). Notably, both tomato and tobacco, members of the Solanaceae family, exhibit several sites of rRNA modification in their 80S ribosomes, which are not present in Arabidopsis, a Brassicaceae. These findings suggest that ribosome structural heterogeneity at the level of chemical modifications is species- and family-specific. (Smirnova *et al.*, 2023). It is noteworthy that only 30% of the common eukaryotic rRNA modifications are conserved across organisms such as plants, yeast, and mammals, while the rest are exclusive to plants. Furthermore, through a comparison with

the amino acid sequences of ribosomal proteins from animals, yeast, and archaea, it has been possible to identify eighty families of ribosomal protein genes in the Arabidopsis genome, consisting of two to six paralogous members (Browning & Bailey-Serres, 2015). The number of paralogs within each RP family varies between species, allowing for extensive heterogeneity among ribosomes (Martinez-Seidel *et al.*, 2020, Smirnova *et al.*, 2023). However, due to high paralog similarity, the ability to discriminate RP isoforms is challenging.

Reversible post-translational modifications (PTMs) of ribosomal proteins (RPs) can increase the diversity of ribosomes without necessitating complete ribosome or RP turnover, in addition to the paralogous RPs (designated by A, B, etc. at the end of their names). Arabidopsis RPs undergo a multitude of covalent modifications, including lysine N-methylation, initiator methionine removal, N-terminal methylation, N-terminal acetylation, phosphorylation, and S-cyanylation (García *et al.*, 2019, Carroll, 2013, Turkina *et al.*, 2011). PTMs are also implicated in translational regulation in other eukaryotes (Simsek & Barna, 2017).

The phosphorylation of eS6 protein by TOR is the most extensively studied functional post-translational modification (PTM) in a eukaryotic RP. TOR is a protein kinase that plays a critical role in integrating energy and nutrient signaling to regulate various cellular processes such as protein synthesis, cell growth, and proliferation (Brunkard, 2020, Jamsheer *et al.*, 2022, Wu *et al.*, 2019, Xiong & Sheen, 2014, Deprost *et al.*, 2007, Meyuhas, 2015, Ren *et al.*, 2011, Ren *et al.*, 2012). In the context of plants,

translational control mediated by TOR occurs via the phosphorylation of S6K1, a 40S ribosomal protein kinase, which then phosphorylates eS6 (eS6-P). While other RPs like P1 uL10, uS5, uS11, eL13, and eL29 are also phosphorylated, the phosphorylation of eS6, uS11, and eL13 is light-stimulated (Boex-Fontvieille *et al.*, 2013, Enganti *et al.*, 2018, Turkina et al., 2011). eS6 and uS11 phosphorylation also correlate with photosynthetic activity. Furthermore, it has been observed that the activation of TOR through the use of auxin or sucrose leads to an increase in eS6-P levels (Schepetilnikov *et al.*, 2013). However, when subjected to auxin treatment, phosphorylated S6K1 also phosphorylates eIF3h, which is a translation initiation factor that is necessary for the promotion of translation reinitiation. It should be noted that unphosphorylated S6K1 is associated with polysomes but after being phosphorylated by TOR, it dissociates from the polysomes (Schepetilnikov *et al.*, 2013). Nonetheless, this results in phosphorylated S6K1 being in close proximity to the ribosomes, which could potentially lead to eS6 phosphorylation together with the phosphorylation of eIF3h, which is consistent with the reports that auxin induces eS6-P (Beltrán-Peña *et al.*, 2002). The protein eS6-P has been recently linked to the process of translation re-initiation, as indicated by its substantial in-vitro association with the Re-initiation Supporting Protein, RISP (Mancera-Martínez *et al.*, 2021). The outcomes of this study imply that eS6-P might have a part to play in the process of translation reinitiation. It has been demonstrated that alterations in the phosphorylation of eS6 are linked to changes in environmental factors that are recognized to influence TOR activity (Deprost *et al.*, 2007, Mahfouz *et al.*, 2006, Williams *et al.*, 2003). In essence, the

upstream connection of eS6-P to TOR, a master regulator of cell growth, and its substrate S6K1 makes a compelling case for the involvement of eS6-P in translation control. However, direct evidence that RP phosphorylation events regulate translation in plants is lacking.

1.1.1 Post-translational modification of eS6 in plants

eS6 is a pan-eukaryotic protein of the small (40S) subunit of the ribosome. The N-terminus of eS6 is located at the 40S-60S subunit interface while its long alpha-helical C-terminal tail wraps around to the solvent-exposed side of the 40S (Khatter *et al.*, 2015). The C-terminal tail harbors a series of between two and six conserved serine residues, which are targeted for phosphorylation by the S6 kinase in a TOR dependent fashion. The structure of this region of eS6 has not been resolved by crystallography or cryo-electron microscopy and is therefore deemed to be flexible.

Post-translational modifications, such as phosphorylation, acetylation, nitrosylation, sulfenylation, and ubiquitination, have been found to be associated with eS6 in plants (**Figure 1.1**). Databases that compile and help visualize PTMs, such as Plant PTM Viewer and qPTMplants are available (Willems *et al.*, 2019, Xue *et al.*, 2022). However, functional roles of these PTMs are not known, except for phosphorylation, the focus of this thesis.

Figure 1.1:Post-translational modifications, secondary structure, disordered regions and surface accessibility of AteS6 using qPTMplants.

The 'Sequence and Structure' function was utilized to generate a representation of the AteS6 AGIs, in order to visually analyze its sequence and structural elements, such as the PTM sites, secondary structure, disordered regions, and surface accessibility. Among total quantitative PTM events, qPTMplants found 886 entries associated with AteS6.

1.1.2 Unlike non-plants, only the TOR-S6K pathway can phosphorylate eS6 in plants

eS6 is a common effector of the TOR-S6K pathway between plants and non-plants. The TOR kinase is a pivotal controller of growth and development in both yeast and mammals, regulating translation, autophagy, ribosome biogenesis, and metabolism in response to various stimuli such as growth hormones, food availability, energy status, and stressors. (Blenis, 2017, Dobrenel *et al.*, 2016a, Laplante & Sabatini, 2012). In both yeast and humans, there exist two distinct complexes, namely TOR Complex 1 (TORC1) and TORC2. However, in the case of plants and green algae, only TORC1 has been confirmed experimentally (Van Leene *et al.*, 2019, Tatebe & Shiozaki, 2017). The composition of TORC1 includes TOR, RAPTOR (TOR regulatory associated protein), LST8, and PRAS40 (proline rich Akt substrate 40) (Meyuhas, 2015). Upon activation, TOR phosphorylates a variety of targets, such as eIF4E-Binding Protein and S6 kinase, (Meyuhas & Dreazen, 2009), which further phosphorylates eS6 and other targets (Meyuhas, 2015). The S6 kinase, a ribosomal protein kinase (S6K), serves as a component of the TORC1 signaling pathway and has a pivotal function in various cellular processes such as cell growth, proliferation, and stress response through regulation of protein synthesis and ribosomal biogenesis (Fingar *et al.*, 2002).

In plants, several investigations in both roots and shoots have revealed a significant sugar–TOR growth-controlling axis (Pfeiffer *et al.*, 2016, Xiong *et al.*, 2013). The activation of meristems by TOR is achieved through the activation of E2F transcription factors in the root apical meristem and WUSCHEL transcription factors in the shoot apical

meristem (Pfeiffer *et al.*, 2016, Xiong *et al.*, 2013). Sugar metabolism in plants is a crucial determinant for activation of the TOR pathway, even though the mechanism is unclear (Dobrenel *et al.*, 2016b, Xiong *et al.*, 2013). The TORC1–S6K signaling axis is a well-known interface between TOR and protein translation in plants, and its downstream components are largely conserved with animal counterparts (Dobrenel *et al.*, 2016b, Henriques *et al.*, 2010, Mahfouz *et al.*, 2006, Xiong & Sheen, 2012). Arabidopsis has two closely related paralogs of S6K, S6K1 and S6K2, which phosphorylate eS6 (Turck *et al.*, 1998) (**Figure 1.2i**). AtS6K1 and AtS6K2 have distinct functions despite their similar sequences, as AtS6K1 is mainly located in the cytoplasm and AtS6K2 is predominantly found in the nucleus (Mahfouz *et al.*, 2006, Sun *et al.*, 2016).

The TOR kinase, which is stimulated by nutrients and energy, is counterbalanced by the SnRK (Snf1-related kinase) 1 and 2 kinases that are induced by starvation in an antagonistic way (Baena-González & Hanson, 2017, Dobrenel *et al.*, 2016b, Jamsheer *et al.*, 2022, Margalha *et al.*, 2019). The deactivation of TOR kinase through phosphorylation of RAPTOR by SnRK1 is a conserved feature across evolution (Nukarinen *et al.*, 2016). The animal counterpart of SnRK1, the AMP-activated kinase, carries out the identical post-translational modification to deactivate TOR under energy limiting conditions (Gwinn *et al.*, 2008).

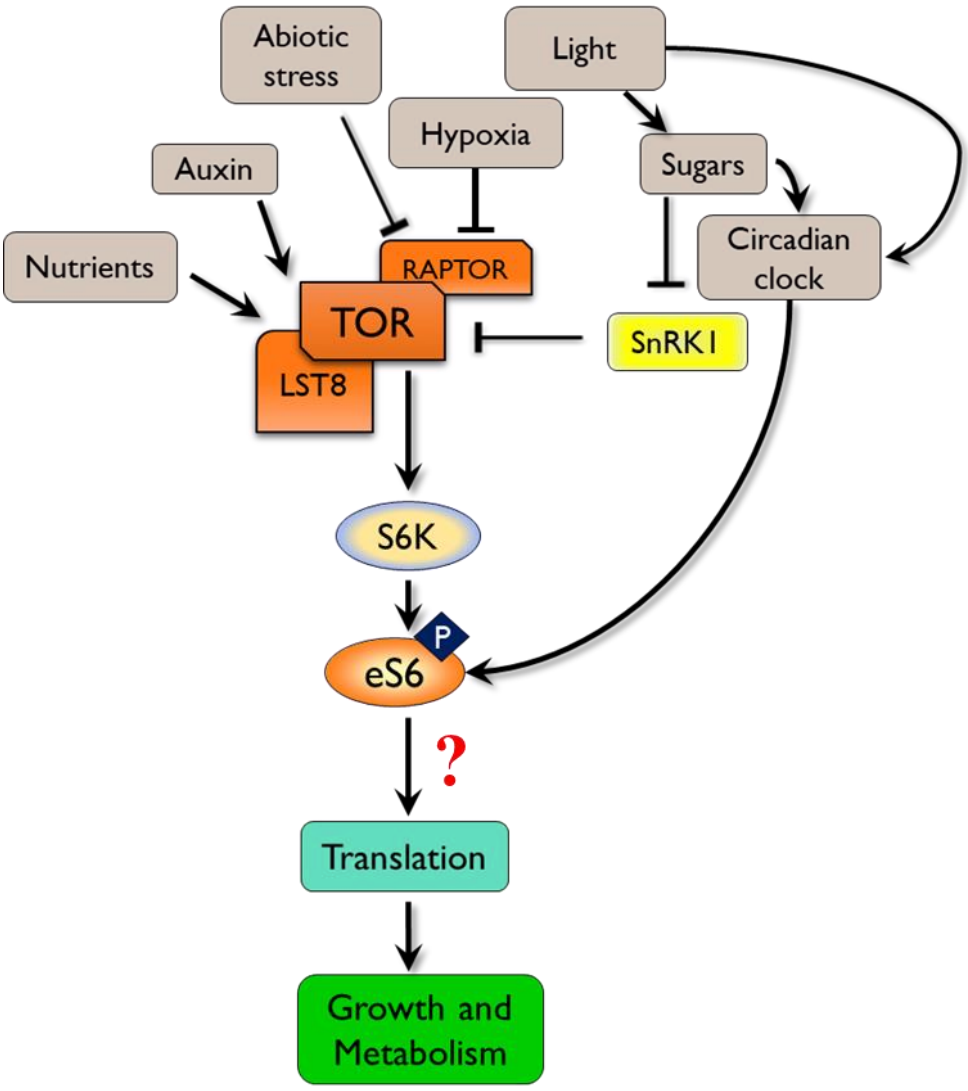

Figure 1.2:TOR kinase is a central regulatory hub to maintain cellular homeostasis.

As elsewhere, plant TOR is active under growth stimulating conditions, promotes translation, ribosome biogenesis and growth and phosphorylates and activates the S6 kinase. eS6 is the common effector of this pathway in all eukaryotes. Despite strong accumulating evidence of variations of eS6P in response to stress conditions, its precise role remains largely elusive.

1.1.3 eS6 phosphorylation and dephosphorylation:

The differential eS6-P dynamics by external signals has been studied extensively in various organisms (Ruvinsky *et al.*, 2009, Ruvinsky & Meyuhas, 2006, Ruvinsky *et al.*, 2005, Scharf & Nover, 1982, Sulic *et al.*, 2005, Turck *et al.*, 2004, Williams *et al.*, 2003, Bohlen *et al.*, 2021, Chen *et al.*, 2018, Mancera-Martínez *et al.*, 2021, Puighermanal *et al.*, 2017) but its functional consequence remains elusive. The use of eS6-P as a bioreporter is a well-accepted method for measuring TOR kinase activity (Bohlen *et al.*, 2021, Conn & Qian, 2013). eS6-P is strongly correlated with TOR-mediated translational stimulation (Dobrenel *et al.*, 2016b, Gonzalez *et al.*, 2015, Meyuhas, 2008, Meyuhas, 2015, Turck *et al.*, 2004, Urban *et al.*, 2007, Yerlikaya *et al.*, 2016), but a causal role for it in translation is missing.

A cluster of phosphorylatable serine residues, S235, S236, S240, S244 and S247, which are conserved across all eukaryotes, have been identified as phosphorylation sites for eS6 in mammals (**Figure 1.3**), though the number of sites varies between species (Bandi *et al.*, 1993, Krieg *et al.*, 1988). The primary kinase responsible for phosphorylating all the serines in eS6, namely S235 (corresponding to S240 in Arabidopsis), S236, S240, and S244, is S6 kinase. On the other hand, RSKs can only phosphorylate S235 and S236 (Roux *et al.*, 2007), and are absent in plants. Drosophila has only a single S6K (Watson *et al.*, 1996). While Sch9 was initially thought to be responsible for phosphorylating eS6 in yeast (Urban *et al.*, 2007), a 2015 study revealed that Ypk3 is the primary kinase required for in-vivo phosphorylation of eS6. Ypk3 is homologous to human S6 kinase and in cells lacking Ypk3, eS6 phosphorylation is eliminated (Gonzalez *et al.*, 2015). In mammals, S6K1 and

S6K2 are both required for phosphorylating eS6, but S6K2 is the primary kinase (Pende *et al.*, 2004). In mammals, multiple kinases namely RSK, PKA, and Casein Kinase1 can induce eS6 phosphorylation. RSK specifically targets S235 and S236 residues for phosphorylation, which can be inhibited by treatment with U1026 or PD184352, inhibitors of MAPK/MEK and ERK, respectively. It is suggested that the ERK pathway mediates the phosphorylation of eS6 by RSK (Pende *et al.*, 2004). Homologs of this kinase have been identified in certain invertebrates, but not in plants and yeast (Hauge & Frodin, 2006, Lara *et al.*, 2013). PKA, on the other hand, can also phosphorylate eS6 at S235 and S236 (Moore *et al.*, 2009). As a sensor for cyclic AMP (cAMP), PKA is involved in glycogen and sugar metabolism (Kirschner *et al.*, 2009). In pancreatic β cells, increased levels of cAMP can lead to the phosphorylation of eS6 at S235 and S236, which can be inhibited by PKA inhibitors (Kirschner *et al.*, 2009). Chemical compounds like haloperidol and forskolin, which are known to activate cAMP signaling, have been found to result in elevated levels of eS6 phosphorylation (Biever *et al.*, 2015, Valjent *et al.*, 2011). Casein Kinase 1 (CK1) can phosphorylate eS6 at S247, and suppressing the activity of CK1 has been shown to reduce eS6 phosphorylation at S247 according to research conducted by Hutchinson (Hutchinson *et al.*, 2011). Additionally, Ataxia Telangiectasia Mutated (ATM) kinase, which is known to be involved in the DNA damage response, has also been found to phosphorylate eS6 at S247 and inhibiting ATM kinase and UV irradiation of HeLa cells inhibits eS6 phosphorylation at S247 (Li *et al.*, 2012). In conclusion, it appears that in mammals, the inhibition or mutation of a single kinase is not sufficient to abolish eS6-P.

Protein Phosphatase type 1 (PP1) has been implicated in dephosphorylating eS6 in yeast. UV induced reduction of eS6-P at S247 is PP1-dependent because a PP1 inhibitor prevents the dephosphorylation at S247 (Li *et al.*, 2012). In yeast, Glc7, the catalytic subunit of PP1, dephosphorylates eS6 in response to rapamycin (Yerlikaya *et al.*, 2016), and in HEK 293T cells, expression of a dominant-negative PP1 catalytic subunit led to increased eS6 phosphorylation levels (Hutchinson *et al.*, 2011). Rapid dephosphorylation of eS6 in plants is seen under low energy stress conditions (Enganti et al., 2018, Turck et al., 1998, Turck et al., 2004). However, the phosphatase that dephosphorylates eS6 in plants, is not known.

1.1.4 eS6-P is differentially regulated by environmental signals

eS6-P is differentially phosphorylated in response to different stimuli (Ruvinsky et al., 2009, Ruvinsky & Meyuhas, 2006, Ruvinsky et al., 2005, Scharf & Nover, 1982, Sulic et al., 2005, Turck et al., 2004, Chen et al., 2018, Enganti et al., 2018). The phosphorylation of eS6 is in mammals can be induced by mitogenic stimuli such as amino acids, androgen, all-trans-retinoic acid, and estradiol in mammals, while hypoxia ,alpha-linoleic acid, and mannitol prevent its phosphorylation. Interestingly, hydrogen peroxide can induce eS6 phosphorylation in an mTOR-independent manner, but it can also downregulate eS6 phosphorylation via the ATM/LKB1/AMPK/TSC2 pathway in the cytoplasm of MCF7 cells (Jia *et al.*, 2013). eS6-P is detected on ribosomes that are in the process of translation (Duncan & McConkey, 1982). A report that has been recently published demonstrated that

A

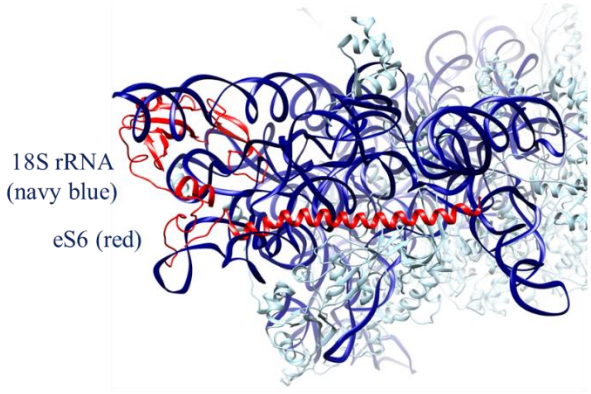

B

```
Saccharomyces cerevisiae  YAQLLAKRLSERKAEKAEI--RKRRASSLKA---------- 236
Arabidopsis thaliana A    YQKLLASRLKEQRDRRSESLAKKRSRLSSAAAKPSVTA--- 250
Arabidopsis thaliana B    YQKLLASRLKEQRDRRSESLAKKRSRLSSAPAKPVAA---- 249
Triticum aestivum         YQKLLAQRLKEQRDRRSESMAKRRSKLSAATKAPAASA--- 250
Zea mays 1                YQKLLAQRLKEQRDRRSESLAKRRSKLSAAAKASAATSA-- 251
Zea mays 2                YQKLLAQRLKEQRDRRSESLAKRRSKLSAAAKASAATSA-- 251
Mus musculus              YAKLLAKRMKEAKEKRQEQIAKRRRLSSLRASTSKSESSQK 249
Homo sapiens              YAKLLAKRMKEAKEKRQEQIAKRRRLSSLRASTSKSESSQK 249
Drosophila melanogaster 1 YAKLLVQRKKESKAKREEA--KRRRSASIRESKSSVSSDKK 217
Drosophila melanogaster 2 YAKLLVQRKKESKAKREEA--KRRRSASIRESKSSVSSDKK 248
                          * :**..* .* : .: *   ::*   *
```

Figure 1.3: eS6-P is evolutionarily conserved.

A) Showing eS6 (red) and 18S rRNA (navy blue) using the cryo-EM structure of a plant (*Triticum aestivum*) 80S ribosome at 5.5-Å resolution (Armache *et al.*, 2010). The image was generated using Chimera. B) S6-phosphorylation sites are highly conserved in eukaryotes. Showing the C-terminus sequence alignment among higher plants (green) and non-plants (red).

eS6-P is relatively more prevalent on shorter coding sequences. This occurrence is due to the progressive dephosphorylation of eS6 as the ribosomes move along an mRNA. In addition, the elevated levels of eS6-P on shorter coding sequences results in a minor improvement in the efficiency of translation (Bohlen *et al.*, 2021). For more detailed regulation of eS6-P in mammals, please refer to this extensive review (Yi *et al.*, 2021).

The levels of eS6 phosphorylation in plants are influenced by a variety of internal and external stimuli such as light, circadian clock, sucrose (Dobrenel et al., 2016b, Enganti et al., 2018, Mancera-Martínez et al., 2021), auxin (Schepetilnikov *et al.*, 2013), cytokinin (Yakovleva & Kulaeva, 1987), heat, cold and hypoxia (Enganti et al., 2018, Williams et al., 2003). However, it remains unclear whether TOR activity is responsible for eS6 phosphorylation in all of these cases. The sole kinase capable of phosphorylating eS6 in Arabidopsis is S6K. However, phosphorylation is reduced with the administration of AZD8055, a TOR inhibitor, though not completely abolished (Dobrenel *et al.*, 2016b). This leads to the suggestion that the process of eS6 phosphorylation may not be entirely dependent on TOR activity or that AZD8055 lacks efficacy in inhibiting TOR. This latter possibility is reinforced by our unpublished findings, wherein roots continue to grow in the presence of AZD8055. It is possible that PDK1, another PI3-type serine-threonine kinase, may phosphorylate S6K and thus stimulate the phosphorylation of eS6. The process of eS6 phosphorylation in maize root tips is negatively impacted by hypoxia and resumes upon reoxygenation. However, treatment with LY294002, which is a PI3K inhibitor, can hinder the phosphorylation experienced during recovery from reoxygenation (Williams *et al.*,

2003), indicating that PDK1, a PI3K type kinase, could enhance S6K activity and consequently boost eS6 phosphorylation, alone or in conjunction with S6K activation by TOR (Mahfouz *et al.*, 2006). Nonetheless, the exact mechanisms of PDK1-mediated regulation pathways are uncertain, and they may be either additive or exclusive. Furthermore, PDK1 could play a role in regulating phosphatase activity, which is evident in both S6K and eS6 phosphorylation.

Regarding the phosphatase driven regulation of eS6-P, a case could be speculated for cold stress. Cold stress induces eS6 phosphorylation (Enganti et al., 2018, Williams et al., 2003). However, TOR activity is reduced under cold stress which leads to decreased S6K phosphorylation (Wang *et al.*, 2017). This raises the question of phosphatase regulation which might play a significant role in regulating eS6 phosphorylation during cold stress or more. Similarly, osmotic stress was shown to have no effect on eS6 phosphorylation (Williams *et al.*, 2003) (unpublished results), even though osmotic stress reduces S6K activity. In conditions of osmotic stress, S6K couldn't phosphorylate eS6 using an in vitro kinase assay (Mahfouz *et al.*, 2006).

Based on these results, although TOR-S6K is the only well-characterized axis of eS6 phosphorylation regulation in Arabidopsis, there may be other players that regulate phosphatase activities that also contribute to eS6 phosphorylation, or maybe specific external conditions affect eS6 phosphorylation via the uncharacterized phosphatase activity. In summary, there is evidence that eS6 phosphorylation in plants can be modulated

by a variety of stimuli, however, no evidence exists for its physiological or biochemical role.

1.1.5 The regulation of eS6 phosphorylation in plants exhibits a diurnal pattern

In Arabidopsis, eS6 is encoded by two paralogous genes, eS6A and eS6B. Both paralogs can undergo phosphorylation on up to five or seven serine or threonine residues located in the C-terminal alpha helix of the protein, respectively. During the light period, eS6-P is regulated in a diel manner, with an elevated level. Recent research has demonstrated that eS6-P cycles in Arabidopsis, peaking during the day under a light-dark cycle and is stimulated by various qualities of light. But lack of a functioning clock leads to eS6-P cycles that are distinctly high in amplitude. However, when a clock-enabled strain entrained in a light-dark cycle was shifted to constant light conditions, eS6-P cycles peaked during the subjective night (Enganti et al., 2018); this result was also confirmed in an independent phosphoproteomic study (Choudhary *et al.*, 2015). The literature reveals that for most cycling mRNA transcripts, the phasing pattern during a clock-driven cycle aligns with that of the light-driven cycle. Notably, the clock-driven cycle permits the transcript to anticipate dawn, although this is not always the case. Nonetheless, it is atypical to observe a phase change of approximately 12 hours involving a diel cycle and a clock-driven cycle, as is documented for eS6-P. A mathematical model of the signaling architecture was constructed and parameterized with the empirical data on eS6-P. Computational simulations using this model suggested that the anti-phasic sensitivity of eS6-P to light and clock makes the pathway sensitive to the timing of dawn (Panchy *et al.*,

2020). Although it is unknown whether the plant uses the pathway in this manner to sense the environmental conditions, the pathway as constructed is capable of providing this information.

1.1.6 Functional significance of eS6 phosphorylation

eS6-P is commonly acknowledged as a bioreporter that efficiently reflects the activity of TOR kinase and is strongly associated with TOR-mediated translational stimulation, although its causal role in translation remains uncertain (Mancera-Martínez *et al.*, 2021, Bohlen *et al.*, 2021, Chen *et al.*, 2018, Dobrenel *et al.*, 2016b, Meyuhas, 2015, Ruvinsky *et al.*, 2009, Meyuhas & Dreazen, 2009, Reiter *et al.*, 2005). All the known phenotypic consequences of eS6-P (Creff *et al.*, 2010, Enganti et al., 2018, Pende et al., 2004, Ruvinsky et al., 2009, Ruvinsky & Meyuhas, 2006, Ruvinsky et al., 2005, Wittenberg *et al.*, 2016, Bohlen et al., 2021, Chauvin *et al.*, 2014, Chen et al., 2018, Mancera-Martínez et al., 2021, Meyuhas, 2015, Puighermanal et al., 2017, Yerlikaya et al., 2016) manifest at the level of the cell, the tissue, or the whole organism. The biochemical basis of eS6-P at the level of cellular biochemistry is not well characterized and controversial to date.

Cell-cycle, growth and proliferation:

eS6 is required for cell proliferation and development. The eS6P−/− knock-in mouse, where five phosphorylatable serine residues were replaced with alanines, exhibited smaller cell size and increased proliferation rate in MEFs, β-pancreatic cells, and muscle cells, while also experiencing hypoinsulinemia, impaired glucose tolerance, and muscle

weakness (Ruvinsky *et al.*, 2009, Ruvinsky *et al.*, 2005, Wittenberg *et al.*, 2016). In yeast, cells with phosphorylatable serines of eS6-P mutated to alanines show a ~30% reduction in cell proliferation and lower protein content compared to WT cells (Yerlikaya *et al.*, 2016).

In the realm of plant biology, it has been suggested that the regulation of growth rate, phase change, and life span are intricately tied to the modulation of TOR-eS6-dependent pathways. These pathways are known to connect nutrition and light signals, thereby serving as a crucial mechanism for controlling various aspects of plant development (Ren *et al.*, 2012). However, prior to this work there were no plants that were fully deficient in eS6-P. Lack of eS6 is embryo-lethal and a 50% reduction of eS6 levels causes severe developmental deficits such as smaller leaves and roots, slow growth, chlorosis and delayed senescence (Creff *et al.*, 2010, Dasgupta *et al.*, 2023); however, these phenotypes are not attributable to eS6-P but rather to reduced gene dosage of eS6 protein. Arabidopsis has two S6K genes, namely AtS6K1 and AtS6K2. Partial depletion of S6K results in an elevation in the occurrence of ploidy and aneuploidy, coupled with a decline in the viability of pollen (Henriques *et al.*, 2010). This shows that S6K plays a crucial role in preserving chromosome stability and also acts as a suppressor of endoreduplication and potentially cell proliferation in Arabidopsis. Nevertheless, the observed phenotypes of S6K mutants cannot be solely attributed to changes in eS6-P as S6K has various other substrates at play.

Protein synthesis:

Being the first ribosomal protein identified to be phosphorylated in addition to being downstream of TOR, a role for eS6 phosphorylation in translation regulation, and specific mRNA translation has remained an attractive area of investigation in non-plants and recently in plants (Pende *et al.*, 2004, Ruvinsky & Meyuhas, 2006, Ruvinsky *et al.*, 2005, Wittenberg *et al.*, 2016, Bohlen *et al.*, 2021, Mancera-Martínez *et al.*, 2021, Puighermanal *et al.*, 2017). Despite its traction, eS6-P in yeast appears to be largely dispensable for translation. Through a comprehensive inquiry and examination of translatome in yeast cells that exclusively express the phospho-mutant $eS6^{AA}$, no evidence was found to support the involvement of eS6-P in the modulation of global translation or in the regulation of particular subsets of mRNAs (Yerlikaya *et al.*, 2016).

In mice with eS6-P deficiency liver ribosomes were associated with polysomes, indicating that eS6-P participation is not necessary for active translation (Ruvinsky *et al.*, 2005). The regulation of mTOR pathways is influenced by the nutritional status of an organism. To investigate the role of TOR in translation in response to nutrient availability through eS6-P, polysome profiles from the livers of eS6-P deficient and wild-type mice were analyzed after a period of starvation or 4-hour refeeding. The analysis showed that eS6-P deficient mice had a slightly higher proportion of polysome-associated ribosomes after refeeding than wild-type mice. However, the loss of phosphorylation did not appear to have a significant effect on global protein synthesis, as indicated by the results (Chauvin

et al., 2014). Surprisingly, phospho-null mouse embryonic fibroblasts (MEFs) had higher global rates of protein synthesis and translation fidelity than WT MEFs (Ruvinsky *et al.*, 2005, Wittenberg *et al.*, 2016). A latest investigation has documented the gradual dephosphorylation of eS6-P on ribosomes as they traverse an mRNA in order to translate the coding sequence. Furthermore, the study revealed that eS6-P levels on shorter coding sequences were higher than those on longer ones, thereby slightly enhancing the translation efficiency of short sequences. Intriguingly, the researchers also observed that if ribosomes that terminated translation on an mRNA were still phosphorylated on eS6, initiation rates on that mRNA would be heightened (Bohlen *et al.*, 2021). Another recent investigation revisited the issue of global translation in phospho-null mice and observed no impact in lysates of the striatum, which includes both dorsal and ventral (nucleus accumbens, Acb) parts. The polysome profiles of both dorsal and Acb lysates from eS6-P-/- mice were comparable to those of the wild type. Nonetheless, a number of transcripts were differentially recruited into the heavy polysomal fractions that were isolated from Acb lysates. The majority of these transcripts were linked to mitochondria-related functions, suggesting a potential consequence of eS6-P deficiency in tissue-specific manner (Puighermanal *et al.*, 2017). In summary, although loss of eS6-P has no substantial impact on global translation, some light evidence of impacting global translation in MEFs and neurons does exist, which could indicate a role in tissue-specific protein synthesis.

Our lab observed a correlation between the eS6-P level and the level of polysomes in WT. eS6-P was very low at the end of night during low translation and the eS6-P was high during the day during high translation (Enganti et al., 2018). This led us to investigate the functional significance of eS6-P. We created homozygous double mutants of *rps6a* and *rps6b* that were supplemented with transgenes expressing versions of eS6 that are either deficient or enabled for phosphorylation. We have performed an in-depth characterization of homozygous double *rps6* mutants that carry either eS6-P enabled or eS6-P deficient eS6. In particular, we have analyzed the effects of these mutations on various aspects of plant physiology including translation, photosynthesis, transcriptome, proteome, plant growth, and development. Our findings provide novel insights into the functional role of eS6 and its phosphorylation status in regulating plant growth and development. Polysome profiles were obtained at two distinct time points; 30 minutes prior to and 2 hours 30 minutes subsequent to the daily transition from darkness to light, as light exposure elicits a considerable and expeditious surge in the loading of mRNA ribosomes (Liu & Bassham, 2012). As elaborated further in Chapter 2, both the transgenic lines expressing eS6-P enabled or eS6-P deficient eS6 demonstrated the same increase in global polysome loading (Dasgupta *et al.*, 2023) in response to light, similar to wild-type. This finding is consistent with findings in mammals where P-deficient eS6 was still able to support high levels of polysome loading and protein synthesis (Ruvinsky *et al.*, 2005).

Furthermore, translation reinitiation after translation termination on particular ORFs is contingent upon the functioning of TOR/S6K1 activity (Schepetilnikov *et al.*, 2011). Arabidopsis eS6-P has been suggested as a promoter of translation re-initiation, as indicated by the contrasting behaviour of phospho-null and phospho-mimic versions in their association with the re-initiation supportive protein, RISP, in yeast two hybrid assays (Mancera-Martínez *et al.*, 2021). In addition, transgenic lines were produced in the *rps6a* single mutant background through the expression of eS6B with a serine 240 mutation to either alanine or aspartate. Similar to the data we have collected, the two versions exhibited no significant difference in global polysome loading. Despite this, the two versions displayed disparity in the translation of the reinitiation-dependent reporter mRNAs, indicating a potential involvement of eS6-P in translation re-initiation (Mancera-Martínez *et al.*, 2021).

Translation fidelity:

eS6-P has been implicated in translation fidelity in MEFs. Constitutively active mTORC1 complex in MEFs lead to increased global protein synthesis but reduced the stability of the newly synthesized polypeptides. Rapamycin treatment suppressed mTORC1 activity resulting in restored stability of nascent polypeptides. The reduced stability of translation products under active mTORC1 was attributed to an increased speed of elongation, which led to an increased rate of stop codon readthrough and misincorporation of amino acids during translation. These data suggested that mTORC1 relaxes translational fidelity. It does

this through the S6 kinases because MEFs lacking both S6 kinases have higher translational fidelity (Conn & Qian, 2013). However, the S6 kinases phosphorylate multiple substrates in mammals, and this study did not test translation fidelity specifically in eS6-P deficient MEFs.

A separate study tested translation fidelity in MEFs expressing un-phosphorylatable eS6. They found that eS6-P deficiency led to reduced translational fidelity (Wittenberg *et al.*, 2016). This result is incoherent with the increase in translational fidelity seen in S6 kinase mutants. Therefore, eS6-P may indeed support the maintenance of the quality of protein synthesis in mammals. The effect of eS6-P on translation fidelity has not yet been investigated in plants.

Ribosome Biogenesis:

Previous studies have demonstrated that TOR functions as a coordinating factor in the regulation of metabolism in response to nutrient status (Brunkard, 2020, Chantranupong *et al.*, 2015, Shi *et al.*, 2018). Among its various functions, mTORC1 plays a crucial role in controlling ribosome biogenesis, a process that involves the maturation and assembly of nucleolar factors, as well as the transcriptional regulation of S6K1 (Chauvin *et al.*, 2014). Despite its importance, the mechanisms underlying this regulation remain poorly understood. Nevertheless, mTORC1 has been shown to have a significant impact on ribosome biogenesis, abundance, protein synthesis, and cell growth, as demonstrated in

previous studies (Delarue *et al.*, 2018, Hannan *et al.*, 2003, Saxton & Sabatini, 2017, Scarpin *et al.*, 2020). Increased TOR activity in mammals has been linked to upregulation of ribosome biogenesis, as evidenced by upregulation of RP genes, rRNA, and other genes involved in ribosome synthesis (Pelletier *et al.*, 2018), as well as the induction of pyrimidine and purine biosynthesis (Ben-Sahra *et al.*, 2013, Robitaille *et al.*, 2013). Recent research has indicated that TOR plays a crucial role in regulating metabolic balance by coordinating nucleotide demand with nucleotide biosynthesis in mammals, as demonstrated by various studies (Emmanuel *et al.*, 2017, Hoxhaj *et al.*, 2017, Valvezan *et al.*, 2017). Similarly, in plants, recent evidence suggests that TOR also has a similar function in promoting nucleotide biogenesis transcriptionally to meet the demands of ribosomal RNA synthesis. Additionally, inhibition of nucleotide biosynthesis has been shown to suppress TOR activity in plants (Busche *et al.*, 2021). Double S6K knockout mouse livers show transcriptional downregulation of the activity of promoters involved in the transcriptional program of ribosome biogenesis. A significant downregulation of up to 78% of ribosome biogenesis genes has been observed in the double S6K mutant livers. As a result, it is reasonable to assume that TOR and its target S6K control this regulation through eS6-P. Similarly, to S6K double mutants, the loss of eS6 phosphorylation also led to a decrease in the ribosome biogenesis genes; however, to a lesser degree. This suggests that eS6-P is involved in the production of translational machinery (Chauvin *et al.*, 2014). A study using HEK293 cells also showed that eS6-P is required for maturation of the 18S rRNA from 30S pre-rRNA (Zhang *et al.*, 2016).

In Arabidopsis, it was reported that eS6 negatively regulates rDNA transcription (Kim *et al.,* 2014) and that overexpression of eS6B results in decreased pre-rRNA transcript. This was further seen in *rps6b* mutants which showed increased pre-18S rRNA compared to WT. In our lab we have analyzed polysome loading, transcriptome and proteome of single paralog *rps6* mutants and homozygous double *rps6* mutants harboring either eS6-P enabled or eS6-P deficient eS6 in Arabidopsis (Dasgupta *et al.*, 2023). In the *rps6* single mutants the gene dosage for eS6 is only 50% of wild type. In these mutants, we have observed an overabundance of 60S subunits, indicating that the *rps6* mutation has a constraining effect on the production rate of 40S subunits. Additionally, there has been an upregulation of proteins related to ribosome biogenesis, ribosomal proteins, as well as other RNA-related proteins. The surplus of 60S subunits seems to have been rectified irrespective of the P-status of eS6. However, the overabundance of ribosomal biogenesis proteins was not as effectively rectified in double *rps6* mutants that contained phospho-deficient eS6 as opposed to phospho-enabled eS6. Based on our findings, it appears that the increase in ribosome biogenesis has been more pronounced than that of RPs and other RNA-related functions such as RNA degradation and translation initiation. Our deductions suggest that eS6-P functions as a repressor of mRNA expression or the accumulation of proteins required for ribosome biogenesis (Dasgupta *et al.*, 2023) consistent with mammals (Chauvin *et al.*, 2014).

Virus infections

Multiple reports have illustrated the susceptibility of eS6 to phosphorylation during viral infection in both human and animal subjects (Li, 2019, Montgomery *et al.*, 2006, Cardinali *et al.*, 1999, Greco *et al.*, 1997, Beaud *et al.*, 1989, Kaerlein & Horak, 1976). The phosphorylation of eS6 has been extensively studied since its discovery in 1976 reporting its increase in phosphorylation in HeLa cells infected with Vaccinia virus (Kaerlein & Horak, 1976) and has since been observed in other viruses such as Polyoma virus, Avian sarcoma virus, Pseudorabies virus (PRV), Simian virus 40, Herpes simplex virus-1, and tumor viruses (Blenis & Erikson, 1984, Decker, 1981, Kennedy & Leader, 1981). The process of eS6 phosphorylation is catalyzed by S6Ks from host cells (Jakubowicz & Leader, 1987, Katan *et al.*, 1986, Maller *et al.*, 1985, Meyuhas, 2008). Despite the findings presented, the precise function of eS6-P in the context of viral infection has yet to be fully elucidated. Given that eS6-P is known to manifest in reaction to a diverse array of physiological, pathological, and pharmacological triggers - encompassing stress, nutritional status, lipid metabolism, hormonal signaling, and mitogenic activation - it is plausible that this molecule serves as a prototypical physiological reaction to viral infection or another similar stimulus (Meyuhas, 2008, Meyuhas, 2015). The persistence of eS6-P in cells that have undergone deactivated PRV transformation signifies that the viral genome expression is not a prerequisite for the occurrence of virus-induced eS6-P (Kennedy *et al.*, 1984). A distinct theory posits that the promotion and accumulation of viruses is facilitated by eS6-P. One important constituent of the alphavirus viral replication complex forms an

association with eS6, and decreased levels of eS6 protein have an adverse effect on the expression of viral mRNA, without impeding host cellular translation. Following exposure to alphaviruses, es6-P levels decline significantly (Montgomery *et al.*, 2006). In summary, the link between virus infection and eS6-P is correlative (Chen *et al.*, 2017).

Plant viruses with differing mechanisms of translation initiation display variation in their demands for eS6 phosphorylation (Rajamäki *et al.*, 2017, Yang *et al.*, 2009). For Turnip mosaic virus (TuMV), eS6 and S6Ks are necessary for viral infection in plant cells. Conversely, eS6 and S6Ks are not required for infection of Tobacco mosaic virus (TMV) which has the 5'm7Gppp cap. (Rajamäki *et al.*, 2017, Yang *et al.*, 2009). The Cauliflower mosaic virus (CaMV) contains the P6 protein, which has been observed to form a complex with RPs (Bureau *et al.*, 2004). The purpose of these interactions is believed to be related to the re-initiation of translation for polycistronic CaMV RNAs. The transactivator/viroplasmin (TAV) is responsible for regulating the reinitiation process in CaMV through activation by TOR, although the mechanism of this activation has yet to be fully determined (Pooggin & Ryabova, 2018, Park *et al.*, 2001, Fütterer & Hohn, 1992). One intriguing possibility for eS6-P to be involved is that S6K1 phosphorylation on serineS267 controls the activity of Reinitiation Supporting Protein (RISP) (Schepetilnikov *et al.*, 2011). Studies have demonstrated that Arabidopsis eS6-P can support translation re-initiation, as evidenced by in vitro interactions between eS6 and phospho-mimic alleles of RISP. Furthermore, *rps6a* and *rps6b* have shown resistance to CaMV infection due to their decreased reinitiation capacity. This may be remedied by the expression of the eS6

phospho-mimetic version in *rps6a* plants (Mancera-Martínez *et al.*, 2021). Therefore, it is plausible that eS6-P could potentially serve as a facilitator of CaMV infection. In synopsis, the aspect of eS6-P differentially promoting the accumulation of select viruses is a fascinating area for further exploration and warrants future investigations.

1.2 SCOPE OF THIS DISSERTATION

Translational control is crucial for cell function because it allows cells to respond to environmental stresses, adjust their energy balance and coordinate cell growth with cell division. In plants, mRNA-ribosome loading changes in response to various changes in the external environment, the underlying mechanisms are not well-understood. Translational control can either be global or gene specific. A classic example is the gene-specific translational control mediated by the target of rapamycin (TOR) kinase pathway. Once activated, TOR kinase functions in part via S6 kinase to phosphorylate components of the translation apparatus, such as ribosomal protein eS6. Phosphorylation of ribosomal protein eS6 by the TOR-S6 kinase pathway is conserved across all eukaryotes. Despite being the first ribosomal protein shown to be phosphorylated, the biochemical consequence of eS6 phosphorylation is still being investigated. In this thesis the role of eS6-P in *Arabidopsis* has been addressed at the level of translation, photosynthesis, plant growth and development using *rps6* knockout plants, and homozygous double *rps6* mutant lines harboring phospho-defective or phospho-enabled versions of eS6. The comprehensive analysis of the transgenic plants echoes similar effects of eS6-P seen in non-plants. This

chapter emphasizes the established literature on eS6-P and its role in ribosome biogenesis, translation, cell growth, and development. Chapter II explores the functional significance of eS6-P using genetic complementation of *rps6* knockout plants with phospho-defective or phospho-enabled versions of eS6. Chapter III explores the potential role of eS6-P in hypoxia-induced autophagy. Chapter IV summarizes the over-arching conclusions and future experimental ideas.

CHAPTER 2: INVESTIGATING THE BIOCHEMICAL AND PHYSIOLOGICAL SIGNIFICANCE OF RIBOSOMAL PROTEIN S6 PHOSPHORYLATION

Results presented in this chapter were published in Dasgupta et al.2023 as a preprint in Biorxiv, together with additional data by other coauthors that are discussed in this chapter but not explicitly presented as results.

A phosphorylation-deficient ribosomal protein eS6 is largely functional in Arabidopsis thaliana, rescuing mutant defects from global translation and gene expression to photosynthesis and growth. Anwesha Dasgupta, Ricardo A Urquidi Camacho, Ramya Enganti, Sung Ki Cho, Lindsey L. Tucker, John S. Torreverde, Paul E. Abraham, Albrecht G. von Arnim bioRxiv 2023.05.30.542942v1

2.1 ABSTRACT

The eukaryote-specific ribosomal protein of the small subunit 6 (eS6) is phosphorylated through the Target of rapamycin (TOR) kinase pathway. Although this phosphorylation event responds dynamically to environmental conditions and has been studied for over 50 years, its biochemical and physiological significance remains controversial and poorly understood. In this chapter, I will present screening strategies and an extensive analysis of transgenic plants that are devoid of WT-eS6 gene expression, harboring only phospho-defective or phospho-enabled eS6. The eS6A (RPS6A) paralog of eS6 functionally rescued double mutations in both *rps6a* and *rps6b* genes when expressed at approximately twice the wild-type dosage. A mutant isoform of eS6A lacking the major six phosphorylatable serine and threonine residues in its carboxyl-terminal tail also rescued the lethality, rosette

growth, and polyribosome loading of the double mutant. It also complemented many mutant phenotypes of *rps6* that were newly characterized here, including photosynthetic efficiency. However, compared to plants rescued with a phospho-enabled version of eS6A, the phospho-deficient seedlings retained a mild pointed-leaf phenotype, and root growth was reduced. Other transcriptomics and proteomics results from our lab revealed that certain cell cycle related mRNAs and ribosome biogenesis proteins were misexpressed, even though the vast majority of the *rps6* mutant's gene expression defects were rescued by the phospho-deficient allele. The residual defects of the phospho-deficient seedlings could be understood as an incomplete rescue of the *rps6* mutant defects, with little or no evidence for gain-of-function defects. As expected, the phospho-deficient eS6A also rescued the *rps6a* and *rps6b* single mutants; however, phosphorylation of the eS6B paralog remained lower than predicted, further underscoring that plants can tolerate phospho-deficiency of eS6 well. Our data also yield new insights into how plants cope with mutations in essential, duplicated ribosomal protein isoforms.

2.2 INTRODUCTION

The central function of ribosomes is conserved across the kingdoms of life. However, eukaryotic ribosomes contain expansion segments in their ribosomal RNAs, eukaryote-specific ribosomal proteins, and covalent modifications that are not found in prokaryotic ribosomes. Ribosomal protein of the small subunit 6 (eS6 or RPS6) is a pan-eukaryotic protein and was the first ribosomal protein reported to be phosphorylated more than four decades ago (Gressner & Wool, 1974a, Gressner & Wool, 1974b, Kabat, 1970). Its amino-

terminus is buried in the 40S-60S subunit interface while its carboxy-terminal tail harboring a string of phosphorylatable serine and threonine residues at the end of a long alpha-helix is located on the solvent exposed side of the 40S. The presence of phosphorylatable residues is highly conserved in all eukaryotes even though the number of the residues varies among species.

Phosphorylation of eS6 occurs in a polysome context (Duncan & McConkey, 1982). Phosphorylation is also highly dynamic. In animals, eS6 phosphorylation is sensitive to nutrients, hormones, growth factors, and a variety of stress conditions (Meyuhas, 2008). In plants, initial evidence for phosphorylation of eS6 came from tomato plants and maize root tips, where phosphorylation was suppressed by abiotic stresses, heat shock and hypoxia, respectively (Bailey-Serres & Freeling, 1990, Scharf & Nover, 1982). In Arabidopsis, where up to seven sites can be phosphorylated, eS6 phosphorylation levels are induced in response to both internal and external signals: light, circadian clock, sucrose (Chen et al., 2018, Dobrenel et al., 2016b, Enganti et al., 2018, Turkina et al., 2011), elevated CO_2 (Boex-Fontvieille *et al.*, 2013), auxin (Schepetilnikov *et al.*, 2013), and cytokinin (Yakovleva & Kulaeva, 1987). eS6-P has evolved to integrate signals in an elaborate manner. As a case in point, phosphorylation is induced in the daylight and repressed during a dark night, but in contrast is induced by the circadian clock during subjective night and repressed during subjective day (Choudhary et al., 2015, Enganti et al., 2018), an incoherent signaling network that may allow eS6-P to sense subtle shifts in photoperiod or diel illumination (Panchy *et al.*, 2020).

eS6 phosphorylation in plants is considered a canonical readout of the Target-of-rapamycin - S6 kinase (TOR-S6K) pathway because this is the only established pathway known to regulate eS6 phosphorylation in plants (Chen *et al.*, 2018, Dobrenel *et al.*, 2016b, Mahfouz *et al.*, 2006). Despite detailed insights into the regulation of eS6-phosphorylation by upstream signals and kinases, the biochemical and physiological role of eS6-P has remained fairly enigmatic. Knock-in mice expressing only the alanine-substituted, nonphosphorylatable version of eS6 exhibit severe whole-body phenotypes, including a reduced size, glucose intolerance, and muscle weakness, along with a higher rate of protein synthesis (Ruvinsky *et al.*, 2009, Ruvinsky *et al.*, 2005). The phosphorylation of eS6 is implicated in cell size control, hyperplasia in pancreatic cancer, glucose homeostasis, and activation of neurons (Ruvinsky *et al.*, 2005, Ruvinsky *et al.*, 2009, Khalaileh *et al.*, 2013, Wittenberg *et al.*, 2016). The consequences of eS6-P at the biochemical level including translation are not well understood. Mouse embryonic fibroblasts lacking phosphorylatable eS6 had decreased translation fidelity, an increased rate of translation overall, and proliferated faster (Wittenberg *et al.*, 2016). The eS6-P was slightly more abundant on shorter coding sequences, and eS6-P slightly boosted their translation efficiency (Bohlen *et al.*, 2021). eS6 phosphorylation has also been linked to transcriptional regulation of genes encoding ribosome biogenesis factors (Chauvin *et al.*, 2014).

In budding yeast, a detailed study of eS6-P deficiency including ribosome footprinting did not discover any effect of the phosphorylation potential on bulk translation

nor a role in regulation of gene expression via (transcription or) translation. An effect on ribosome biogenesis was attributed to reduced protein expression (Yerlikaya *et al.*, 2016). Recently, Arabidopsis eS6-phosphorylation was proposed to support translation re-initiation, based on differences between phospho-null and phospho-mimic versions with respect to (i) their in-vitro interaction with the re-initiation supporting protein, RISP and (ii) their ability to support expression of a reinitiation-dependent reporter mRNA (Mancera-Martínez *et al.*, 2021).

In my manuscript (Dasgupta *et al.*, 2023) we report our findings from an extensive characterization study of plants lacking either one or both wild-type *RPS6* paralogs and harboring either wild-type or phospho-deficient eS6 transgenes. With the exception of the polysome loading data analysis, transcriptome and proteome data analysis, which was not analyzed by me, all the data presented in this dissertation chapter are generated by me. In Arabidopsis the two genes encoding eS6, *RPS6A* and *RPS6B*, are functionally largely equivalent but non-redundant; double *rps6a rps6b* mutants are embryonic lethal (Creff *et al.*, 2010). We found that the phospho-deficient allele of eS6 rescued the lethality of plants lacking both wild-type *RPS6* genes. We also found it to be largely functional in complementing the growth defects in single-paralog mutants. Double *rps6a rps6b* mutants complemented with a P-deficient eS6 had reverted to normal photosynthetic efficiency (Qy_{max}) and had largely normal mRNA and protein levels for photosynthesis proteins. These P-deficient plants also had no striking defects in global translation, again complementing defects seen in the single *rps6* mutants. However, transcriptome analysis

revealed that the plants displayed subtle defects in gene expression of several cytokinesis related genes. They also tended to have asymmetric cotyledons and transiently pointed first leaves, defects hinting at incomplete complementation of the *rps6* mutations and potentially indicating a whole-plant defect stemming from the P-deficiency. These results mirror and extend findings on the function of this core phosphorylation event from yeast and vertebrates to photosynthetic organisms.

2.3 MATERIALS AND METHODS

2.3.1 Arabidopsis growth conditions and segregation screening

Seeds were sterilized and stratified at 4°C for 2 d. The seeds were germinated on half strength Murashige and Skoog (MS) salt plant medium (MP Biomedicals) solidified with 0.65% Phytoagar (Bioworld). Standard conditions are a long-day cycle of 16 h white light /8 h dark at 22°C and 50% humidity. Unless stated otherwise, seedlings were grown on medium 1% sucrose. The RPS6A (At4g31700) gene knockout mutant is from the GABI-KAT T-DNA collection with an insertion in intron 4 (Kleinboelting *et al.*, 2012). For RPS6B (At5g10360) the *rps6b* allele is SALK_012147C from the SALK collection with an insertion in exon 4 (Creff *et al.*, 2010).

To analyze segregation of the transgenes, seedlings were grown on medium supplemented with 1% sucrose with either 50 μg/ml kanamycin, 7 μg/ml sulfadiazine or Basta. 50 seeds were plated on either kanamycin or sulfadiazine to score the 3:1 segregation of *rps6b-1* or *rps6a-2*, respectively, and 70 seeds were plated on Basta plates to score for a 3:1 or 15:1

or 63:1 segregation of the transgene. Resistance versus sensitivity was scored 7 days after plating, and a Chi-square test was performed to confirm the segregation ratio. The line was then planted in soil and the progeny from the plants was again scored the same way on the way to identify families homozygous for *rps6a*, *rps6b* and a transgene.

2.3.2 Protein Extraction and Immunoblot Analysis

Total protein extraction was performed as described previously by Zhang et al in 2008 (Zhang *et al.*, 2008). In brief, 12-day old whole seedlings were harvested after the desired treatments and flash frozen in liquid nitrogen. For total protein extraction, seedlings were ground using a plastic pestle in a 1.5-mL tube with ice-cold extraction buffer containing 25 mM Tris-HCl (pH 7.5), 75 mM NaCl, 5% (v/v) glycerol, 0.05% (v/v) Nonidet P-40, 0.5 mM EDTA, 0.5 mM EGTA, 2 mM DTT, and 2% (w/v) insoluble polyvinylpyrrolidone (Sigma Aldrich P-6755) supplemented with 1× protease and phosphatase inhibitor cocktail (Thermo Fisher Scientific; cat. no. PIA32959). Total protein content was quantified by Bradford assay (Thermo Fisher Scientific, cat. no. 23,236).

For immunoblot analysis, 40 μg of total protein was separated on a 15% (w/v) SDS-PAGE gel and electroblotted onto a polyvinylidene fluoride membrane. After overnight blocking at 4°C with TBST buffer (1× Tris-buffered saline [pH7.6], 0.1% Tween-20, 10% non-fat dry milk), the membrane was washed 10min each for three repeats with 1X TBST. After the washes, the membrane was incubated for 1h at 22°C with either anti-eS6 rabbit polyclonal antiserum (dilution 1:2500) or anti-eS6 S237-P rabbit polyclonal IgG (dilution 1:5000) or anti-eS6 S240-P rabbit polyclonal IgG (dilution 1:5000). Following washing

with 1X TBST, 10 min each for 3 repeats, the membrane was incubated with 1:5000 dilution of horseradish peroxidase conjugated anti-rabbit IgG (Vector Labs, cat. no. PI-1000) in blocking buffer for 1 h at room temperature as the secondary antibody. After incubation, the membrane was washed with 1X TBST, 10 min each for 3 repeats. Following the washes, chemiluminescence was performed (WesternBright Quantum, Advansta) as per manufacturer's protocol using the Chemidoc Imaging System from Bio-Rad.

2.3.3 Polysome Profiling

The aerial portion of 12 days-after-germination seedlings grown under long day conditions was collected by flash freezing at ZT23.5 (30 minutes before lights on) and ZT2.5 (two and a half hours after lights on). Plant tissue was ground in liquid nitrogen and extracted in polysome isolation buffer (200 mM Tris-HCl pH 8.4, 25 mM $MgCl_2$, 50 mM KCl, 1% deoxycholic acid and 2% polyoxyethylene 10 tridecyl ether). Sucrose gradients were prepared by layering 1.7 ml, 3.3 ml, 3.3 ml, and 1.7 ml each of 50% sucrose, 38.4% sucrose, 26.6% sucrose, and 15% sucrose, respectively. After addition of each gradient layer, the centrifuge tube was frozen at -80°C for 1 h. On the day before use, the gradients were thawed overnight without shaking at 4°C. Plant extracts (1 ml) were loaded on top of a 10 ml 15–50% sucrose gradient and centrifuged at 35,000 rpm for 3.5 h without brake (Beckmann Coulter SW 41Ti). After recording the RNA absorbance profile at 254 nm, the gradient was fractionated into 12 equal fractions. Samples from the fractions were then separated on SDS–PAGE gels followed by immunoblotting to determine eS6 protein levels

and phosphorylation levels in the samples. Equal volumes of sample from each fraction were loaded onto the gels.

Area under the curve for the polysome profile traces were calculated as described (Enganti et al., 2018, Lokdarshi *et al.*, 2020a). In brief, gradient traces were manually split into 40S, 60S, 80S, small polysomal (2-4 ribosomes) and large polysomal sections (5+ ribosomes). Blank gradient traces were subtracted from the sample traces and the area under the curve was calculated for each section. If applicable, areas were combined into non-polysomal (sum of areas from 40S, 60S and 80S) and polysomal (sum of areas from small and large polysomal) sections. Abundances of different ribosomal complexes were compared between genotypes or time points by using Welch's t test.

2.3.4 Transient gene expression in Nicotiana benthamiana

Coding sequences of eS6 were cloned as N-terminal fusions to enhance yellow fluorescent protein and expressed from the CaMV 35S promoter. Overnight cultures of *Agrobacterium tumefaciens* harboring the T-DNA plasmid of interest were grown with appropriate antibiotics. The cultures were pelleted and resuspended in infiltration buffer (10mM MES buffer, 10mM $MgCl_2$, pH 5.4) to an optical density of 1.0 at 600nm. Acetosyringone was added to a final concentration of 200µM to the culture and incubated with agitation for 2h. Young leaves on three-week-old *N. benthamiana* plants were infiltrated with the cultures using a 1ml syringe. The plants were kept in the dark overnight and shifted to normal growth conditions for 36h, following which the leaves were imaged to detect fluorescence by confocal laser scanning microscopy.

2.3.5 Root phenotyping

To measure root lengths, seedlings were grown vertically on square petri plates with a grid and photographed on day 7 after germination. Images were imported into ImageJ and root lengths were measured by tracing each primary root using the segmented line tool.

2.3.6 Photosynthetic efficiency measurement

The maximum quantum yield of photosystem II (PS II) (Qymax = F_v/F_m) was measured on a FluorCam 800MF (Photon Systems Instruments, Drásov, Czechia) as per the manufacturer's instructions and modifications (Murchie & Lawson, 2013). Briefly, plants were dark adapted for 1 min (F_0) prior to applying a saturating pulse of 1800 μEin m^{-2} s^{-1} for 0.8 s (F_m). Variable fluorescence (F_v) was calculated as the difference between F_0 and F_m to get the maximum quantum yield (F_v/F_m) (Lokdarshi *et al.*, 2020b).

2.4 RESULTS

This chapter relies on Arabidopsis specific notation of T-DNA insertion mutants and the updated nomenclature of plant RPs (Lan *et al.*, 2022, Scarpin *et al.*, 2022) that are summarized for easy interpretation of the following results, in **Figure 2.1**. The *rps6a* and *rps6b* mutants are T-DNA insertion mutants marked by sulfadiazine resistance (*rps6a*) and kanamycin resistance (*rps6b*). The transgenes are referred to as *eS6*-transgenes in order to distinguish the transgenic version from the endogenous version. Transgenes carry Basta resistance. The transgenes express phospho-deficient versions (serine to alanine mutations marked S>A) or phospho-mimic versions (serine to aspartate, S>D) or wild-type versions.

The transgenes had been constructed and introduced into Arabidopsis *rps6a rps6b* mutant backgrounds prior to my involvement in the project (Enganti, 2018).

2.4.1 Screening results of rps6a rps6b double mutant lines deficient for eS6-P, identified by the Mendelian segregation of their selectable marker genes for rps6a, rps6b and the RPS6 transgene.

Identification of rps6a rps6b double mutant lines harboring P-deficient and WT alleles of eS6A and eS6B:

To identify successful transformants harboring *rps6a* and *rps6b* single mutations and the transgene, the T1 seeds were screened on ½ strength MS medium supplemented with 1% sucrose with 1X Basta. Before my involvement in the project, the T2 seeds were screened on the MS medium with sulfadiazine (selection marker for *rps6a*), kanamycin (selection marker for *rps6b*) and basta (selection marker for transgenes). I started the screening process with each transgenic line plated on four separate plates: ½ strength MS medium supplemented with 1% sucrose with (a) kanamycin, (b) sulfadiazine, (c) basta and (d) all three selection markers. Resistance versus sensitivity was scored 7 days after plating, and a Chi-square test was performed to confirm the segregation ratio. The selection marker combination plate was to select for the presence of at least one copy of the individual insertions before transplanting seedlings onto the soil. The progeny was screened through the same strategy to identify families homozygous for *rps6a, rps6b* and a transgene. My work began with establishing the screening strategy to identify double mutants complemented with various phospho-mutant versions of eS6. **Figure 2.2** details the result of the screening project. In summary, I identified individual double mutant lines

complemented with wild-type eS6A (eS6A ^{WT}) an HA-tagged version of eS6A (eS6A $^{WT\text{-}HA}$), phospho-deficient version of eS6A, where 5 serines and 1 threonine were replaced with alanine (eS6A $^{\Delta 6S>A}$), wild-type eS6B (eS6B^{WT}) and a phospho-deficient version of eS6B, where 3 serines were replaced with aspartate Δ3S>D allele of eS6B.

Genotyping using PCR to confirm the genotypes of the rps6a rps6b double mutant lines harboring P-deficient and WT alleles of RPS6:

The seedlings harboring mutant alleles for both *rps6a* and *rps6b* were genotyped via PCR to check for the allelic status of the endogenous *RPS6A* and *RPS6B* genes and their respective T-DNA insertions. To differentiate between transgenic eS6A and endogenous wild type eS6A (allele: *RPS6A*), I designed a primer that extends from the 3'UTR of endogenous eS6A into the intergenic region. The PCR strategy along with example gels showing genotyping result of WT and a double mutant with eS6A transgene are presented in **Figure 2.3**.

2.4.2 Subcellular localization of phosphorylation-deficient allele of eS6A

In order to investigate if phospho-deficiency of eS6 has an effect on its subcellular localization, we decided to use a transient expression assay in *Nicotiana benthamiana.* The constructs used in the assay were constitutive expression constructs of wild-type eS6A and a fully phosphodeficient allele, eS6A $^{\Delta 7S>A}$ with N-terminus enhanced YFP (EYFP) fusion tags. Both the wildtype and P-deficient eS6A accumulated strongly in the nucleus and

A. RPS6 genes in *Arabidopsis*: AtRPS6A (At4g31700) and AtRPS6B (At5g10360).

B. Proteins: AteS6A and AteS6B, respectively.

```
                              229 231     237 240 241     247 249
AteS6A  RLKEQRDRRSESLAKKRSRLSSAAAKPSVTA
AteS6B  RLKEQRDRRSESLAKKRSRLSSAPAKPVAA
```

C. Single paralog gene knockout mutants: *rps6a(-/-)* and *rps6b(-/-)*.

D. Double heterozygous mutants: *rps6a(+/-)rps6b(+/-)*.

E. Double homozygous mutants harboring eS6A or eS6B transgenes with serines or threonine changed to alanine (ΔS>A alleles) or to aspartate (ΔS>D alleles): *rps6a(-/-)rps6b(-/-);* eS6A/B$^{\Delta S>A/\Delta S>D}$

F. eS6A transgenes with serines or threonine changed to alanine (ΔS>A alleles).

Name	Residues altered to alanine						
eS6A$^{\Delta 3S>A}$		S231	S237	S240			
eS6A$^{\Delta 5S>A}$		S231	S237	S240		S247	T249
eS6A$^{\Delta 6S>A}$		S231	S237	S240	S241	S247	T249
eS6A$^{\Delta 7S>A}$	S229	S231	S237	S240	S241	S247	T249

G. eS6B transgenes with serines or threonine changed to aspartate (ΔS>D alleles).

Name	Residues altered to aspartate				
eS6B$^{\Delta 3S>D}$		S231	S237	S240	
eS6B$^{\Delta 4S>D}$		S231	S237	S240	S241

Figure 2.1: Notation review.

(A) The two *RPS6* genes will be referred to as *RPS6A* and *RPS6B*. Their AGIs are in parentheses. (B) To incorporate the updated nomenclature of plant RPs, the protein from the two *RPS6* genes will be designated eS6A and eS6B respectively. The serine or threonine residues in the C-terminal tails of eS6A and eS6B are highlighted in green with their corresponding numbers above them. Notation for (C) single homozygous mutants and (D) double heterozygous mutants and (E) double homozygous mutants with transgenes. Tables show the double mutants with (F) phospho-deficient eS6A transgenes and (G) phospho-mimic eS6B transgenes that were generated and screened.

Figure 2.2: **Summary of screening results of *rps6a rps6b* double mutant lines harboring transgenes that are either phospho-enabled or phospho-defective for eS6-P, identified by the Mendelian segregation.**

Transgenes encoding phospho-deficient and wild-type alleles of eS6A were introduced into Arabidopsis lines with mutations in (A) eS6B, and (B) eS6A. The tables list all individual transgene integration events and indicates whether single or multiple T-DNAs are present and whether the line contains mutations in *rps6a*, *rps6b* or both. The screening results were documented and verified using Chi square tests. Expected segregation ratios were 3:1 for *rps6a*, and *rps6b* T-DNA insertions. For transgenes that were either P-enabled for eS6 or P-deficient the expected segregation ratios were 3:1, and 15:1. Column 1 indicates the version of phospho-defective or WT eS6 transgene in each family. Each row depicts a transgenic line and their current genotype. Column 2 indicates the generation that was screened. Column 3 represent the lineage of each plant analyzed in the generation followed by column 4 that shows the number of offsprings analyzed, in that specific transgenic line. Column 5 indicates the number of offsprings in that specific family that are *rps6a* and *rps6b* double mutants (homozygous for both). Column 6 specifies the number of siblings that are homozygous **only** for *rps6a* and Column 7 **only** for *rps6b*. The transgene column has three sub-columns to denote the number of transgenes that a specific family is expected to have. The first sub-column lists the number of siblings in the corresponding family that mostly have one transgene, second sub-column lists the number of siblings that are homozygous for at least one of the transgenes and the third, lists the number of siblings that likely have two or more transgene

A

TRANSGENE	GENERATION	FAMILY	OFFSPRING	*rps6a(-/-) rps6b (-/-)*	*rps6a (-/-)*	*rps6b (-/-)*	Transgene		
							(+/-)	(+/+)	(+/-)(+/-)
eS6B^{WT}	T3	1.1-1.15	15	0	0	0	10	0	5
	T3	2.1-2.14	14	0	3	2	0	8	6
	T3	5.1-5.14	14	0	5	2	4	6	2
	T3	3.1-3.13	13	0	2	3	0	8	3
	T4	1.6.1-1.6.9	9	0	0	0	2	0	7
	T4	1.2.1-1.2.2	2	0	1	0	2	0	0
	T4	3.9.1-3.9.14	14	3	5	10	0	9	5
	T4	5.5.1-5.5.15	15	2	6	6	4	7	3
	T4	3.2.1-3.2.12	12	2	2	10	0	10	1
	T4	3.5.1-3.5.13	13	4	5	12	0	12	1
	T4	2.2.1-2.2.15	15	6	15	6	0	14	1
	T4	1.15.1-1.15.8	8	0	6	0	4	0	4
eS6B$^{\Delta 3S>D}$	T3	36.1-36.14	14	0	4	1	1	8	4
	T3	27.1-27.6	6	0	0	0	2	2	2
	T3	29.1-29.9	9	0	0	0	1	4	3
	T4	36.6.1-36.6.14	14	2	7	3	2	4	8
	T4	36.8.1-36.8.7	7	0	1	1	2	2	2
	T4	36.12.1-36.12.6	6	4	6	4	0	5	1
	T4	27.3.1-27.3.7	7	0	0	7	0	5	2
	T4	27.4.1-27.4.10	10	0	0	8	3	4	2
	T4	29.3.1-29.3.3	3	0	1	0	0	0	3
	T4	29.2.1-29.2.9	9	0	2	0	1	1	7
	T5	29.2.1.1-29.2.1.10	10	0	2	0	0	7	3
eS6B$^{\Delta 4S>D}$	T3	22.1-22.13	13	0	0	0	0	4	6
	T4	22.6.1-22.6.14	14	0	5	0	0	9	4
	T4	22.2.1-22.2.10	10	0	1	0	0	1	3
	T4	2.9.1-2.9.9	9	1	2	2	0	1	8
	T4	2.11.1_2.11.8	8	0	1	0	1	3	3

Figure 2.2 continued

B

TRANSGENE	GENERATION	LINEAGE	OFFSPRING	*rps6a(-/-) rps6b (-/-)*	*rps6a (-/-)*	*rps6b (-/-)*	Transgene		
							(+/-)	(+/+)	(+/-)(+/-)
eS6A^{WT}	T2	1-14	14	0	0	0	7	0	4
	T3	2.1-2.11	11	2	3	3	6	1	3
	T3	3.1-3.14	14	0	1	4	0	0	14
	T3	5.1-5.11	11	0	2	0	2	5	3
	T3	6.1-6.15	15	0	0	0	3	2	12
	T3	11.1-11.12	12	0	2	1	2	5	4
	T3	14.1-14.10	10	0	0	0	1	2	6
	T4	5.1.1-5.1.5	5	0	0	0	0	0	4
	T4	5.10.1-5.10.11	11	0	0	0	0	0	0
	T4	14.10.1-14.10.11	11	1	3	1	0	1	10
	T4	2.4.1-2.4.8	8	6	8	6	1	4	2
	T4	5.6.1-5.6.11	11	0	0	0	1	0	0
	T4	6.1.1-6.1.17	17	0	2	7	0	0	17
	T5	2.2.1.1-2.2.1.5	5	5	5	5	0	2	3
	T5	2.2.2.1-2.2.2.5	5	4	5	4	0	3	2
	T5	2.2.3.1-2.2.3.5	5	5	5	5	0	2	3
	T5	2.2.4.1-2.2.4.5	5	4	5	4	0	1	4
	T5	2.2.5.1-2.2.5.5	5	5	5	5	0	1	4
	T5	2.2.6.1-2.2.6.5	5	5	5	5	0	0	5
	T5	2.2.7.1-2.2.7.6	6	5	6	5	0	0	6
	T5	14.10.3.1-14.10.3.4	4	0	1	0	0	2	1
	T5	14.10.7.1-14.10.7.5	5	3	4	3	0	1	3
	T5	5.10.11.1-5.10.11.3	3	0	3	0	0	0	3
	T5	5.10.6.1-5.10.6.4	4	0	4	0	0	2	0
	T5	5.1.1.1-5.1.1.5	5	0	5	0	0	0	5
	T5	6.1.1.1-6.1.1.5	5	4	5	4	0	4	1
	T5	6.1.7.1-6.1.7.5	5	0	5	0	0	0	5
eS6A^{WT-HA}	T3	2.1-2.11	11	0	0	3	1	3	4
	T4	2.8.1-2.8.10	10	0	0	5	0	4	4
	T5	2.5.4.1-2.5.4.15	15	1	4	6	0	11	4
eS6A$^{\Delta 3S>A}$	T3	1.1-1.15	15	0	3	0	3	7	4
	T3	5.1_5.15	15	0	5	0	0	3	11
	T5	1.7.3.1-1.7.3.3	3	3	3	3	0	1	2
	T5	1.7.2.1-1.7.2.3	3	0	2	0	0	1	1
eS6A$^{\Delta 6S>A}$	T5	10.5.12.1-4	4	0	3	0	1	1	2
	T5	10.5.13.1-2	2	0	2	0	0	1	1
	T5	10.24.2.1-5	5	0	2	0	0	2	2
	T5	10.24.3.1-3	4	0	2	0	0	1	2
	T6	10.24.3.2.1-2	2	1	2	1	0	0	2
	T6	10.24.11.1.1-6	6	0	0	2	0	1	5
	T6	10.24.2.1.1-9	9	5	8	5	0	1	6
	T6	10.24.3.3.1-8	8	6	8	6	0	6	2

Figure 2.2 continued

in the nucleolus, as well as in the cytosol, as expected for ribosomal proteins (**Figure 2.4** A). The eS6A wild-type and eS6A $^{\Delta 7S>A}$ mutant proteins also appeared in structures resembling mini-nucleoli and other more or less numerous small granules, collectively referred to as nuclear punctae. eS6A $^{\Delta 7S>A}$ formed punctae more often than eS6A wild type (**Figure 2.4** A,B). eS6A $^{\Delta 7S>A}$ transformed cells also tended to have more than one nucleolus, but this trend was not statistically significant (**Figure 2.4** C). eS6 was tagged at the N-terminus because tagging the C-terminus was more likely to disrupt the phosphorylation at that site. If EYFP-eS6 were incorporated into the 40S, then the bulky YFP may disrupt subunit joining with the 60S. It is plausible that the YFP-tagged eS6 is showing us the localization pattern of free eS6 protein, and eS6 in the process of ribosome biogenesis until the 40S is exported from the nucleus. Taken together, the phosphorylation status did not appear to affect the subcellular targeting of eS6 in a major way.

2.4.3 The eS6A^{WT-HA} and eS6B^{WT} transgenes fully complement the root growth defect in rps6 double mutants while the eS6A$^{\Delta 6S>A}$ transgene complement the defect partially.

The majority of the work was done with a double *rps6a rps6b* mutant that harbored a transgene with variably phospho-deficient versions of eS6A, where 5 serines and 1 threonine were replaced with alanine (Δ6S>A). As controls, double mutants were complemented with an HA-tagged version of eS6A (eS6A $^{WT-HA}$) or with wild-type eS6B and with a Δ3S>D allele of eS6B.

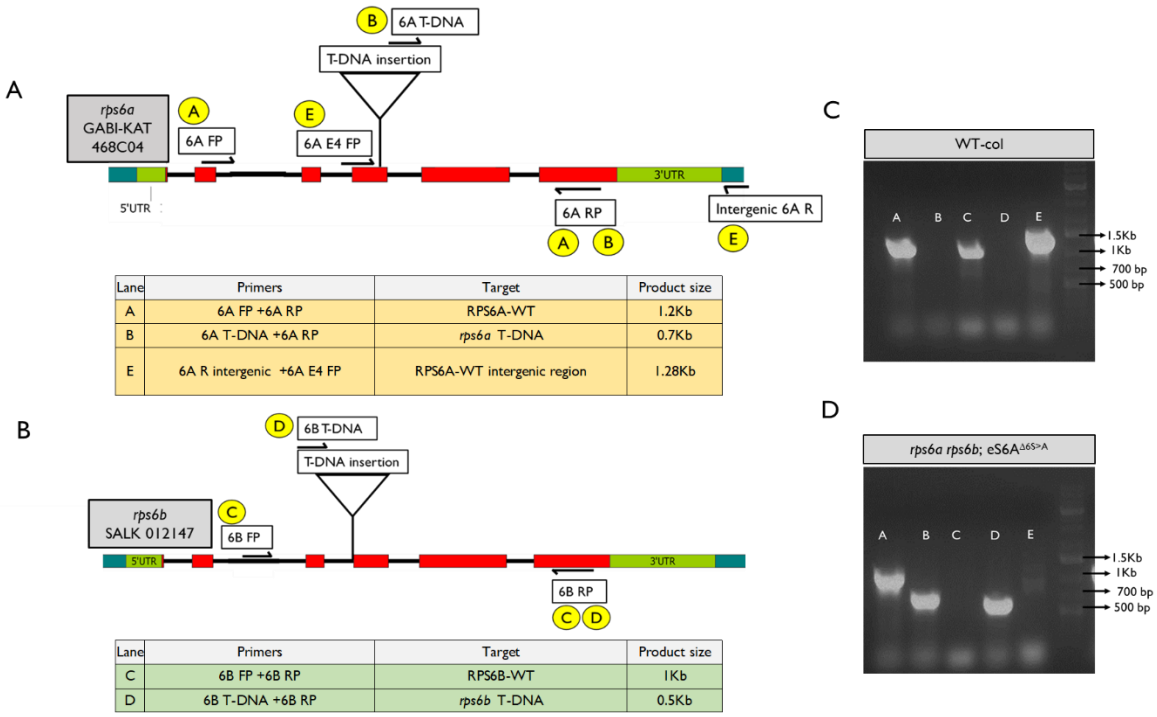

Figure 2.3: Confirming genotypes of double mutants with transgenes using PCR.

(A, B) Gene models of (A) *AtRPS6A* and (B) *AtRPS6B* with their respective primers and their respective T-DNA insertion positions. Each primer pair is labelled with an alphabetic character, which is cross-referenced in the tables below each gene model. The table lists the target that is amplified by the primer pair and the PCR product size in basepairs.

(C, D) Example gels of PCR genotyping results for (C) WT-col and (D) a double *rps6a rps6b* mutant with an eS6A$^{\Delta 6S>A}$ transgene.

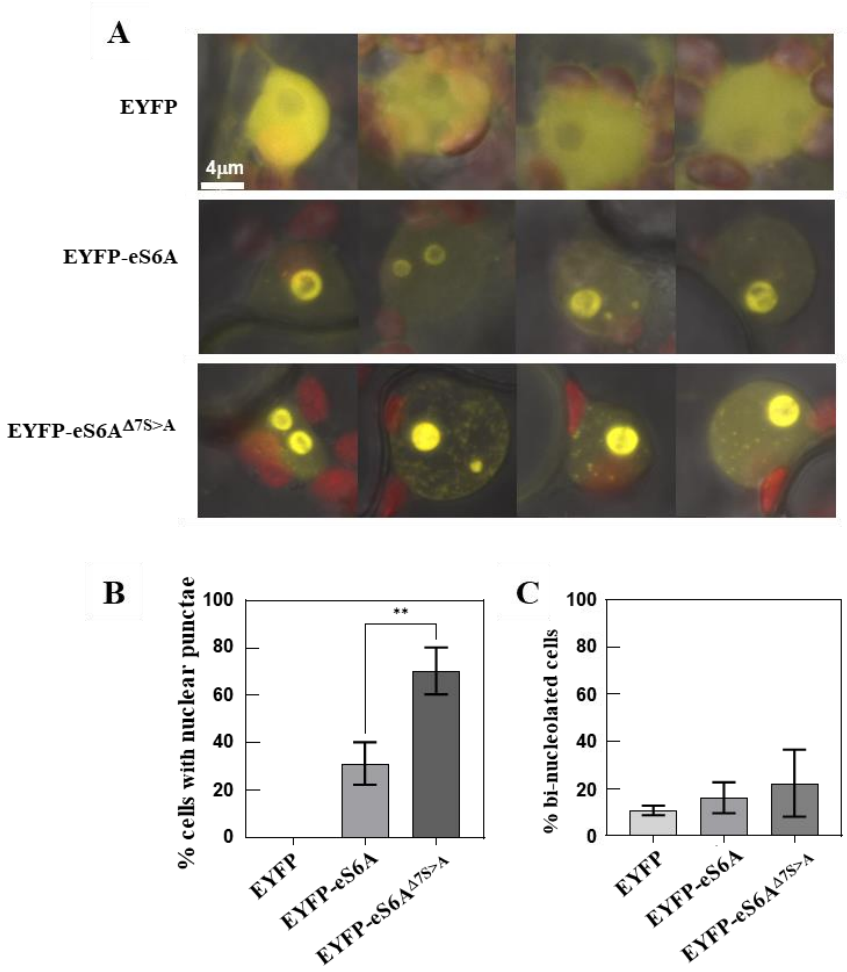

Figure 2.4: Nuclear and nucleolar localization of YFP-tagged eS6A 7SA in transiently transformed *Nicotiana benthamiana* leaves.
Expression was driven by the 35S promoter. Plants were kept in the light prior to microscopic observation to allow for robust phosphorylation of wild type eS6. Data was collected approximately 48 hours after transformation. Four representative micrographs per construct are shown. Three independent experiments yielded equivalent results. (A) The range of typical localization patterns for eYFP alone, wild type eS6A, and eS6A $^{\Delta 7SA}$. (B) Quantification of cells containing nuclear punctae. ** p=0.0073. (C) Quantification of the fraction of cells with more than one nucleolus.

Considering that *rps6a rps6b* double mutants are embryo-lethal (Creff *et al.*, 2010), it was striking that the P-deficient plants were fully viable. However, a number of subtle growth defects were observed. First, root growth was reduced in a repeatedly selfed, homozygous, phospho-deficient line as compared to P-enabled eS6A$^{WT\text{-}HA}$ and eS6B (**Figure 2.5** A,B). Second, young eS6A$^{\Delta 6S>A}$ complemented seedlings had pointed first leaves, a common phenotype in ribosomal protein mutants, including *rps6a* and *rps6b*. The pointed leaf phenotype is not due to the fact that eS6B is missing because *rps6a rps6b* heterozygotes (which contain 50% each of eS6A and eS6B) also have the pointed leaf phenotype (Creff *et al.*, 2010, Ren *et al.*, 2012), and eS6A$^{WT\text{-}HA}$ plants did not have pointed leaves (**Figure 2.5** C).

2.4.4 rps6a single mutant and eS6A$^{\Delta 6S>A}$ complemented double mutant seedlings display a higher proportion of asymmetric cotyledons.

In the course of embryonic development in dicotyledonous plants, the cotyledons, also known as embryonic leaves, undergo a distinct developmental process compared to the true leaves, which are formed through the activity of the apical meristem. As part of this developmental process, the cotyledons transition from being a sink to a source in order to facilitate the biogenesis of chloroplasts in the leaf. This is a crucial process for the survival of the plant after germination. We newly observed that *rps6a* mutants, and to a lesser degree *rps6b* as well, tend to have cotyledons that differ in size (**Figure 2.5** C,D,E). This asymmetry was retained in the eS6A$^{\Delta 6S>A}$ seedlings.

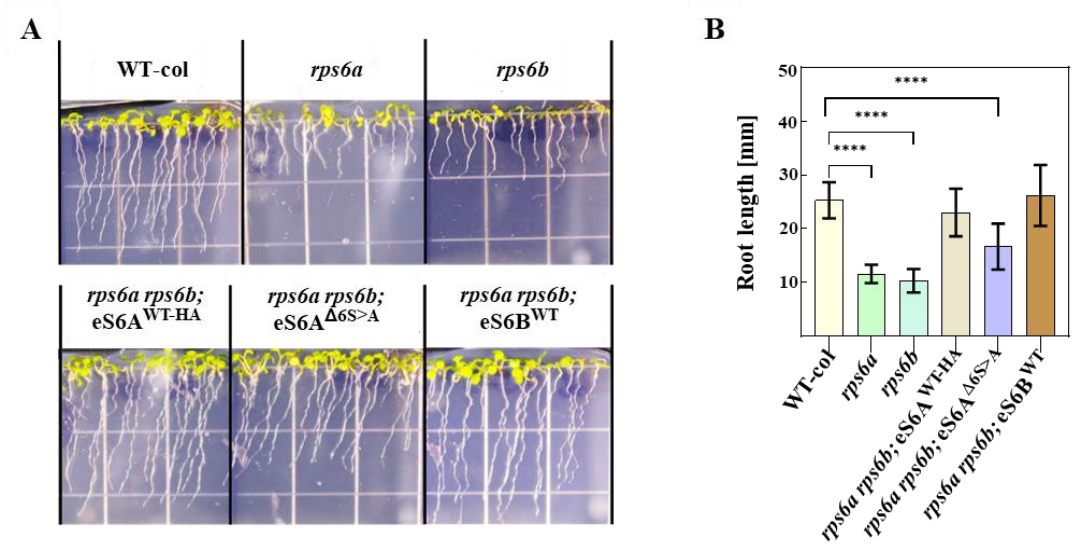

Figure 2.5: Plants that are deficient for eS6-P grow largely normally with exceptions during seedling establishment.

(A) Phenotype of 11-day-old seedlings complemented with a phospho-deficient version of eS6A, as compared to controls. (B) Root lengths of seedlings from experiment (A). Error bars indicate standard deviations, and **** indicates $p<0.0001$ by Welch's t-test. (C) Pointed-leaf and asymmetric cotyledon phenotypes in 7-day-old seedlings of P-deficient plants and controls. (D) Cumulative histogram and (E) violin plot of the asymmetric cotyledon phenotype. Medians are indicated by red bars. ** $p=0.0056$ and **** $p<0.0001$ by Mann-Whitney test.

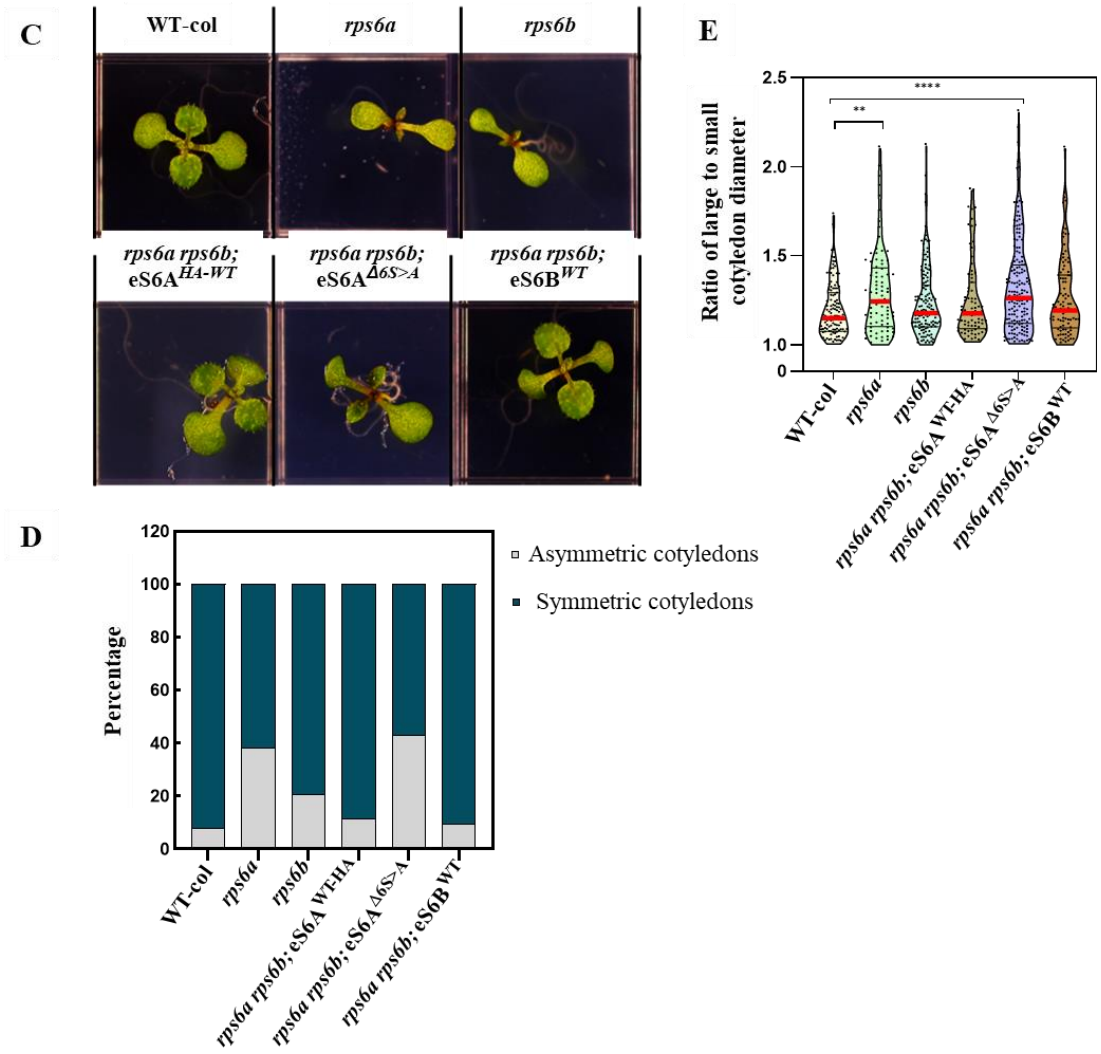

Figure 2.5 continued

2.4.5 rps6a and rps6b single mutants have significantly lower quantum efficiency of Photosystem-II (PS-II) as compared to WT.

To characterize the phospho-deficient plants in more detail, we measured the photosynthetic efficiency of photosystem II (Qy_{max} = F_v/F_m). In keeping with misexpression of photosynthesis genes in *rps6a* mutant seedlings from the RNA-Seq experiment (Urquidi Camacho, 2023), PS II efficiency was reduced in *rps6a* and *rps6b* mutants in seedlings and in rosette-stage plants grown at 22ºC or at 12ºC **(Figure 2.6)**. The phospho-deficient plants (*rps6a rps6b*; $eS6A^{\Delta 6S>A}$) were largely rescued for photosynthetic efficiency at all stages.

2.4.6 $eS6A^{\Delta 6S>A}$ complemented double mutants have normal levels of total eS6 but are devoid of eS6-P.

After identifying the double mutants homozygous for endogenous eS6 only harboring transgenes, I determined their eS6 protein and eS6-P phosphoprotein levels. The $eS6A^{WT\text{-}HA}$ and $eS6B^{WT}$ complemented double mutants show total eS6 and eS6-P levels comparable to WT (**Figure 2.7** A) suggesting the expression of sufficient eS6 to complement the lethal, double-mutant phenotype. The $eS6A^{\Delta 6S>A}$ complemented plants were indeed deficient for eS6-P for both S237 and S240.

Additionally, RNA-Seq and proteomics experiments (Urquidi Camacho, 2023) demonstrated that the $eS6A^{\Delta 6S>A}$ mRNA and protein were expressed at an elevated level, equivalent to about 1.3- and 1.6-fold, respectively, of the native eS6A **(Figure 2.7** B**)**. Therefore, it appears that the homozygous $eS6A^{\Delta 6S>A}$ transgene provides about as much eS6 mRNA and protein as can be expected in a heterozygous *rps6b* mutant, which is considered a recessive mutation with a fully wild-type phenotype.

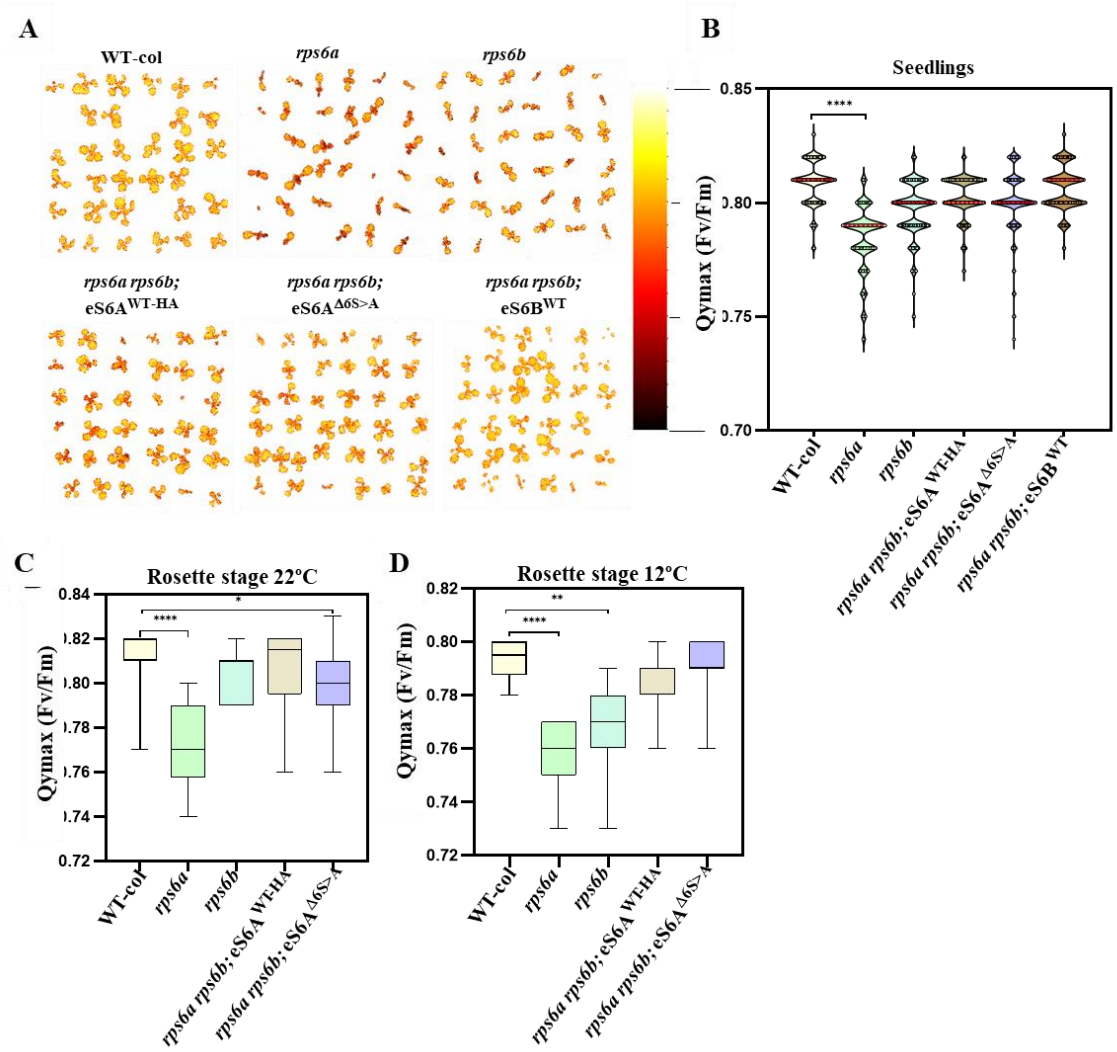

Figure 2.6: Phenotypes of P-deficient plants in mature rosettes and photosynthetic efficiency.

(A) Qy_{max} heatmaps in 11-day-old seedlings for the indicated genotypes of P-deficient plants and controls. (B) Quantification of data from experiments such as panel (A).(C, D) Qy_{max} in 3-week-old rosettes for the indicated genotypes of P-deficient plants and controls at (C) 22ºC and (D) 12ºC.

2.4.7 eS6A$^{\Delta 6S>A}$, eS6A$^{WT\text{-}HA}$ and eS6B^{WT} complemented double mutants are translationally competent as seen by the translation upregulation upon dark to light transition.

To determine translational competency, in our lab we analyze polysome profiles from samples that collected both 0.5 h before and 2.5h after the daily dark to light shift (i.e. at zeitgeber times ZT23.5 and ZT2.5) because light exposure induces a large and rapid increase in mRNA ribosome loading (Liu *et al.*, 2012). Increase in polysome loading after dark to light shift indicates that plants can respond adequately to light by upregulating translation needed for cellular functions under light. From our analysis of the polysome profiles of the *rps6a* and *rps6b* mutants we knew that even though they were able to ramp up translation upon light exposure, the overall polysomes were slightly decreased in both. An increase in the relative abundance of the 60S subunit, which had been suggested earlier (Creff *et al.*, 2010) was also found to be statistically significant for both *rps6a* and *rps6b* in the light in our data (Dasgupta *et al.*, 2023). This data led us to conclude that production of sufficient 40S subunit is rate limiting in the *rps6* single mutants, because only a single paralog is available for eS6, not only for growth but also for ribosome production. That is why the 60S subunit overaccumulates; indicating that the amount of 40S and 60S subunit are slightly out of balance in both *rps6* mutants as compared to wild type. However, polysome profiles in the phospho-deficient eS6 complemented single mutant showed that the dark-to-light transition triggered the typical rise in polysome loading, without the significant abundance in the level of the 60S subunit or any other striking defects in polysome loading (Dasgupta *et al.*, 2023). These results suggest that the phosphodeficient isoform rescues the ribosome biogenesis defects in single mutant background.

To determine the effects of the phospho-deficiencies in eS6 on the translation apparatus, we next analyzed polysome profiles of the eS6A$^{\Delta 6S>A}$, eS6A$^{WT\text{-}HA}$ and eS6B^{WT} complemented double mutants from samples collected according to the same sampling scheme before and after the daily dark to light shift. The *rps6a rps6b* double mutants that were complemented with the phospho-deficient eS6A$^{\Delta 6S>A}$ transgene showed essentially normal polysome loading before and after the dark-to-light shift **(Figure 2.7** C; quantified in **Figure 2.8** B**)**. However, exposure to light increased the polysome loading in both the phospho-enabled eS6A$^{WT\text{-}HA}$ and the P-deficient eS6A$^{\Delta 6S>A}$ mutant. Similar results were obtained when the double mutants were complemented with eS6B, or eS6B$^{\Delta 3S>D}$ **(Figure 2.8** A**)**. As expected, light-induced phosphorylation of eS6 in polysomes was detected in wild-type plants and in double mutants complemented with eS6A$^{WT\text{-}HA}$, but not in plants complemented with eS6A$^{\Delta 6S>A}$ **(Figure 2.7** D). Therefore, eS6 protein functions apparently normally in supporting polyribosome loading despite being unphosphorylated (Δ6S>A) or harboring *bona fide* phospho-mimic mutations (Δ3S>D). In addition, in these experiments all the transgenes in the double mutant background suppressed the overaccumulation of the 60S subunit similar to the transgenes in the single mutant background **(Figure 2.8** A,B**)**.

2.4.8 Phospho-defective eS6 gets incorporated into actively translating ribosomes.

For Wt-col, polysomal eS6 phosphorylation at S240 and S237 increased robustly within 2.5h of light exposure (**Figure 2.7** D). This is consistent with the increase in global polysome loading and higher eS6 phosphorylation in response to light. A similar pattern

was observed for double mutant seedlings harboring HA-tagged WT-eS6A. Both of these results confirm that phosphorylated eS6 gets incorporated into actively translating polysomes. The eS6A$^{\Delta 6S>A}$ complemented seedlings lacked S240 and S237 phosphorylation, as expected **(Figure 2.7** D**)**. However, total eS6 was still detected in polysomal fractions, suggesting that the eS6A$^{\Delta 6S>A}$ protein, despite lacking six major sites of phosphorylation, gets incorporated into polysomes **(Figure 2.7** D**)**.

2.5 DISCUSSION

2.5.1 Tracking tri-hybrid segregation using Mendelian genetics.

The screening work identified transgenic lines that are devoid of endogenous eS6A and eS6B. Those lines now harbor only complementing transgenes. These lines were used for phenotypic analysis and polysome profiling experiments, and - in experiments not shown here (Dasgupta *et al.*, 2023) - for RNA-seq analysis of their transcriptomes and proteomics. The lines complemented with eS6A$^{WT\text{-}HA}$ and with phospho-deficient eS6A$^{\Delta 6S>A}$ presented us with a unique opportunity to study the effects of paralog absence and eS6-P at both the organismal and the biochemical level of the complete absence of endogenous eS6. Ideally, if we were to find a line that has only one transgene, we expect those plants to behave like single mutants *rps6a* and *rps6b* with pointed leaves, shorter roots, and chlorotic leaves. We believe that the developmental phenotypes observed in the *rps6a* and *rps6b* plants are largely due to lower dosage of eS6 expression. The issue is intricate in nature, given that the majority of our familial units have multiple transgenes.

Figure 2.7: **Biochemical characterization of plants lacking eS6 phosphorylation.**

(A) Phosphorylation of eS6 is not detected in *rps6a rps6b* double mutants that harbor the phospho-deficient $eS6A^{\Delta 6S>A}$ transgene. Whole protein extracts from seedlings were probed with phospho-specific antibody for P-S240 or P-S237. Note: Our S-237 antibody detects two bands consistently. Repeated results and experience with the $eS6A^{\Delta 6S>A}$ allele have convinced us that the upper band running at ~35 KDa is the eS6 band.

(B) mRNA read counts for eS6A and eS6B from an RNA-Seq experiment with the indicated genotypes. Proteomics data from the same genotypes expressed as a $\log_2$-fold difference to wild type. Note that the three transgenes provide elevated levels of eS6 protein, as expected given the elevated mRNA read counts. The mRNA read counts are expected to be elevated if one assumes that the plants contain multiple transgenes, although this was not confirmed independently.

(C) Polysome loading in *rps6a rps6b* double mutants complemented with phospho-enabled and phospho-deficient transgenes. Polysome loading was examined 30 minutes prior to lights-on (ZT23.5) and 2.5h after lights-on (ZT2.5). Representative polysome profiles show that eS6-P deficient plants are able to increase their ribosome loading during the dark-to-light shift.

(D) Immunoblots demonstrating that eS6 is phosphorylated in a polysome context in double *rps6a rps6b* mutants complemented by an HA-tagged eS6A (middle). In contrast, in the phosphodeficient plants (bottom) no phosphorylation is detectable at the position corresponding to eS6 (arrowhead). Note that fractions 3-4 at the top of the gradient contain several crossreacting proteins.

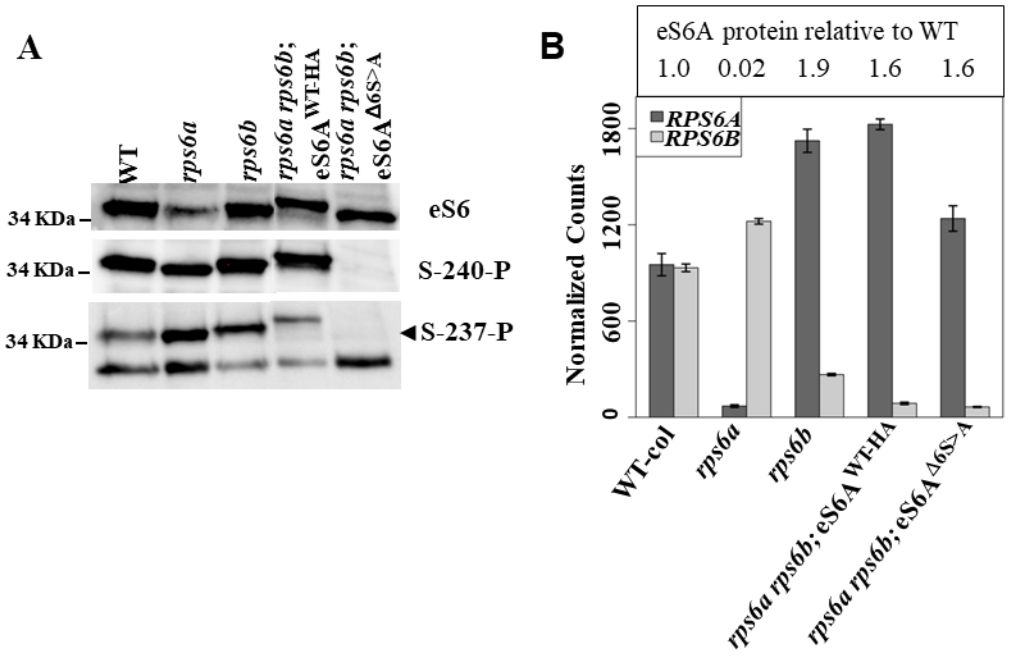

Figure 2.7 continued

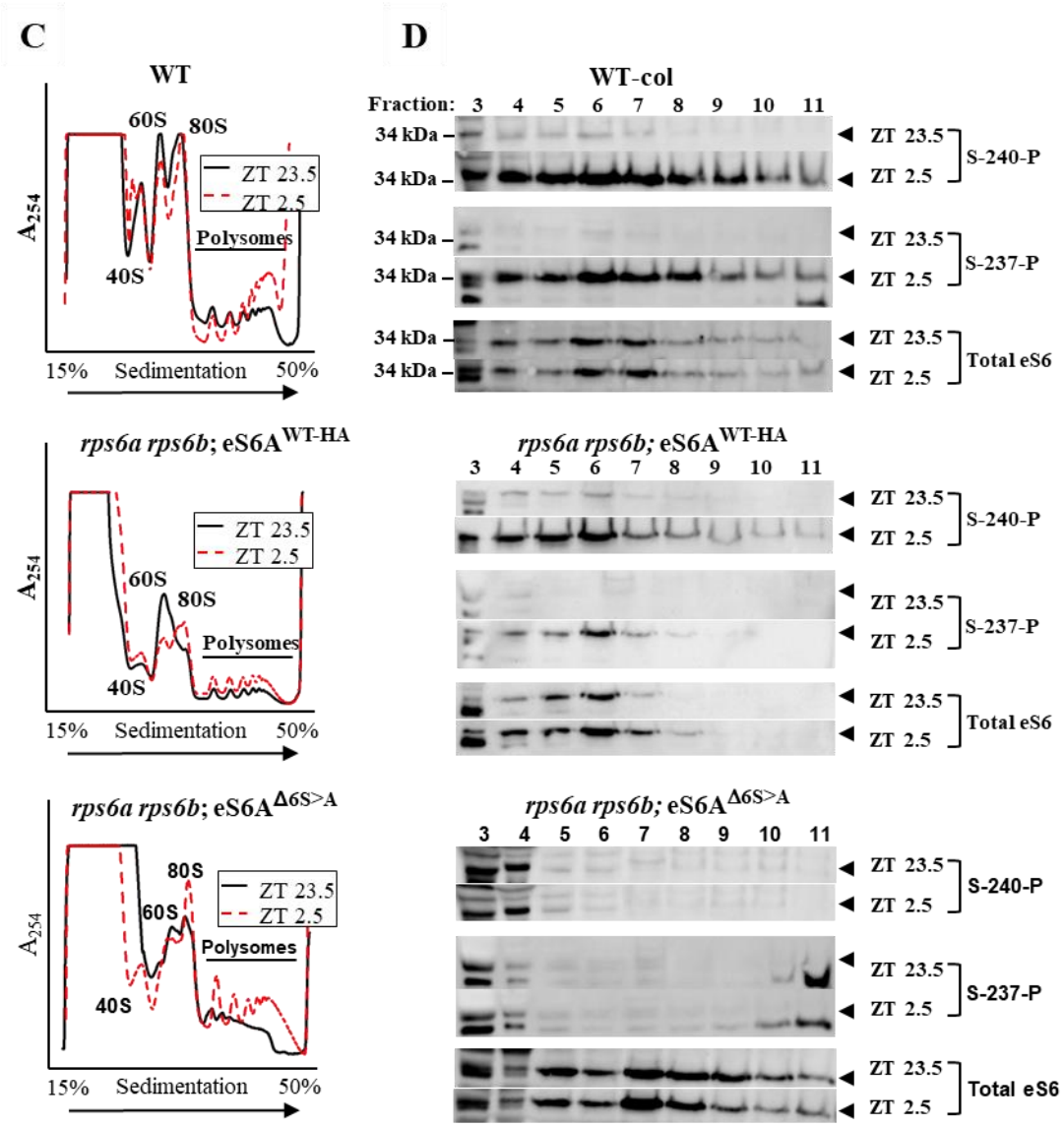

Figure 2.7 continued

A

***rps6a rps6b* background**

Genotype	Sampling	P/(NP+P)	Ratio to ZT23.5	t-test to ZT23.5	N
Col WT	ZT23.5	0.324 ± 0.072			8
	ZT2.5	0.539 ± 0.071	1.67	***	11
rps6a rps6b	lethal	NA	NA		
6B WT	ZT23.5	0.340 ± 0.020			2
	ZT2.5	0.630 ± 0.002	1.85		2
6B 3SD	ZT23.5	0.385 ± 0.001			2
	ZT2.5	0.630 ± 0.005	1.64		2

***, P<0.001

***rps6a rps6b* background**

Sampling	Genotype	60S/(NP+P)	Ratio to WT	t-test w WT	N
ZT23.5	Col WT	0.188 ± 0.026	1.00		8
	rps6a rps6b	lethal	NA		
	6B	0.161 ± 0.002	0.86		2
	6B 3SD	0.159 ± 0.001	0.85		2
ZT2.5	Col WT	0.129 ± 0.040	1.00		11
	rps6a rps6b	lethal	NA		
	6B	0.088 ± 0.008	0.69		2
	6B 3SD	0.124 ± 0.001	0.96		2

(average ± stdev)

B

***rps6a rps6b* background**

Genotype	Sampling	P/(NP+P)	Ratio to ZT23.5	t-test to ZT23.5	N
Col WT	ZT23.5	0.182 ± 0.009			3
	ZT2.5	0.269 ± 0.052	1.48	N.S	3
rps6a rps6b	lethal	NA	NA		
6A HA	ZT23.5	0.190 ± 0.014			4
	ZT2.5	0.272 ± 0.026	1.44	**	4
6A 6SA	ZT23.5	0.178 ± 0.068			4
	ZT2.5	0.239 ± 0.050	1.34	N.S	5

**, P<0.01

***rps6a rps6b* background**

Sampling	Genotype	60S/(NP+P)	Ratio to WT	t-test w WT	N
ZT23.5	Col WT	0.345 ± 0.100	1.00	N.S	3
	rps6a rps6b	lethal	NA		
	6A HA	0.326 ± 0.040	0.94	N.S	4
	6A 6SA	0.354 ± 0.040	1.02	N.S	4
ZT2.5	Col WT	0.320 ± 0.111	1.00	N.S	3
	rps6a rps6b	lethal	NA		
	6A HA	0.228 ± 0.045	0.71	N.S	4
	6A 6SA	0.313 ± 0.081	0.98	N.S	5

(average ± stdev)

Figure 2.8: Phosphodeficiency of eS6A has minor effects on global polysome loading.

Summary of polysome profiles of *rps6a rps6b* double mutants complemented with various P-enabled and P-deficient eS6 isoforms. N indicates the number of replicate gradients. The first table in A and B presents the fraction of RNA in polysomes P/(NP+P), focusing on the dark-to-light shift. The second table shows quantification of the relative fraction of RNA in the 60S subunit. t-test results are shown for experiments at least 3 biological replicates. (A) Complementation of double mutants with alleles of eS6B. The data for WT are from Supplemental Fig. 5C. (B) Complementation of double mutants with alleles of eS6A. In the 6A 6SA line all eS6 is phosphodeficient.

2.5.2 New phenotypes of ribosomal protein mutants

Our analysis discovered several new phenotypes of *rps6* mutants. The two cotyledons of *rps6* mutants often differ in size. The pale green color of the seedlings and rosette-stage plants is accompanied by reduced quantum efficiency of photosystem II (QY_{max}), an effect exacerbated at cooler temperature. Consistent with the QY_{max} data the detrimental effects of cytosolic ribosomal protein mutations on the chloroplast were also evident at the level of the transcriptomic and proteomic level, with defects in gene expression of many photosynthetic genes (Urquidi Camacho, 2023). Interestingly, in *rps6a* the photosynthesis functions were more strongly affected than in *rps6b*, while in *rps6b* the cytosolic translation functions were more strongly upregulated than in *rps6a*. Because transgenes of eS6A that use the *RPS6A* promoter complemented both the photosynthesis and translation functions well, we suspect that the difference in phenotype is not due to differences in the amino acid sequences of eS6A and eS6B. Instead, this difference could arise if eS6B had a shifted spatial expression pattern, biased towards growing cells, which produce more ribosomes, rather than cells fated to become mesophyll, which produce the photosynthetic apparatus.

This project also produced the first proteomics data for plant ribosomal protein mutants (Urquidi Camacho, 2023). Proteomic analyses largely echo the defect in photosynthesis functions and an upregulation of ribosomal proteins and ribosome biogenesis proteins in both *rps6a* and *rps6b*, consistent with the transcriptome data. In each mutant the other paralog is upregulated, together with many other ribosomal proteins. Together, these results suggest the mutants' growth is rate limited by production of *rps6*

mRNA. In the *rps6b* mutant it takes arguably twice as long to accumulate enough *RPS6* mRNA per cell than in wild type. Hence the mutants grow more slowly. Meanwhile, they accumulate excess mRNAs for other ribosomal proteins, whose gene dosage is normal, and which over accumulate as a result. Ribosome biogenesis proteins are expressed at a higher level as well, perhaps driven by the excess of yet to be assembled ribosomal proteins.

2.5.3 eS6A and eS6B paralogs are functionally equivalent

This project enabled us to look for evidence that the A and B paralogs of eS6 have different functions. In short, our data suggest that the two paralogs are functionally equivalent. First, the eS6B paralog was able to complement the *rps6a* mutant phenotype as well as the eS6A paralog, with respect to root growth and general appearance, as observed earlier (Creff *et al.*, 2010, Ren *et al.*, 2012). Second, the double mutant *rps6a rps6b* was complemented effectively by $eS6A^{WT\text{-}HA}$, a hemagglutinin-tagged wild-type version of eS6A, as well as a wild-type version of eS6B. Even though both wild-type alleles were absent, both eS6A and eS6B were able to complement essentially completely and equally. The phenotypic rescue was evident at the biochemical level (polysome profiles and loading), photosynthetic efficiency, root growth, and other developmental phenotypes.

2.5.4 Phospho-deficient eS6 performs many functions of the wild-type eS6

Light, sucrose and auxin can boost translation. These signals also boost TOR activity, which then causes phosphorylation of eS6 in its C-terminal tail. This has led to the hypothesis that eS6-P is causally involved in mediating these effects on translation. However, evidence for this idea has been mostly correlative (Boex-Fontvieille *et al.*, 2013,

Chen *et al.*, 2018, Dobrenel *et al.*, 2016b). For example, eS6-P is accompanied by increased expression of plastid ribosomal proteins (Dobrenel *et al.*, 2016b) and by increased polysome loading in the cytosol (Chen *et al.*, 2018, Liu *et al.*, 2012); however, our data indicate that eS6-P-deficient plants express chloroplast ribosomal proteins about normally, and can boost polysome loading in the morning as effectively as wild type. Recently, Mancera-Martinez *et al.* addressed this question by manipulating the phosphorylation potential of eS6 by expressing ΔS>A and ΔS>D versions of eS6B from a cauliflower mosaic virus 35S promoter in *rps6a* single-mutant plants. Similar to our data, the two versions did not differ in global polysome loading. However, the two versions differed in the translation of two reinitiation-dependent reporter mRNAs, suggesting that eS6 phosphorylation may regulate the translation of specific mRNAs (Mancera-Martínez *et al.*, 2021).

To reveal the role of eS6 phosphorylation we compared the biochemical, molecular, cellular, and organ-level phenotypes of *rps6* double mutants complemented with either a phosphorylation-enabled allele (WT-HA) or a phosphorylation-deficient allele (Δ6S>A). This is the first study to examine P-deficient alleles in a genetic background mutated for both *RPS6* paralogs. It is also the first to compare the P-deficient eS6 against the wild type, rather than P-deficient against P-mimic (Mancera-Martínez *et al.*, 2021). We chose the eS6A paralog, rather than both eS6A and eS6B for simplicity. This was a reasonable choice because eS6A and eS6B were confirmed to be functionally equivalent. We constructed the phospho-deficient allele as close to the native version as possible. Aside from keeping its

native promoter, untranslated regions, and exon-intron structure, we left it untagged in order to not introduce confounding features. We did tag the corresponding wild type eS6A with HA to be able to distinguish it from the native version, but our data suggest that this did not compromise its function in a major way. As described in results, a series of phospho-deficient versions of eS6A and eS6B were created and screened, anticipating that this would allow us to define the minimal changes necessary for a robust phenotype. In the end, a version with six codons altered to alanine revealed only rather subtle phenotypes, and therefore we did not pursue the versions with fewer changes in detail.

Overall, the phospho-deficient eS6A proved to be largely functional, given that it reverted the lethal phenotypes of the *rps6a rps6b* double mutant back to normal. In detail, polysome loading was normal, including the boost in polysome loading during the daily dark-to-light transition. And while *rps6* single mutants had an excess of the 60S subunit (Dasgupta *et al.*, 2023), the phospho-deficient double mutants reverted back to normal. The phospho-deficient eS6A also partitioned to cellular compartments, nucleus, nucleolus, and cytosol, similar to wild type. And it rescued most gene expression defects commonly seen in *rps6a* and *rps6b* mutants (Urquidi Camacho, 2023), as well as misregulation of protein levels in translation and photosynthesis. Accordingly, photosynthetic efficiency was mostly back to wild-type levels.

The conclusion derived here is not solely based on the *rps6a rps6b* double mutants. Even in *rps6a* single mutants, the presence of a phospho-deficient eS6A suppressed the phosphorylation of the eS6B paralog, yet rescued the polysome profiles of *rps6a* and

allowed for normal growth (Dasgupta *et al.*, 2023). Although the mechanism for this coordinated loss of phosphorylation is not understood, this result bolsters the conclusion that phospho-deficient eS6 is largely functional, and ribosomes lacking eS6 phosphorylation are functional as well.

2.5.5 Emerging roles of eS6 phosphorylation

Detailed analysis of the phospho-deficient plants did, however, reveal several notable abnormalities and deficiencies. The YFP-tagged eS6A$^{\Delta 7S>A}$ tended to aggregate a bit more readily in the nucleus than did the wild-type version. In the transcriptome analysis, certain defects in the mitotic cell cycle functions and responses to phosphate starvation, which are characteristic of *rps6* mutants, failed to get fully rescued by the phospho-deficient Δ6S>A allele, although they were rescued by the phospho-enabled WT-HA allele (Urquidi Camacho, 2023). The pointed-leaf phenotype suggested that leaf expansion was slightly delayed, as was the rate of root elongation, a sensitive indicator of cell division. At the proteome level, certain misregulations of ribosome biogenesis proteins also failed to get fully rescued (Urquidi Camacho, 2023). In this context it is notable that eS6 functions as part of the small subunit processome in ribosome biogenesis (Bernstein & Baserga, 2004). The increase in ribosomal proteins and the excess free 60S subunit seen in our *rps6* mutants mirror similar increases in yeast and mammalian ribosomal protein mutants (Pachler *et al.*, 2004, Robledo *et al.*, 2008).

Together, these results are our best indicator as to the cellular function of eS6-phosphorylation in Arabidopsis. The phospho-deficient plants had morphological defects as seedlings, cotyledon asymmetry and pointed leaves. Although these phenotypes were not as severe as in the original *rps6* mutants (Dasgupta *et al.*, 2023), it is plausible that it was the misregulation of cell cycle related mRNAs and ribosome biogenesis proteins that led to the growth inhibition in cotyledons and first leaves.

It was plausible that the eS6 phospho-deficient plants would reveal a phenotype not seen in *rps6* mutants, a gain-of-function defect. Notably, few if any of the defects observed in the phospho-deficient plants look like a clear gain-of-function defect. Instead, the phenotypes in the *rps6a rps6b* eS6A$^{\Delta 6S>A}$ line are incomplete rescues of defects germane to *rps6a* mutants.

Additionally, we note that although the phospho-deficient version of eS6A was expressed at a level higher than the native eS6A (**Figure 2.7** B), it did not quite reach the two-fold increase. Our proteome data in the *rps6a rps6b* background pegged eS6A$^{\Delta 6S>A}$ at 1.6-fold the level of eS6A in wild type. Because *RPS6A* and *RPS6B* are expressed equally at the transcriptome level, the phospho-deficient plants thus have eS6 at 20% below wild type. We consider this acceptable because *rps6a* heterozygotes, whose gene dosage is 25% below wild type, do not have major phenotypes, i.e. *rps6a* and *rps6b* are recessive mutations, as is also true for other *rps* mutations (Van Lijsebettens *et al.*, 1994). I did not screen for recovery or survival phenotypes under several stress conditions. It is possible

that the P-deficient plants might reveal phenotypic defects under conditions that alter eS6-P, such as hypoxia, heat, or light and darkness.

Taken together, my data presented here along with the transcriptomics and proteomics analyses (Urquidi Camacho, 2023) and findings of Mancera-Martinez and coworkers (Mancera-Martínez *et al.*, 2021) extend what we know about the functional consequences of eS6-P to a photosynthetic organism, Arabidopsis. In each eukaryote that has been studied, yeast, the mouse, and now Arabidopsis, global translation is largely unaltered (Ruvinsky *et al.*, 2005, Yerlikaya *et al.*, 2016), although Wittenberg and coworkers reported a lower rate of translation and increased translation fidelity in eS6-P-enabled cells (Wittenberg *et al.*, 2016). Evidence for effects on mRNA-specific translation exists but is sparse (Bohlen *et al.*, 2021, Mancera-Martínez *et al.*, 2021, Puighermanal *et al.*, 2017). This is also true for effects at the transcriptome and proteome level (Yerlikaya *et al.*, 2016). Translatome defects were not examined in our study. These minimal phenotypes stand in contrast to the diverse consequences of the environmental stimuli that regulate eS6-P and the diverse phenotypic effects from inhibiting the TOR-S6 kinase pathway genetically or pharmacologically (Ahmad *et al.*, 2019, Ingargiola *et al.*, 2023, Margalha *et al.*, 2019, Ren *et al.*, 2012, Scarpin *et al.*, 2022). Yerlikaya and coworkers (Yerlikaya *et al.*, 2016) concluded conservatively that none of their phenotypes in eS6 P-deficient yeast could be firmly ascribed to the P-deficiency but were probably due to reduced eS6 protein levels. For this work in Arabidopsis, a similar conclusion is acceptable. Essentially all the phenotypes seen in eS6 phospho-deficient plants are also seen in *rps6*

mutants. They are hypomorph (loss-of-function) phenotypes rather than neomorph (gain-of function) phenotypes. It is therefore difficult to rule out that these phenotypes are due to the reduced level of the eS6A$^{\Delta 6S>A}$ protein or subtle insufficiencies in its pattern of expression, rather than its lack of phosphorylation.

CHAPTER 3: INVESTIGATING THE EFFECTS OF RIBOSOMAL PROTEIN OF THE SMALL SUBUNIT 6 PHOSPHORYLATION IN HYPOXIA INDUCED AUTOPHAGY

3.1 ABSTRACT

Autophagy is an essential process for plants to cope with various stressors. The inability of Arabidopsis autophagy mutants to endure extended periods of insufficient nitrogen and/or carbon supply, and the occurrence of untimely leaf senescence even under optimal conditions, underscores the criticality of autophagy. When sufficient nutrients are available, cells sustain a basal level of autophagy that effectively eliminates outdated and faulty cellular constituents. TOR functions as a suppressor of autophagy in yeast, animals, and plants, yet there exist circumstances where autophagy may be managed by mechanisms that are not dependent on TOR. This chapter lays out a preliminary investigation into the possibility that TOR inhibits autophagy via es6-P. The approach taken was to induce autophagy with a hypoxia treatment; and to score the degree of autophagy using live-cell staining with monodansylcadaverine, a stain for autophagic vesicles, in Arabidopsis seedlings defective for eS6 phosphorylation. I confirmed that 24h hypoxia induces autophagy under both light and dark conditions. Although there were differences in the vesicle staining pattern between phospho-defective and phospho-enabled seedlings, suggesting that eS6-P may play a role in the response, the results were complicated in several ways. For example, the assay was confounded by a high level of background staining; the *rps6* mutant had a striking phenotype with the assay used; and the presence of sucrose in the medium convoluted the effects of hypoxia. The fact that sucrose, eS6-genotype, light, and hypoxia interacted in complex and unexpected ways, eventually did not allow a firm conclusion whether eS6-P mediates the autophagy response.

3.2 INTRODUCTION

In plant cells, regulation of energy homeostasis is crucial to fine-tune growth and development. The factors that influence energy homeostasis are often environmental conditions leading to transient or persistent energy deprivation phases or shifts in developmental programs (Chen *et al.*, 2021, Qi *et al.*, 2021, Signorelli *et al.*, 2019, Sirko & Masclaux-Daubresse, 2021). Autophagy is a crucial cellular process for degrading and recycling cellular components, particularly during stressful conditions when it serves as a valuable resource for energy. Constitutive or basal autophagy occurs under favorable conditions to control the quality of cellular contents (Marshall & Vierstra, 2018, Su *et al.*, 2020a, Su *et al.*, 2020b, Yoon & Chung, 2019).

3.2.1 Autophagy and its components

Within the plant kingdom, there are three distinct types of autophagy which are micro-autophagy, macro-autophagy, and mega-autophagy. The former of these pertains to the creation of an intravacuolar vesicle via invagination of the tonoplast, in which cytosolic components are directly engulfed into the vacuole. (Sieńko *et al.*, 2020). Macro-autophagy, a widely studied process, entails the generation of autophagosomes, double-layered vesicles that can capture cytosolic substances for eventual degradation in the central vacuole. Following this, the resultant products can either be stored in the vacuole or transported to the cytosol depending on metabolic requirements. (Marshall & Vierstra, 2018). The induction of macro-autophagy is observed during stress conditions in various plant species (Chen *et al.*, 2021, Signorelli *et al.*, 2019, Sirko & Masclaux-Daubresse,

2021, Su *et al.*, 2020a). Mega-autophagy is the most extreme form of autophagy in plants, which involves disruption of the tonoplast leading to the digestion of the entire cell content, including the cell wall, and is often observed as the final step of programmed cell death, during development, pathogen attack, or prolonged stress (Hatsugai *et al.*, 2015, Marshall & Vierstra, 2018, Tyutereva *et al.*, 2022, van Doorn & Papini, 2013).

The process of autophagosome formation involves several autophagy (ATG) genes in yeasts, animals, and plants, with six core protein sets involved in autophagosome biogenesis in plants (Lai *et al.*, 2019, Nakatogawa, 2020, Soto-Burgos *et al.*, 2018). ATG8 is a crucial component in the process of autophagy, as it is responsible for both the conjugation reaction with membrane lipid phosphatidylethanolamine and the interaction with adaptor proteins to facilitate selective autophagy (Bu *et al.*, 2020, Marshall & Vierstra, 2018, Stephani & Dagdas, 2020). Numerous ATG8 orthologs in plants have been discovered for binding with ATG8-interacting proteins that contain the ATG8-interacting motif (AIM) or ubiquitin-interacting motif (UIM), and ATG8 is crucial for bulk and selective autophagy (Johansen & Lamark, 2011, Kellner *et al.*, 2017, Marshall & Vierstra, 2018, Nakatogawa, 2020, Noda *et al.*, 2010, Seo *et al.*, 2016).

3.2.2 Regulation of autophagy

The TOR protein kinase complex is a key regulator of autophagy, inhibiting autophagy while promoting growth. In plants, autophagy is activated by repressing TOR activity during nutrient deficiency, salt stress, and osmotic stress, but not during oxidative stress or ER stress, where TOR is not involved (Biever *et al.*, 2015, Dobrenel *et al.*, 2016a, Liu *et*

al., 2009, Pu *et al.*, 2017). The relationship between TOR and autophagy in Arabidopsis is influenced by nutrient availability, as demonstrated by the low binding capacity of highly phosphorylated ATG13 for ATG1, which maintains basal autophagy levels under normal conditions, while TOR has no effect on autophagy activation by oxidative or ER stress. However, there is ongoing debate as to whether the assembly of the ATG1-ATG13 complex is regulated by nutrient availability (Pu *et al.*, 2017). .Arabidopsis SnRK1 is a complex composed of catalytic α subunit and regulatory β and γ subunits that inhibits TOR activity in yeast and mammals as its homolog SNF1/AMPK (Smeekens *et al.*, 2010). The SnRK subunits in Arabidopsis consist of three isoforms of the α-subunit, three isoforms of the β-subunit, and one isoform of the βγ-subunit (Martínez-Barajas & Coello, 2020, Ruiz-Gayosso *et al.*, 2018). The activation of SnRK1 proteins requires phosphorylation at specific threonine residues in the catalytic domain. SnRK1 can also autophosphorylate. Sugar phosphates such as trehalose-6-phosphate (T6P) can inhibit SnRK1 and affect TOR activity, making T6P a useful indicator of cellular metabolic status(Baena-González & Hanson, 2017, Crepin & Rolland, 2019, Lastdrager *et al.*, 2014, Nukarinen *et al.*, 2016). Under different stress conditions, mutants lacking SnRK1 inhibit autophagy while overexpression of SnRK1 promotes autophagy, specifically under abiotic stressors, and under nutrient deprivation SnRK1 promotes autophagy by phosphorylating ATG1 and RAPTOR to inhibit TOR activity (Chen *et al.*, 2017, Nukarinen *et al.*, 2016). These results suggested that nutrient deficiency-, salt- and osmotic stress-induced autophagy is both SnRK1 and TOR-dependent.

3.2.3 Hypoxia, ROS and autophagy

Autophagy is necessary for regulating the plant response to hypoxia during submergence in Arabidopsis, as demonstrated by the accumulation of MDC-stained autophagosomes in wild-type plants and a decrease in *atg* mutants (Chen *et al.*, 2015, Guan *et al.*, 2019). The Arabidopsis response to hypoxia entails a decrease in expensive translation (Branco-Price *et al.*, 2008, Branco-Price *et al.*, 2005). Under conditions of hypoxia, both animals and plants have been observed to exhibit autophagy (Chen *et al.*, 2015, Guan *et al.*, 2019, Mazure & Pouysségur, 2010). In particular, plants exposed to submergence or low oxygen levels have been found to experience a significant increase in ROS levels, which in turn leads to the induction of autophagy (Chen *et al.*, 2015, Guan *et al.*, 2019). Furthermore, it has been observed that prolonged hypoxia can result in Arabidopsis *atg* mutants displaying heightened levels of ROS and programmed cell death, compared to wild-type plants, thereby indicating their heightened sensitivity to submergence. These mutants also exhibit an increase in hypoxia responsive gene (HRG) expression (Chen *et al.*, 2015). Abiotic and biotic stressors can lead to an increase in reactive oxygen generation, which can cause damage to organelles and biomolecules, but mitochondrial ROS can act in retrograde signaling to modify energy management during oxygen deprivation in yeast, mammalian cells, and plants (Guzy *et al.*, 2007, Hamanaka *et al.*, 2016). It has been observed that plants experience a burst of mitochondrial ROS when oxygen levels drop (Chang *et al.*, 2012), and a plasma membrane-localized burst via calcium-dependent NADPH oxidases (Schmidt *et al.*, 2018b); however, it is still unclear how these signals are specific to low oxygen

availability. Arabidopsis has 10 NADPH oxidases, three of which have been linked to low-oxygen responses (Bellemer *et al.*, 2010, Lin *et al.*, 2017, Liu *et al.*, 2017). Autophagy aids the antioxidant system by eliminating damaged organelles that could otherwise generate ROS, while the conventional antioxidant system consists of superoxide dismutase isoforms, catalases, and peroxidases, and the non-canonical system comprises ROS scavengers such as glutathione, ascorbate, tocopherol, and sugars (Minibayeva *et al.*, 2012). Autophagy plays multiple roles in plant responses to hypoxia, as demonstrated by the impaired autophagy and lower tolerance to submergence in *rboh* mutants, and the degradation of S-nitrosoglutathione reductase1 via the selective autophagy pathway to promote seed germination in low-oxygen environments (Chen *et al.*, 2015, Guan *et al.*, 2019, Zhan *et al.*, 2018). CML 38 (CALMODULIN-LIKE 38), classified as a core-hypoxia gene, is selectively transcribed and translated during hypoxia in Arabidopsis, and plays an essential role in hypoxia tolerance response (Lokdarshi *et al.*, 2016). Furthermore, a recent study showed that prolonged hypoxia induces autophagy to degrade stress granule-like bodies via a CML38-dependent mechanism (Field *et al.*, 2021). Taking all the evidence together, it establishes that autophagy is required for regulation of the response to hypoxia tolerance and survival in Arabidopsis.

3.2.4 Mechanisms of oxygen sensing

Oxygen is essential for the survival of aerobic organisms. In both animals and plants, cells respond to a lack of oxygen through various survival strategies, such as autophagy in animals and gene regulation and morphological adaptive responses in plants (Branco-Price

et al., 2008, Kroemer *et al.*, 2010, Loreti *et al.*, 2016). Hypoxia is characterized by a reduction of oxygen level that constraints aerobic respiration (usually between 1% and 5%), and anoxia occurs when oxygen is absent in the environment (Sasidharan *et al.*, 2017). Flooding events can lead to hypoxia in non-photosynthetic roots, resulting in reduced energy production. Mammals use Hypoxia Inducible Factor (HIF-1) to sense low-oxygen and induce the cell-survival response (Gibbs & Holdsworth, 2020, Mazure & Pouysségur, 2010). In mammals, under normal hypoxic conditions BH3-only proteins mediate the response, but under severe hypoxic or anoxic conditions, an HIF-independent autophagic response can be induced. This response is mediated through the AMPK-mTOR and UPR pathways and can lead to autophagic cell death due to failed adaptation. However, if glucose is provided, hypoxia-induced autophagy can occur without cell death (Azad *et al.*, 2008, Mazure & Pouysségur, 2010).

In the realm of plants, the detection of oxygen has been attributed to the group VII of the Ethylene Response Factors (ERF-VIIs). This category of transcription factors possesses a cysteine (cys) residue at their N-terminal, which is persistently oxidized in the presence of oxygen by the Plant Cysteine Oxidases (PCOs), a group of plant enzymes. The cys branch of the N-degron pathway directs the ERF-VII proteins to degradation via the proteasome. In hypoxia, however, the lack of oxygen suppresses PCOs from oxidizing the cys residue, rendering ERF-VIIs stable. Consequently, the stable ERF-VII proteins relocate to the nucleus and activate the transcription of Hypoxia-Responsive Genes (HRGs), including genes that encode proteins necessary for carbohydrate metabolism and

fermentation. Furthermore, aerobic respiration in the mitochondria decreases dramatically under hypoxia, and ATP is exclusively produced through enhanced glycolytic activity. The purpose of fermentative metabolism is to generate ATP by reusing NAD+ via the glycolytic pathway, resulting in only 2 moles of ATP production rather than the usual 36 during aerobic respiration, which is crucial for hypoxia endurance and survival (Loreti *et al.*, 2016). The presence of acyl-CoA binding protein (ACBP) serves to safeguard RAP2.12 from degradation in aerobic environments. Activation of HRG induction can be attributed to the redundancy of ERF-VII proteins RAP2.12 and RAP2.2, which is presumed to result from the collective impact of RAP2.12 synthesized de novo and RAP2.12 liberated from ACBP (Kosmacz *et al.*, 2015, Licausi *et al.*, 2011, Schmidt *et al.*, 2018a).

3.2.5 Carbohydrates and hypoxia tolerance

For efficient energy production via glycolysis coupled to fermentation under hypoxia, an adequate sugar supply is required (Cho *et al.*, 2021). In such cases, starch functions as a substantial sugar source, both in cereals and in Arabidopsis (Cho *et al.*, 2021). Although other cereals are unable to germinate under hypoxia due to their lack of production of the key enzymes required for starch degradation, rice is able to do so by utilizing α-amylases even in low oxygen conditions, which is a crucial component of its anaerobic response (Guglielminetti *et al.*, 1995, Perata *et al.*, 1997, Yu *et al.*, 2021). Although Arabidopsis and rice have different mechanisms for tolerating hypoxia, starch remains a crucial component of the anaerobic response in Arabidopsis. The expression of HRGs is stimulated and the submergence tolerance of Arabidopsis plants is augmented by exogenous sucrose or starch

reserves, which suggests that sugars have a “protective effect” on the plant's ability to endure hypoxia. The level of HRGs increases significantly at the onset of hypoxia, peaking after 12 hours, and then gradually decreasing over time. The anaerobic response at the transcriptional level is weakened by prolonged hypoxia, which regulates HRG induction intensity through a homeostatic mechanism to coordinate oxygen and sugar sensing. (Cho *et al.*, 2021, Loreti *et al.*, 2005, Loreti *et al.*, 2018).

3.2.6 TOR kinase and hypoxia

The exact mechanisms by which autophagy improves hypoxia tolerance in plants remain unclear, despite substantial evidence suggesting a favorable outcome. One such pathway that has been implicated in the process of optimal hypoxia response is the TOR kinase pathway (Kunkowska *et al.*, 2023). TOR function is necessary for effective HRG induction, which is crucial for resource conservation during long periods of low oxygen. Sucrose and glucose activate TOR through glycolysis and mitochondrial bioenergetics, as well as the pPCO1 promoter, while DCMU and oligomycin suppress photosynthesis and mitochondrial ATP generation, ultimately resulting in inhibited TOR activity and less induction of HRGs during hypoxia (Kunkowska *et al.*, 2023). Darkness, like DCMU and oligomycin, decreases TOR activity, as does hypoxia in the dark. RAP2.12 activity is dependent on active TOR for HRG production, as evidenced by trials in which darkness and hypoxia both lead to decreased TOR activity, which is necessary for HRG production. The observed reduction in HRG expression subsequent to an initial surge following a brief period of hypoxia was attributed to insufficient TOR activity as an activator of RAP2.12

by means of phosphorylation of two serine residues located within the activation domain of this transcription factor. Furthermore, the administration of treatments such as darkness, DCMU, and AZD8055 have all been found to elevate RAP2.12 nuclear localization. (Kunkowska *et al.*, 2023). However, sugar deprivation reduces the expression of HRG through decreased activity of the transcription factor RAP2.12, which is independent of known repressors and stabilizing mechanisms, and also dampens the transcriptional hypoxia response (Burkart & Brandizzi, 2021, Giuntoli *et al.*, 2014, Loreti *et al.*, 2018, Wu *et al.*, 2019).

This chapter will focus on our attempts at understanding the hypoxia induced autophagy response and its potential regulation of eS6-P as a TOR activity readout. In the context of this chapter, it is important to mention that active TOR kinase functions in part via activating S6 kinase, to phosphorylate components of the translation apparatus, such as ribosomal protein eS6. eS6-P is conserved across eukaryotes and is the common effector between plants and non-plants. Hence, eS6-P is widely regarded as a bioreporter for TOR kinase activity. In Arabidopsis, eS6-P is elevated during the day when translation is very active and is low during the night when translation is also low. eS6-P is also downregulated under various abiotic stress conditions and including hypoxia (Bailey-Serres & Freeling, 1990, Williams *et al.*, 2003). This led us to hypothesize that the phosphorylation of eS6 by TOR may be part of the mechanism whereby TOR represses autophagy, aside from TOR hyperphosphorylating ATG13. It has been previously demonstrated that extended oxygen deprivation in Arabidopsis thaliana seedlings leads to overall downregulation of global

translation, with the exception of a specific group of highly induced mRNAs (Branco-Price *et al.*, 2005). Hence, consequences at the level of translation due to hypoxia are well-understood. Since eS6-P is a ribosomal protein and linked to the master regulator TOR, we chose to study effects of eS6-P on autophagy after 24h hypoxia treatment using *rps6* knock-out mutants and the double mutant *rps6a rps6b* complemented with either phospho-enabled eS6 or phospho-deficient eS6. Monodansylcadaverine (MDC) is a frequently used fluorescent stain due to its specific ability to stain autophagosomes in both mammals and plants, making it ideal for initial stages of experiments (Bassham, 2015, Biederbick *et al.*, 1995, Contento *et al.*, 2005, Munafó & Colombo, 2001). The results presented here show that prolonged hypoxia indeed triggers autophagy (MDC vesicles) in Arabidopsis. I also show differences in the vesicle staining pattern between phospho-defective and phospho-enabled seedlings, suggesting the involvement of eS6-P in the response. However, the results were complicated to draw firm conclusions. Therefore, my observations here provide preliminary evidence on the role of eS6-P in the regulation of autophagy. But further investigation is necessary to understand the specific role of eS6-P and its contribution to autophagy regulation.

3.3 MATERIALS AND METHODS

3.3.1 Plant Growth Conditions

Arabidopsis (Arabidopsis thaliana) ecotype Columbia-0, *rps6a*, *rps6a rps6b*; eS6A$^{\Delta 6S>A}$ and *rps6a rps6b* ;eS6A^{WT-HA} seeds were sterilized and stratified at 4°C for 2 d followed by their germination on half strength Murashige and Skoog (MS) salt plant medium (MP

Biomedicals) solidified with 0.65% Phytoagar (Bioworld). They were grown vertically under a long-day cycle of 16 h white light /8 h dark at 22°C and 50% humidity. Seedlings were grown on medium without sucrose for experiments that doesn't state otherwise. 1% sucrose was used for experiments that indicate presence of exogenous sucrose.

3.3.2 Hypoxia Treatment Protocol

Hypoxia was administered to 10-day-old Arabidopsis seedlings grown vertically on Murashige and Skoog agar medium, by replacing the air supply with nitrogen gas, and time of hypoxia was initiated at 2% or less oxygen. The dissolved oxygen concentration was monitored with an oxygen monitor (YSI model 55). For dark normoxia, plates with seedlings were placed in a box in the incubator under regular growth conditions. For dark hypoxia the plates with seedlings were placed in a box inside the hypoxia chamber.

3.3.3 MDC staining, imaging and image analysis

Seedlings were stained by immersion in 0.05mM MDC in Phosphate buffered saline (PBS) for 10 mins, followed by two PBS washes. All samples were kept in the dark while staining. Fluorescence was detected, with an excitation wavelength of 335nm and an emission wavelength of 508nm. MDC-stained Arabidopsis seedling root transition zones were imaged using Zeiss AxioObserver Z1 microscope with a DAPI-specific filter.

For particle quantitation images of single optical sections of root epidermal cells were analyzed in ImageJ using the built-in Particle Counter program (Schneider *et al.*, 2012). Data were collected from between 50-90 cells per genotype, per condition and per

replicate. Data represents three independent biological blinded experiments. Particles smaller than $0.1\mu m^2$ and larger than $10\mu m^2$ were excluded. Statistical analysis was done in GraphPad Prism. Violin plots of data were generated by using the "show all points" option in Prism with each plot containing bars indicating the median, and the first and third quartile values.

3.4 RESULTS

3.4.1 Hypoxia upregulates MDC-stained foci in WT-col as compared to normoxia

MDC is a viable alternative for fast analysis of living tissue without the need for autophagy biomarker expressing transgenic plants, owing to its accumulation within acidic lumen membrane compartments and subsequent fluorescence. Because MDC stains later stages of autophagosome maturation, we chose to use 24-hour hypoxia treatments (Le Bars *et al.*, 2014). We sought to test the induction of MDC-stained autophagosomes after treating seedlings with sustained hypoxia under supplemental lighting. Compared to the basal level of MDC vesicles during normoxia in WT seedlings, the number of MDC vesicles in the hypoxia treated seedlings showed a significant increase (**Figure 3.1)**.

3.4.2 The rps6a single mutant displays a non-canonical response to hypoxia.

To investigate the role of eS6-P in hypoxia induced autophagy, we treated the *rps6a* single mutant with sustained hypoxia. The basal levels of MDC-vesicles in both genotypes were found to be comparable. However, the autophagosome (MDC vesicles) induction seen in WT seedlings upon hypoxia treatment was absent in the *rps6a* mutant (**Figure 3.2**).

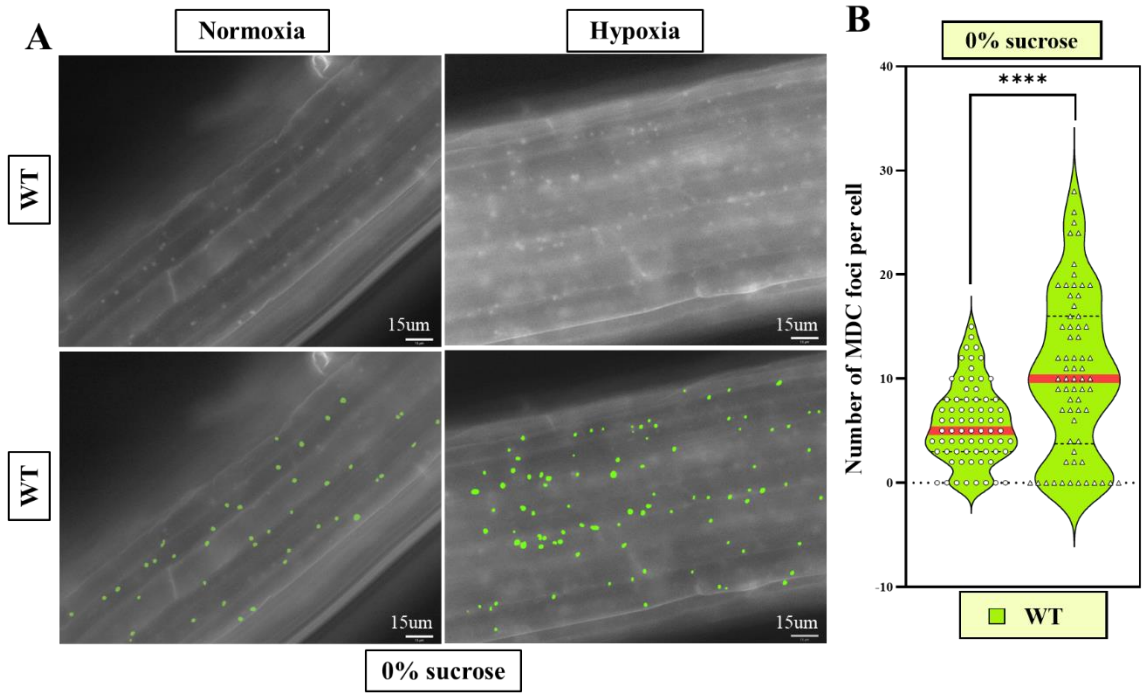

Figure 3.1: Hypoxia upregulates MDC-vesicles in WT-col as compared to normoxia.

(A) Vertically grown 10-day old seedlings of WT-col were used in this experiment. A set of these seedlings were kept in the incubator for normoxia while the other set was treated with hypoxia for 24h in light. Please note that the contrast on these pictures is hard to adjust well, so MDC-stained foci were manually highlighted with green for easier viewing. The figure shows one representative micrographs per condition. **(B)** Quantified results show a significant induction of autophagosomes (MDC vesicles). **** indicates $p<0.001$ by Mann-Whitney test.

Although MDC may be staining vesicles other than just autophagosomes, the complete absence of MDC vesicles in many *rps6a* cells under hypoxia cannot be explained by just a loss of these 'other' vesicles but suggests that autophagosomes and by implication autophagy are reduced in *rps6a*. Thus, *rps6a* mutants may have a higher threshold for autophagy than WT. However, we have not ruled out the possibility that the vesicles in *rps6a* are present but recalcitrant to staining because of a higher pH.

3.4.3 Autophagy induction upon hypoxia treatment seen in WT can also be seen in the rps6a rps6b double mutants complemented with eS6A$^{\Delta 6S>A}$ and eS6A$^{WT\text{-}HA}$.

To investigate whether of eS6-P contributes to hypoxia-induced autophagy, we extended the experiment to include *rps6a rps6b* double mutants complemented with phospho-enabled eS6A;eS6A$^{WT\text{-}HA}$ (P-enabled transgenics) or with phospho-defective eS6A;eS6A$^{\Delta 6S>A}$ (P-deficient transgenics). The 24h hypoxia treatment started and ended during the daily light period, because plants show higher TOR activity as evidenced by eS6-P under light conditions (Dobrenel et al., 2016b, Enganti et al., 2018), and translation is upregulated after the dark-to-light transition. We hypothesized that eS6 phosphorylation is involved in TOR mediated inhibition of autophagy. If TOR was relaying signals to inhibit autophagy, then the P-deficient plants might display an increase in autophagosomes (MDC vesicles), especially under normoxia, and perhaps under hypoxia as well. The double mutants showed a significant induction of autophagosomes (MDC vesicles) similar to the WT seedlings under hypoxia (**Figure 3.1**). Their induction of MDC-vesicles was independent of the status of eS6-P. Therefore, under these conditions any TOR-mediated

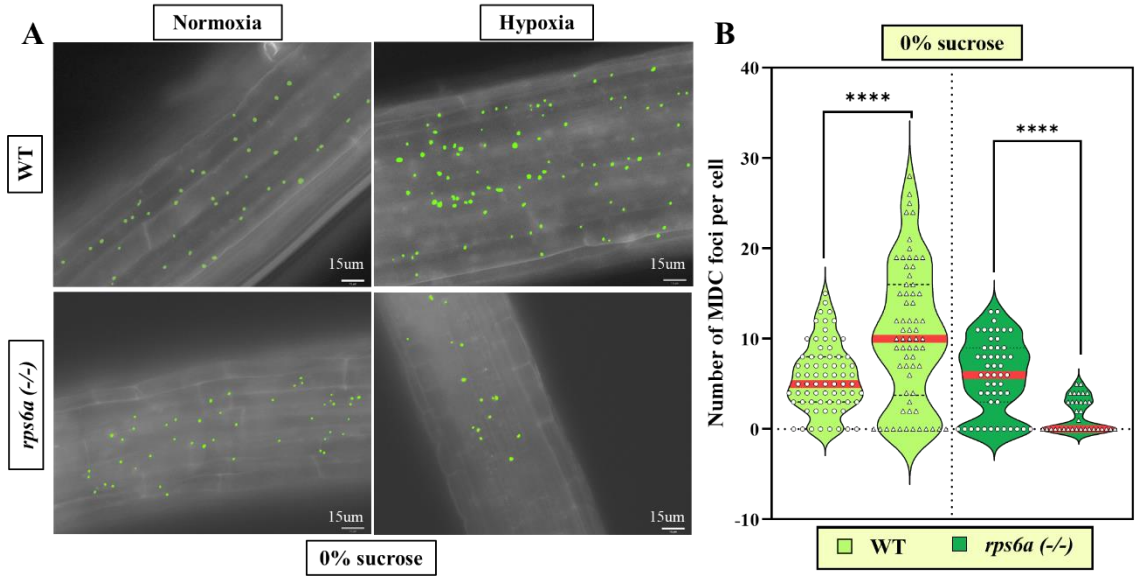

Figure 3.2: The *rps6a* single mutant displays a non-canonical response to hypoxia.

(A) Vertically grown 10-day old seedlings of WT-col and *rps6a* were treated with hypoxia or mock-treated as in Fig.3.1. The WT data are replicated from Fig. I-i (B) Quantification of results shows a significant induction of autophagosomes (MDC vesicles) only in the WT. **** indicates $p<0.001$ by Mann-Whitney test.

inhibition of autophagy does not require eS6 phosphorylation.

If TOR was relaying the inhibition of autophagy via eS6-P, then the P-deficient transgenics would have excess autophagosomes especially under normoxia and would not display a strong induction of autophagosomes (MDC vesicles) in response to hypoxia. The results showed that the P-enabled transgenics ($eS6A^{WT\text{-}HA}$) and the P-defective transgenics ($eS6A^{\Delta 6S>A}$) upregulate autophagosome (MDC vesicles) formation just like WT (**Figure 3.3**). Hence, the upregulation of autophagosomes (MDC vesicles) under hypoxia is likely following a pathway that is eS6-P independent.

3.4.4 Hypoxia treatment in presence of sucrose reveals a phenotypic difference between double mutants complemented with $eS6A^{\Delta 6S>A}$ and $eS6A^{WT\text{-}HA}$

The experiments so far have been conducted in the absence of sucrose in the medium. To evaluate our hypothesis that TOR suppresses autophagy under hypoxia via eS6-P, we repeated the hypoxia treatment in the presence of 1% sucrose, because sucrose is expected to boost TOR activity. For example, the diel cycles of eS6-P are disrupted by 3% sucrose (Enganti et al., 2018) possibly due to over-active TOR. Therefore, one might expect that any role for TOR-mediated eS6-P in hypoxia-induced autophagy might be highlighted. Specifically, autophagosomes might be reduced in an eS6-P dependent manner (with or without hypoxia, but specifically with hypoxia). This experiment indeed showed a difference between WT or P-enabled transgenics ($eS6A^{WT\text{-}HA}$) and P-defective transgenics ($eS6A^{\Delta 6S>A}$) (Figure 3.4). The robust induction of autophagosomes that had been seen after 24h hypoxia in the absence of sucrose was no longer visible when sucrose was present,

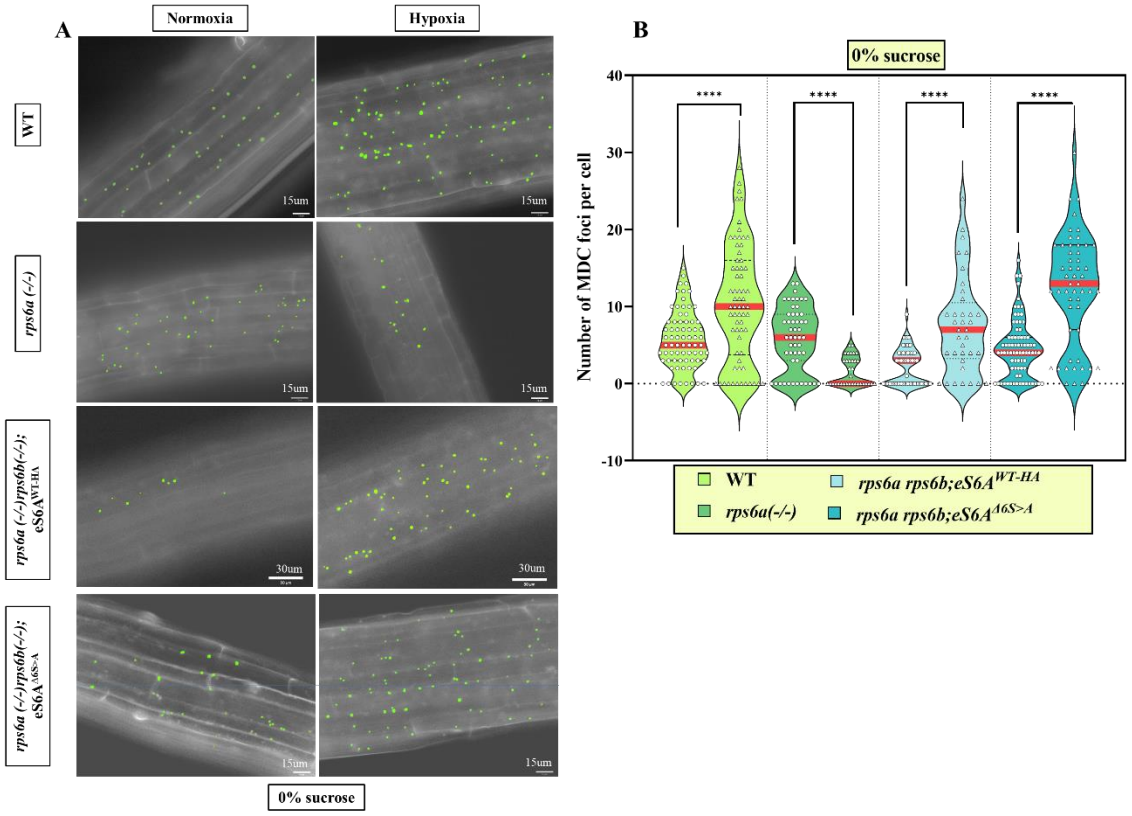

Figure 3.3: Autophagy induction upon hypoxia treatment seen in WT can also be seen in the *rps6a rps6b* double mutants complemented with eS6A$^{\Delta 6S>A}$ and eS6A^{WT-HA} .

(A) Vertically grown 10-day old seedlings of Wt-col, *rps6a*, *rps6a rps6b* double mutant complemented with phospho-enabled eS6A (eS6A^{WT-HA}) or with phospho-defective eS6A (eS6A$^{\Delta 6S>A}$)were used in this experiment. A set of these seedlings were kept in the inclubator for normoxia while the other set was treated with hypoxia for 24h. **(B)** Quantified results show a significant induction of autophagosomes. **** indicates $p<0.001$ by Mann-Whitney test.

Interestingly, the behavior of the P-defective transgenics (eS6A$^{\Delta 6S>A}$) remained unchanged in absence or presence of sucrose (**Figure 3.4**). Very surprisingly, however, in the *rps6a* mutant, where hypoxia had previously suppressed the autophagosomes (MDC vesicles), now, in the presence of sucrose, we could see a significant induction of autophagosomes (MDC vesicles) (**Figure 3.4**).

At face value these data formally show a difference between P-enabled and P-deficient plants and therefore are consistent with our hypothesis that eS6-P suppresses autophagosomes and, by inference, that TOR suppresses autophagy via eS6-P. However, this difference arose in the context of three surprising results that did not match what our hypothesis predicted: first, under normoxia, MDC vesicles were not reduced by sucrose (compare **Figure 3.3** B and **Figure 3.4** B) and may even be increased throughout. Second, with sucrose, hypoxia did not simply fail to boost the number of MDC vesicles, but it clearly reduced them, at least in the WT and P-enabled transgenics. Third, with sucrose, *rps6a* now showed the standard increase in MDC vesicles under hypoxia, different from before. These observations contradict our assumptions that (a) sucrose-stimulated TOR represses autophagy, and (b) hypoxia increases autophagy by inactivating TOR. Sucrose caused a lot of changes that cannot be explained under the assumptions. Alternatively, it is also possible that sucrose may have several effects that are not accounted for in our simplistic model.

3.4.5 Hypoxia treatment in dark maintains a similar pattern of formation of MDC vesicles to hypoxia treatment done in light.

Ribosome loading significantly increases for a substantial portion of the transcriptome during the transition of dark-grown Arabidopsis seedlings to light, while the reverse transition leads to the translational repression of multiple mRNAs (Bailey-Serres *et al.*, 2012, Juntawong *et al.,* 2014). Our lab has previously shown that eS6-P is dependent on light because the phosphorylation is dramatically reduced in continuous darkness and the diel cycling of the phosphorylation is no longer seen in continuous darkness (Enganti et al., 2018).

According to the previous results in this chapter under light conditions, the boost in autophagosomes by hypoxia was independent of eS6-P. Hence, we decided to next test their behavior under 24h hypoxia in darkness. If TOR works through eS6-P to suppress autophagy, then one expects that autophagosomes would generally be more numerous in darkness and any effect of eS6-P would be abolished, because TOR is inactive. Darkness was established by placing the seedlings in a box. The box was either kept in the incubator for normoxia or placed in the hypoxia chamber for 24h for hypoxia. The dark treatment was “unanticipated darkness”, out of phase with the diel LD cycle, starting around ZT5.

As shown in **Figure 3.5**, in darkness the pattern of autophagosome induction after 24h hypoxia remained approximately the same as in light. Thus, although the hypoxic response occurs in darkness, and TOR activity is generally reduced by 24h of darkness as shown by eS6-P (Enganti et al., 2018), the MDC vesicles formed to an approximately similar extent

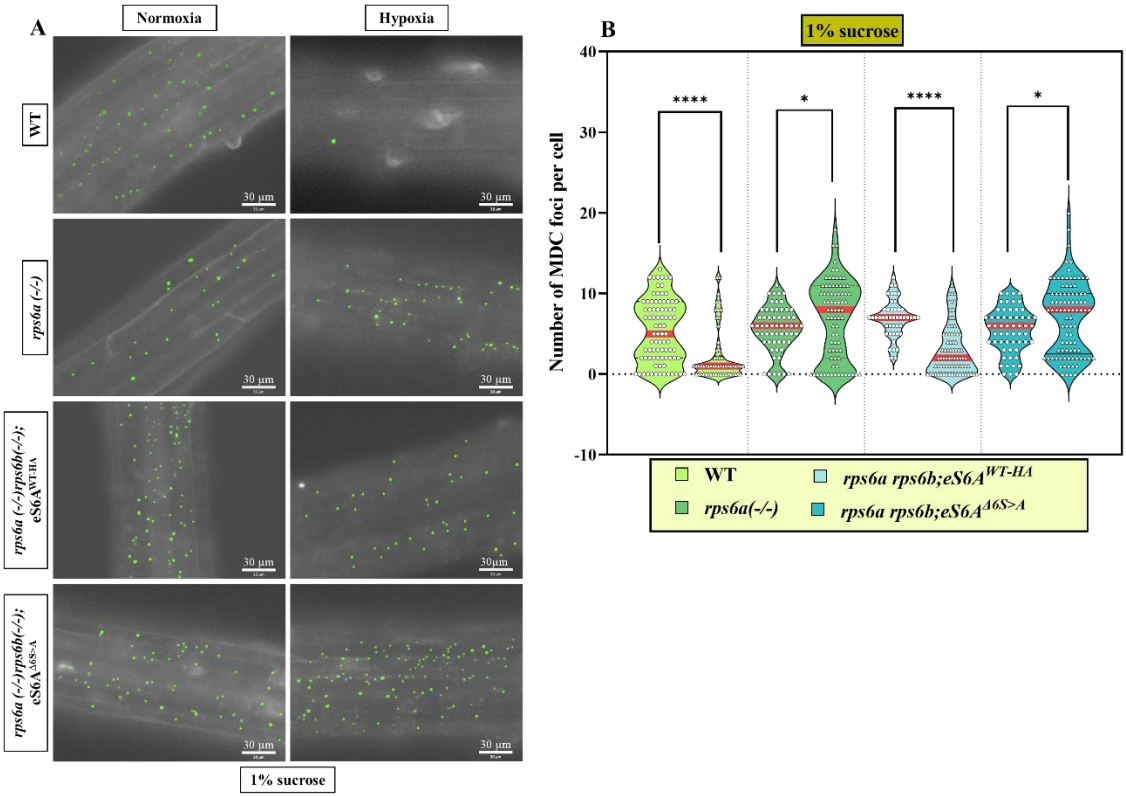

Figure 3.4: Hypoxia treatment in presence of sucrose reveal a phenotypic difference between double mutants complemented with eS6A$^{\Delta 6S>A}$ and eS6A$^{WT\text{-}HA}$.

(A) Vertically grown in presence of 1% sucrose, 10-day old seedlings of Wt-col, *rps6a*, *rps6a rps6b* double mutant complemented with phospho-enabled eS6A (eS6A$^{WT\text{-}HA}$) or with phospho-defective eS6A (eS6A$^{\Delta 6S>A}$) were used in this experiment. A set of these seedlings were kept in the incubator for normoxia while the other set was treated with hypoxia for 24h. **(B)** Quantified results show a significant induction of autophagosomes. **** indicates $p<0.001$ and * indicates $p<0.05$ by Mann-Whitney test.

in darkness as in the light. This indicates that the autophagosome (MDC vesicle) formation is buffered against the level of TOR activity. In addition, there was again no clear role for eS6-P in autophagosome (MDC vesicle) formation. The *rps6a* mutant also reproduced its unconventional response. Its behavior may be attributed to its struggle with ribosome biogenesis, or the numerous indirect consequences from this that were amply documented earlier at the transcriptome and proteome level (Chapter 2) (Dasgupta *et al.*, 2023).

Dark induced de-phosphorylation of eS6 can be seen as early as 4h despite having exogenous sucrose in the medium (Enganti et al., 2018). Keeping that in mind, we decided to repeat the hypoxia treatment in darkness but in presence of 1% sucrose. The experiment reproduced some of the results seen previously with sucrose in the light, including the 'standard' behavior of *rps6a* and no boost in autophagosomes (MDC vesicles) in the P-enabled transgenic, but a sharp induction of autophagosomes (MDC vesicles) in the P-defective transgenics (eS6A$^{\Delta 6S>A}$) (**Figure 3.6**). This could be explained if lack of eS6-P causes even a minor disruption in the sugar sensing and homeostasis especially during stress conditions. However, WT seedlings showed a different result; while in the light, induction of autophagosomes (MDC vesicles) was completely abolished when exogenous sucrose was present, in the dark the upregulation of autophagosomes (MDC vesicles) was visible again (**Figure 3.6**). It seems that the "protective effect" of 1% (30mM) exogenous sucrose is best seen if prolonged hypoxia is not done in dark conditions. In darkness, we may need to consider adding higher concentrations of sucrose to impart enhanced tolerance, as demonstrated by the authors of Loreti 2005 (Loreti *et al.*, 2005), where 30mM

of sucrose was barely enough to survive 6h anoxia in darkness while 90mM had a substantial protective effect. Interestingly, the "sucrose-rescued" autophagy response observed in light-grown *rps6a* did not change if hypoxia was administered in the dark (**Figure 3.6**). This is probably because the response seen in the light experiment is not majorly due to the immediate "protective effect" by exogenous sucrose. Instead, it may be due to sucrose supporting the entire early development of the *rps6a* seedlings, i.e., ribosome biogenesis, which probably prepared the *rps6a* mutants to better mitigate survival under stress.

3.5 DISCUSSION

This chapter is the result of an attempt to investigate the role eS6 phosphorylation plays in TOR mediated regulation of autophagy. Hypoxia was chosen to be the stimulus to induce autophagy given the extensive characterization of its effects on translation in Arabidopsis. Autophagy was scored using MDC stain which is a fluorescent dye enabling rapid analysis of autophagy in live tissue (Bassham, 2015, Contento *et al.*, 2005, Pu & Bassham, 2023). However, the autophagy community encourages caution when interpreting results solely using fluorescent dye staining since autophagy is sensitive to specific stress conditions. Acidotropic fluorescent dyes, are widely used for initial analysis of autophagy but are strongly recommended to be coupled with the use of specific autophagosome markers such as ATG8 to ensure accurate interpretation of results (Bassham, 2015, Pu & Bassham, 2023).

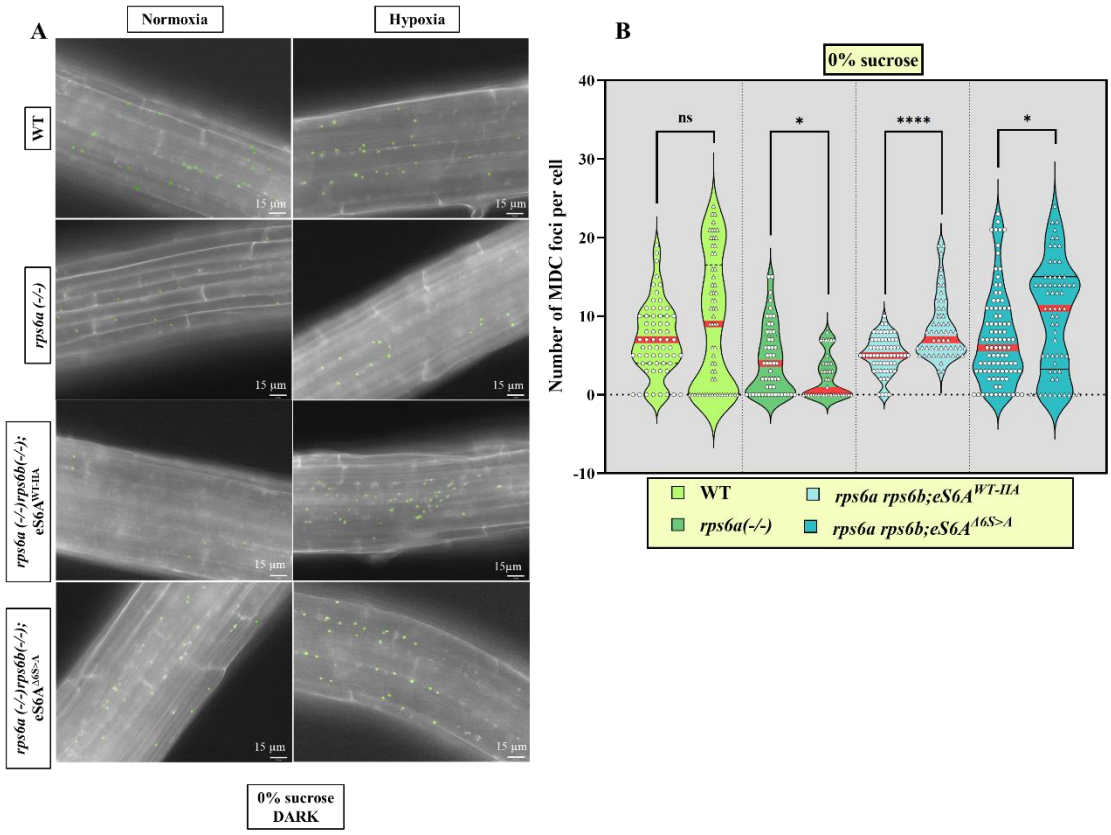

Figure 3.5: Hypoxia treatment in dark maintains similar pattern of formation of acidic vesicles to hypoxia treatment done in light.

(A) Vertically grown 10-day old seedlings of Wt-col, *rps6a*, *rps6a rps6b* double mutant complemented with phospho-enabled eS6A (eS6A^{WT-HA}) or with phospho-defective eS6A (eS6A$^{\Delta 6S>A}$) were used in this experiment. A set of these seedlings were kept in the incubator in a box for normoxia in dark while the other set was treated with hypoxia for 24h in dark. **(B)** Quantified results show a significant induction of autophagosomes (MDC vesicles). **** indicates $p<0.001$ and * indicates $p<0.05$ by Mann-Whitney test.

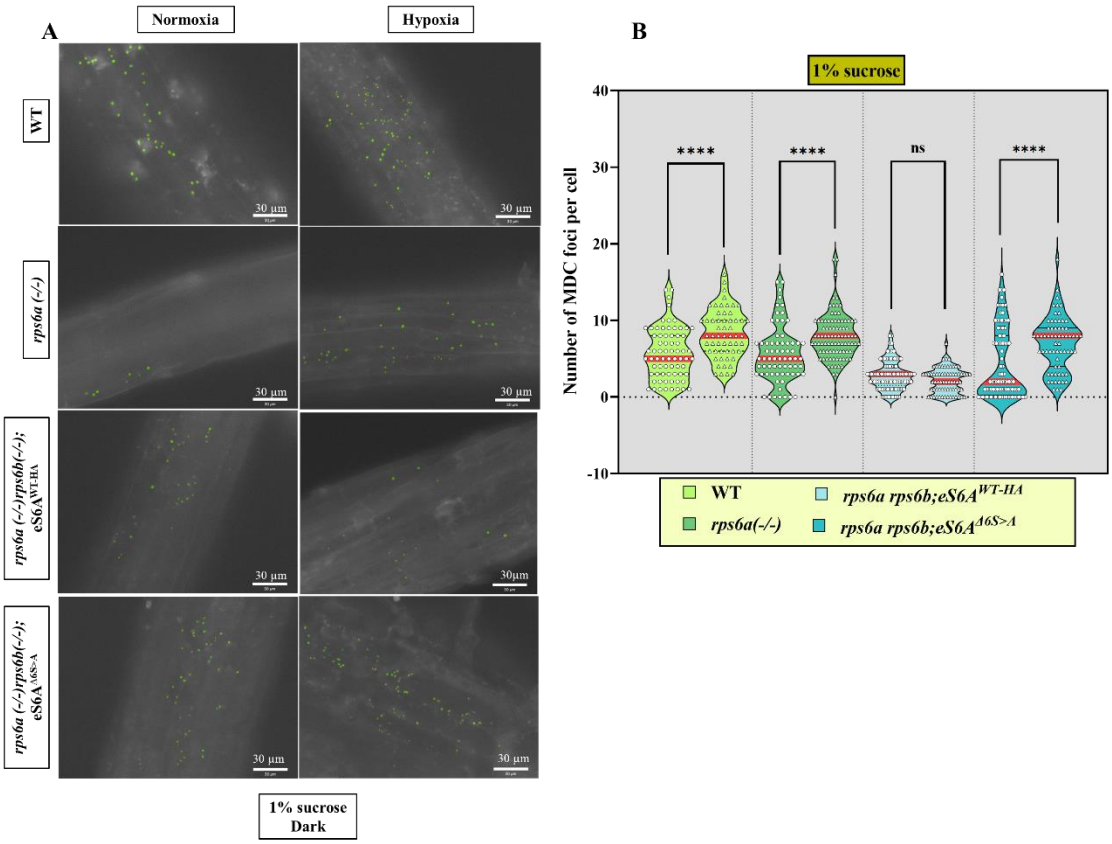

Figure 3.6: Sucrose dependent enhanced tolerance is no longer seen under hypoxia in dark.

(A)Vertically grown in presence of 1% sucrose, 10-day old seedlings of Wt-col, *rps6a*, *rps6a rps6b* double mutant complemented with phospho-enabled eS6A ($eS6A^{WT\text{-}HA}$) or with phospho-defective eS6A ($eS6A^{\Delta 6S>A}$) were used in this experiment. A set of these seedlings were kept in the incubator in a box for normoxia in dark while the other set was treated with hypoxia for 24h in dark. (B) Quantified results show a significant induction of autophagosomes (MDC vesicles). **** indicates $p<0.001$ and * indicates $p<0.05$ by Mann-Whitney test.

We find that hypoxia induces autophagy reproducibly under light and dark conditions. Interestingly, the *rps6a* single mutant fails to induce autophagosomes (MDC vesicles) in the absence of sucrose under hypoxia in light and dark, but it is rescued in the presence of sucrose. Double *rps6* mutant complemented with P-deficient eS6 showed induction of hypoxia induced autophagosomes (MDC vesicles) in every condition tested. Therefore, absence of eS6-P did show a consistent phenotype under the conditions tested here. However, to interpret this behavior in light of the direct involvement of eS6-P in TOR mediated regulation of autophagy, we need additional experiments. In summary, this preliminary study raises the intriguing possibility eS6 protein and its phosphorylation regulate autophagy. However, further investigation is necessary to clarify the interaction between eS6 paralogs and their contribution to autophagy maintenance. Moreover, the consistent upregulation of MDC vesicles in all conditions of the phospho-null mutant brings the possibility of another specific and targeted function of this event.

3.5.1 Role of eS6-P in hypoxia-induced induction of autophagosomes in absence of exogenous sucrose.

Organisms that thrive in oxygen have adapted to low oxygen levels with adaptive responses at various levels such as cellular, tissue and organism levels. Limited ATP production in hypoxia calls for an adequate supply of carbohydrates for efficient glycolysis coupled with fermentation, where alcoholic fermentation replaces mitochondrial respiration (Loreti *et al.*, 2016, Yu *et al.*, 2021). The role of starch in providing energy during prolonged hypoxia is known in cereals and Arabidopsis, but plants produce sugar catabolic enzymes only in

the presence of adequate carbohydrate reserves to generate ATP for survival-related processes (Cho *et al.*, 2021, Loreti *et al.*, 2018, Loreti *et al.*, 2016). This balance is established with the sharp increase in the expression of HRGs at the beginning of hypoxia, peak expression after 12 h, followed by a gradual decline. The observed behavior with WT, and P-enabled transgenics ($eS6A^{WT\text{-}HA}$) aligns with existing literature on sugar consumption in plants under prolonged hypoxia (Loreti *et al.*, 2018). However, the upregulation of autophagosomes (MDC vesicles) under hypoxia is likely not because of TOR-eS6-P activity. During hypoxia induced metabolic reprogramming, ATP generated is lower than aerobic respiration, which creates a large energy debt for the plant to survive the stress which possibly activates SnRK1. However, low ATP production under hypoxic conditions might render low activity of TOR. Hence it is possible that autophagy triggered by early hypoxia could be a consequence of low TOR and high SnRK1 activity. Since fermentative metabolism slows down after 12h hypoxia, the resulting carbohydrate starvation likely inactivates TOR further resulting in upregulation of autophagy. Since our experiment setup is assaying induction of autophagosomes (MDC vesicles) after 24h hypoxia, it's likely that the role of eS6-P is insignificant since TOR is expected to be inactive at that stage. However, it was still a reasonable experiment because a) the increase in MDC vesicles at 24h could reflect autophagosome formation in the early hours when TOR was still active and b) we had the light on, so there could be photosynthesis and active TOR. The role of SnRK1 in mediating autophagy during late hypoxia needs further

investigation. The lack of autophagy induction seen in *rps6a* will be explained in the next paragraphs.

3.5.2 Role of eS6-P in enhanced tolerance to hypoxia induced autophagy in presence of exogenous sucrose.

Plants experience transcriptional reprogramming during periods of sugar deprivation that is partially influenced by SnRK1 protein kinases. SnRK1 subfamily members are considered crucial in generating an optimal response to darkness and hypoxia, although HRG expression induced by sugar starvation is largely independent of SnRK1.1. Activation of SnRK1 occurs earlier than the decline in T6P under hypoxia, suggesting the potential involvement of additional factors in coordinating hypoxia response and SnRK1 activation (Baena-González *et al.*, 2007, Branco-Price *et al.*, 2008, Cho *et al.*, 2016, Loreti *et al.*, 2018, Loreti *et al.*, 2016).

24h hypoxia in presence of exogenous sucrose upregulates autophagy perhaps by active SnRK1 but inhibited by low levels TOR. The opposite actions of SnRK1 and TOR could explain the sharp decline in autophagosome (MDC vesicles) induction in WT and P-enabled transgenics ($eS6A^{WT\text{-}HA}$) after 24h hypoxia. However, the presence of exogenous sucrose has demonstrated an improvement in the capacity to endure anoxia. This is achieved by the activation of genes that facilitate the breakdown of sucrose, as well as the accumulation of HRGs. The utilization of starch and sucrose is therefore deemed necessary for an effective anoxia/hypoxia response and metabolic reprogramming (Loreti *et al.*,

2005). These results signify that an adequate level of sugar is imperative for a comprehensive reaction to hypoxia.

These findings offer a plausible explanation as to why WT and P-enabled transgenics ($eS6A^{WT\text{-}HA}$) did not display autophagy induction after 24h hypoxia in light, in presence of sucrose. The presence of exogenous sucrose likely triggered an adequate response to the stress but by 24h the plant may have switched to conserving carbohydrate reserves for recovery i.e no autophagosomes and expressing only survival related genes. However, in the same experimental conditions the *rps6a* mutant significantly induces an autophagy response in contrast to the experiment in absence of sucrose. The continuous presence of exogenous sucrose during its growth probably primed it for a stress response but was insufficient to execute survival response seen in WT. The P-defective transgenics ($eS6A^{\Delta 6S>A}$) retain a similar pattern as in prior experimental conditions, indicating a possible of role of eS6-P in hypoxia induced autophagy regulation. Taken together, we cannot rule out the possibility that sucrose caused changes that are beyond the scope of our simple model. The presence of sucrose may also cause rapid turnover of hypoxic autophagosomes in WT and P-enabled transgenics (eS6AWT-HA) but not in rps6a and the P-defective transgenics ($eS6A^{\Delta 6S>A}$). Another possibility could be a caveat in MDC staining which demands follow-up experiments with GFP-ATG8 fusion proteins to confirm the findings. It is also feasible that TOR might have some unexpected counterintuitive repressive effect on the hypoxia response. It is of interest to us in light of our suprising results with *rps6a*. Additional experiments specifically looking at residual

TOR activity via phosphorylation of S6K in similar experimental conditions could also simplify interpretation of the observations.

3.5.3 Absence of light induces autophagosomes even in presence of sucrose

Under 24h hypoxia in light, in the WT, induction of autophagosomes (MDC vesicles) was completely abolished when exogenous sucrose was present, but in dark hypoxia upregulation of autophagosomes (MDC vesicles) was visible again. One possibility is that the amount of exogenous sucrose in this experiment was probably enough to trigger a stress survival response in the light, while in darkness it was insufficient. While it is tempting to speculate that the light can allow residual levels of carbon fixation, resulting in this enhanced tolerance of hypoxia, it is not likely. Otherwise, the protective effect of exogenous sucrose seen in prolonged hypoxia (12h or more) such as ours, may require higher concentration of sucrose. Since dark treatment of 24h is a substantial stress for plants, it is logical to surmise that 1% or 30mM sucrose is probably enough to impart tolerance against transient anoxia or long hypoxia but not long hypoxia and dark at the same time. Notably, while the wild-type strain did not exhibit an increased tolerance to hypoxia in darkness in presence of sucrose, the *rps6a* mutant was able to elicit autophagy after 24h hypoxia in both light and dark conditions. These findings suggest the possibility of disruption in the sensing of all the experimental components, including hypoxia, light conditions, and sucrose. The disruption could be due to its defects arising from 50% less dosage of eS6 protein both of which require further experimentation to determine. The *rps6a rps6b* double mutant complemented with phospho-enabled eS6A ($eS6A^{WT\text{-}HA}$), did

not show induction of autophagy unlike WT. It can be speculated that due to the absence of eS6B paralog, the pathway responsible for this sucrose dependent effect exerts a stronger effect on phospho-enabled eS6A ($eS6A^{WT\text{-}HA}$). Nevertheless, the *rps6a rps6b* double mutants complemented with phospho-defective eS6A ($eS6A^{\Delta 6S>A}$) maintained the sharp induction of autophagosomes (MDC vesicles) as in other conditions. We know that eS6-P starts declining at about 4h after being shifted to light in presence of 1% exogenous sucrose but stays moderately phosphorylated in presence of 3% sucrose in the media. It has been shown that 90mM or 3% sucrose does allow WT plants to have enhanced tolerance. eS6-P in the dark requires a high level of sucrose to be present. This further suggests that the upregulation of autophagy under 24h hypoxia in presence of exogenous sucrose could be eS6-P mediated via an alternative pathway than TOR.

3.5.4 Role of eS6-P in the non-canonical response of rps6a to hypoxia induced autophagy.

Across our experiments, the lack of induction of autophagy by *rps6a* after 24h hypoxia is striking. *rps6a* mutants have 50% less dosage of the *RPS6*/eS6 gene and are known to upregulate ribosome biogenesis to make enough 40S subunits to support its growth and development. To survive sustained hypoxia plants requires a coordinated effort of multiple signaling pathways. While upregulation of ribosome biogenesis might be enough to meet regular demand of translation it might not be sufficient to trigger a sustained stress-survival response. While it is plausible that the reduction of the gene dosage of RPS6 is solely responsible for it, the autophagy induction observed in presence of sucrose cannot be

simply explained by it. Further, in 24h dark hypoxia with exogenous sucrose, *rps6a* can show the same pattern of induction as in light. This indicates a possible mis regulation of an alternative pathway involved in hypoxia tolerance and survival which might or might not be a consequence of dosage reduction. We could speculate that *rps6a* mutant has a higher threshold for autophagy than WT. It could be due to the fact that *rps6a* mutants make ribosomes more slowly, at approximately half the speed of wild type, despite upregulating ribosome biogenesis. *rps6a* behavior could also occur due to the absence of eS6A paralog which could be responsible for a hypoxia specific behavior, a function that eS6B is unable to compensate.

3.5.5 Potential mechanisms resulting in the non-canonical behavior of rps6a

To gain a better understanding of the potential mechanisms responsible for the unexpected behavior of *rps6a*, we sought to determine the expression status of genes that are involved in the processes of autophagy and hypoxia response from our transcriptome dataset of *rps6a* (Dasgupta *et al.*, 2023), *rps6b* and P-enabled regular growth conditions without exogenous sucrose. Among 2800 genes that show significant differential expression in *rps6a* vs WT, a subset of carbohydrate metabolism genes exhibits differential expression summarized in Figure 3.8. Seventeen out of twenty-one T6P metabolism enzymes are expressed in our dataset of which 7 show differential expression resulting in 24 percent reduction of expression in *rps6a* vs WT in regular growth conditions. Additionally, several carbohydrate metabolism genes including T6P biosynthesis genes are differentially expressed. The carbohydrate metabolism gene subset that shows differential expression in

rps6a are summarized in Figure 3.8. Modulation in carbohydrate metabolism as mentioned earlier (see introduction of chapter 3) has been shown to be crucial to hypoxia tolerance. Together, the gene expression changes at the transcript level can cause the non-canonical behavior of rps6a across our experiments. Additionally, ATG8E, ATG8F, ATG18 and ATG4A are also downregulated in *rps6a*. ATG8E and ATG8F, the two highly expressed ATGs in our dataset collectively contribute to around sixteen percent reduction in overall expression in *rps6a*. It should be noted that these perturbations in carbohydrate metabolism and autophagy are occurring at regular growth conditions in *rps6a*. Stress conditions likely exacerbate these perturbations leading to a lack of response or a non-canonical response. However, further experiments are needed to address these hypotheses.

Since uORFs are well-known to be involved in regulation of carbon/nitrogen metabolism, as demonstrated by the sucrose-induced translational repression of the transcription factor bZIP11 (Ma *et al.*, 2011, Smeekens *et al.*, 2010, Wiese *et al.*, 2004), we tested for presence of uORFs for the subset of genes against uORF database (Urquidi Camacho, 2023) for the genes curated in Figure 3.8. Intriguingly, more than 50% of the carbohydrate metabolism genes summarized in Figure 3.8 appear to contain uORFs including bZIP11 (Figure 3.7). The primary outcome of carbon deprivation with regards to the ability to withstand hypoxic conditions is presumably at the metabolic level. However, it is plausible that sugars may have a regulatory role in the transcriptional level of the anaerobic response signaling pathway. The redundant response of *rps6a rps6b* double mutant harboring phospho-defective eS6A (eS6A$^{\Delta 6S>A}$) for hypoxia induced autophagy

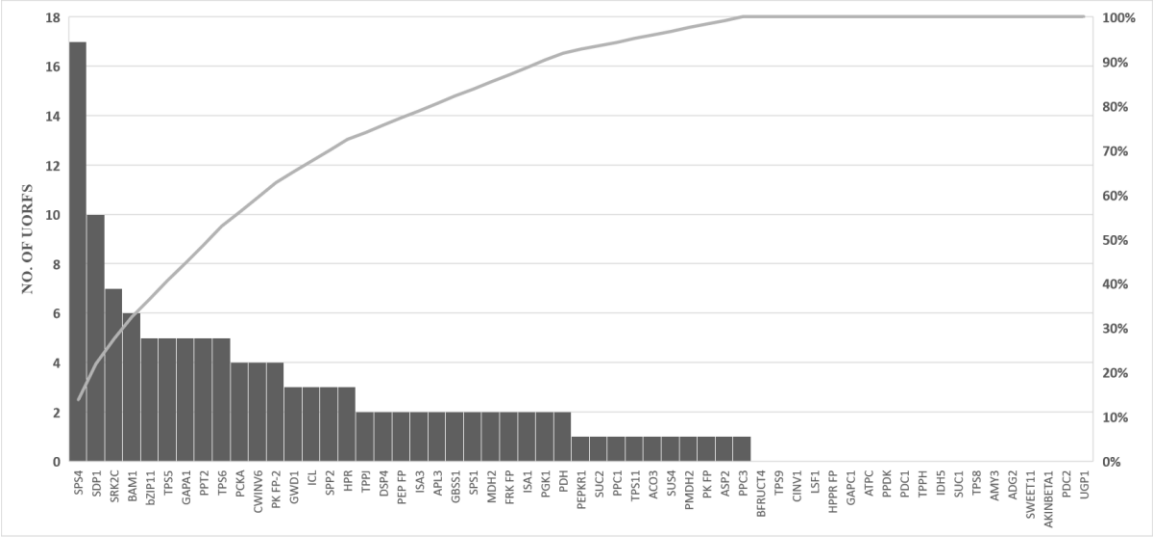

Figure 3.7: 40 out of 60 differentially expressed carbohydrate metabolism genes in our transcriptome data set contain uORFs.

uORF presence tested in uORF database (Urquidi Camacho, 2023).

under all conditions tested could have a potential basis on perturbed sucrose sensing in absence of eS6-P.

Figure 3.8 also has a short list of ethylene response factors including the upregulated ERF VII protein RAP2.12, which plays a central role in induction of HRGs under hypoxia (Kosmacz *et al.*, 2015, Licausi *et al.*, 2011). Activity of RAP2.12 has recently been shown to rely on TOR activity and for the induction of HRGs (Kunkowska *et al.*, 2023). They also found that activation of a smaller amount of nuclear localized RAP2.12 by TOR activity, is enough to produce a sufficient production of HRGs.

In summary, the modulation of T6P metabolism, and ATGs seen in *rps6a* could be one of the potential directions of future investigation to elucidate the complexity of oxygen sensing, sugar signaling and autophagy in plants. Future experiments should include *rps6b* in these experimental conditions since the majority of the transcriptome differential expression pattern in *rps6a* is also retained by *rps6b*. Even though MDC-vesicles has been one of the major tools to visualize autophagy, results described here should be corroborated with identical experiments using a fusion protein between GFP or any other fluorescent protein and the autophagosomal membrane protein ATG8 (Bassham, 2015, Pu & Bassham, 2023).

Figure 3.8: List of a subset of genes that show significant differential expression in *rps6a* vs WT transcriptome analysis.

Upregulation is denoted by blue font color in the "log2fold change" column and downregulation is denoted by red font color. The functional classification was manually curated from the literature.

	Locus.Identifier	log2FoldChange	padj	Primary.Gene.Symbol
ETHYLENE RESPONSE FACTORS	AT1G53910	0.404975152	2.96E-03	RELATED TO AP2 12 (RAP2.12)
	AT3G16770	0.677502813	1.83E-08	ETHYLENE-RESPONSIVE ELEMENT BINDING PROTEIN (EBP)
	AT5G67190	-1.20642417	6.40E-05	DREB AND EAR MOTIF PROTEIN 2 (DEAR2)
	AT1G22190	-0.405271803	1.46E-02	RELATED TO AP2 4 (RAP2.4)
AUTOPHAGY RELATED GENES	AT2G44140	-0.414497343	1.24E-02	AUTOPHAGY 4A (ATG4A)
	AT2G45170	-0.727391626	1.91E-04	AUTOPHAGY 8E (ATG8E)
	AT4G16520	-0.294582462	4.35E-03	AUTOPHAGY 8F (ATG8F)
	AT5G54730	-0.62016773	4.93E-04	HOMOLOG OF YEAST AUTOPHAGY 18 (ATG18) F (G18F)
TREHALOSE-6-PHOSPHATE METABOLISM	AT1G23870	-0.941871168	2.93E-09	TREHALOSE-PHOSPHATASE/SYNTHASE 9 (TPS9)
	AT1G68020	-0.383895189	6.67E-03	(ATTPS6)
	AT1G70290	-1.336091865	2.47E-28	TREHALOSE-6-PHOSPHATASE SYNTHASE S8 (TPS8)
	AT2G18700	-1.699715298	4.28E-28	TREHALOSE PHOSPHATASE/SYNTHASE 11 (TPS11)
	AT4G17770	0.696455106	2.96E-08	TREHALOSE PHOSPHATASE/SYNTHASE 5 (TPS5)
	AT5G65140	-0.96328719	1.80E-07	TREHALOSE-6-PHOSPHATE PHOSPHATASE J (TPPJ)
	AT4G39770	-0.609525949	1.59E-03	TREHALOSE-6-PHOSPHATE PHOSPHATASE H (TPPH)
CARBOHYDRATE METABOLISM	AT4G34590	0.636852522	9.55E-03	BASIC DOMAIN LEUCINE ZIPPER 11 (bZIP11)
	AT3G04120	0.535167727	2.03E-13	GLYCERALDEHYDE-3-PHOSPHATE DEHYDROGENASE C SUBUNIT 1 (GAPC1)
	AT5G43330	0.664714843	4.14E-05	CYTOSOLIC-NAD-DEPENDENT MALATE DEHYDROGENASE 2 (c-NAD-MDH2)
	AT5G54960	0.603203794	6.67E-03	PYRUVATE DECARBOXYLASE-2 (PDC2)
	AT4G33070	2.495999761	6.19E-04	PYRUVATE DECARBOXYLASE 1 (PDC1)
	AT5G08570	0.411589512	3.88E-04	Pyruvate kinase family protein
	AT1G69830	0.598457969	3.56E-07	ALPHA-AMYLASE-LIKE 3 (AMY3)
	AT5G11920	0.628320793	2.53E-02	6-&1-FRUCTAN EXOHYDROLASE (cwINV6)
	AT2G31390	0.584005681	3.18E-03	FRUCTOKINASE 2 (FRK2)
	AT5G19550	0.443198941	1.56E-03	ASPARTATE AMINOTRANSFERASE 2 (ASP2)
	AT3G43190	0.754528602	1.79E-02	SUCROSE SYNTHASE 4 (SUS4)
	AT1G10760	0.521505813	7.91E-06	STARCH EXCESS 1 (SEX1)
	AT1G53310	0.32280007	7.07E-03	PHOSPHOENOLPYRUVATE CARBOXYLASE 1 (PPC1)
	AT1G71880	0.744660906	3.26E-09	SUCROSE-PROTON SYMPORTER 1 (SUC1)
	AT1G21440	0.475042016	9.83E-05	Phosphoenolpyruvate carboxylase family protein
	AT2G05710	0.213991405	4.05E-02	ACONITASE 3 (ACO3)
	AT2G39930	0.350620175	6.41E-03	ISOAMYLASE 1 (ISA1)
	AT3G01510	0.369117607	3.70E-02	LIKE SEX4 1 (LSF1)
	AT3G12780	0.157798755	2.76E-02	PHOSPHOGLYCERATE KINASE 1 (PGK1)
	AT3G13930	0.322771066	2.28E-03	MITOCHONDRIAL PYRUVATE DEHYDROGENASE SUBUNIT 2-2 (MTE2-2)
	AT3G14940	0.665590757	3.08E-03	PHOSPHOENOLPYRUVATE CARBOXYLASE 3 (PPC3)
	AT3G21720	2.402597944	1.42E-13	ISOCITRATE LYASE (ICL)
	AT3G52180	1.480241953	4.13E-15	STARCH-EXCESS 4 (SEX4)
	AT3G52990	0.290042539	2.71E-02	Pyruvate kinase family protein
	AT4G09020	1.319875263	2.41E-07	ISOAMYLASE 3 (ISA3)
	AT4G37870	0.518280105	5.41E-08	PHOSPHOENOLPYRUVATE CARBOXYKINASE 1 (PCK1)
	AT4G39210	0.434600552	4.97E-03	(APL3)
	AT5G20280	0.220861263	4.77E-02	SUCROSE PHOSPHATE SYNTHASE 1F (SPS1F)
	AT2G33040	0.316815672	2.61E-04	GAMMA SUBUNIT OF MT ATP SYNTHASE (ATP3)
	AT5G03290	0.417899295	4.12E-03	ISOCITRATE DEHYDROGENASE V (IDH-V)
	AT5G04040	-0.450457959	1.29E-03	SUGAR-DEPENDENT1 (SDP1)
	AT1G12580	-0.281145087	4.14E-02	PHOSPHOENOLPYRUVATE CARBOXYLASE-RELATED KINASE 1 (PEPKR1)
	AT5G09660	-0.429537986	2.89E-09	PEROXISOMAL NAD-MALATE DEHYDROGENASE 2 (PMDH2)
	AT5G17310	-0.343479336	1.18E-03	UDP-GLUCOSE PYROPHOSPHORYLASE 2 (UGP2)
	AT4G10120	-0.312207425	2.43E-04	SUCROSE PHOSPHATE SYNTHASE 4F (SPS4F)
	AT4G15530	-0.258086752	3.67E-02	PYRUVATE ORTHOPHOSPHATE DIKINASE (PPDK)
	AT1G78290	-0.712627224	7.63E-05	SNF1-RELATED PROTEIN KINASE 2-8 (SNRK2-8)
	AT5G19220	-0.224065444	1.52E-02	ADP GLUCOSE PYROPHOSPHORYLASE LARGE SUBUNIT 1 (APL1)
	AT3G52340	-0.3080533	2.41E-02	SUCROSE-6F-PHOSPHATE PHOSPHOHYDROLASE 2 (SPP2)
	AT3G23920	-0.605190952	3.20E-07	BETA-AMYLASE 1 (BAM1)
	AT1G35580	-0.283116323	4.66E-02	CYTOSOLIC INVERTASE 1 (CINV1)
	AT3G26650	-0.231546891	2.41E-03	GLYCERALDEHYDE 3-PHOSPHATE DEHYDROGENASE A SUBUNIT (GAPA)
	AT2G45630	-0.383955384	4.99E-02	HYDROXYPHENYLPYRUVATE REDUCTASE 4 (HPPR4)
	AT3G48740	-0.340298396	1.48E-03	(SWEET11)
	AT1G12240	-0.475040829	5.27E-07	(ATBETAFRUCT4)
	AT1G22710	-0.746215347	2.28E-10	SUCROSE-PROTON SYMPORTER 2 (SUC2)
	AT1G32900	-0.260845896	4.79E-03	GRANULE BOUND STARCH SYNTHASE 1 (GBSS1)
	AT1G68010	-0.405227564	4.16E-08	HYDROXYPYRUVATE REDUCTASE (HPR)
	AT3G01550	-0.854307763	2.26E-08	PHOSPHOENOLPYRUVATE (PEP)/PHOSPHATE TRANSLOCATOR 2 (PPT2)
	AT5G21170	-1.295175325	7.49E-08	(AKINBETA1)

CHAPTER 4: CONCLUSIONS AND FUTURE PERSPECTIVES

4.2 BRIEF SUMMARY OF RESULTS

The research presented in this study indicates that plants that express a predominantly phospho-deficient isoform of eS6 are able to grow normally under laboratory conditions. Furthermore, the AteS6A paralog was able to effectively rescue double mutations in both *rps6a* and *rps6b* genes when expressed at twice the wild-type dosage. Additionally, a phospho-deficient isoform of eS6A, with six phosphorylatable serine and threonine residues in its carboxyl-terminal tail mutated to alanine, was also able to rescue the lethality, rosette growth, and polyribosome loading of the double mutant. This isoform was able to complement various phenotypes of *rps6* mutants such as photosynthetic efficiency, as well as most gene expression defects that were measured through transcriptomics and proteomics (Chapter 2) (Urquidi Camacho, 2023). The phenotype of seedlings that were deficient in eS6-P was characterized by pointed leaves, reduced root growth, and impaired expression of mRNAs associated with proteins implicated in cell cycle and ribosome biogenesis, in stark contrast to the plants rescued by a phospho-enabled variant of eS6A. The phospho-deficient eS6 mutant was also challenged with hypoxia to test its ability to upregulate autophagy (MDC vesicles were scored) and compared with the phospho-enabled eS6 mutant. Wild-type seedlings showed upregulation of autophagosomes (MDC vesicles) after 24h hypoxia along with the phospho-enabled eS6 mutant and the phospho-deficient eS6 mutant. However, 24h hypoxia with sucrose resulted in convoluted phenotypes in wild type in terms of autophagy (MDC vesicles). Interestingly, *rps6a* showed a clear phenotype of only being able to respond to hypoxia by upregulating autophagy in presence of sucrose which indicates a potential role of eS6-P in this hypoxia

induced response. Nonetheless, we have not ruled out the possibility of *rps6a* behavior to be a mere consequence of lack of 50% dosage of eS6 in the plants.

4.3 FUTURE PERSPECTIVES ON PHYSIOLOGICAL ROLES OF eS6-P

Despite showing a "largely functional" behavior pattern across the numerous analyses shown in this thesis, the phospho-deficient plants did reveal some notable abnormalities and deficiencies. The EYFP-tagged eS6A$^{\Delta 7S>A}$ showed a significant preference towards forming aggregated foci in the nucleus than did the wild-type version. While this finding lacks a direct physiological consequence at this stage, future experiments with nucleolar markers such as FIBRILLARIN2 (FIB2) along with time course analysis could be used to determine a distinct localization characteristic associated with WT and the phospho-deficient eS6. A similar set of localization experiments can also be performed with the other paralog eS6B and its phospho-null version to investigate paralog specific localization patterns. A differential nucleolar localization pattern for RP paralogs in Arabidopsis was observed for uL23 (Degenhardt & Bonham-Smith, 2008). Additionally in the transcriptome analyses, defects in the mitotic cell cycle functions and responses to phosphate starvation were detected, representative of incomplete complementation of *rps6* mutants by the phospho-deficient Δ6S>A allele, although completely rescued by the phospho-enabled WT-HA allele. The pointed-leaf phenotype of the Δ6S>A complemented double mutant plants indicate a delay in leaf expansion similar to the rate of root elongation, a sensitive indicator of cell division. The proteomic analyses also revealed defects in ribosome biogenesis proteins, again indicative of a lack of full complementation. This is

not surprising since eS6 is known to function as part of the small subunit intermediate in ribosome assembly (Bernstein & Baserga, 2004). The increase in ribosomal proteins and the accumulation of 60S subunits seen in our *rps6* mutants mirror similar behavior in yeast and mammalian ribosomal protein mutants (Pachler *et al.*, 2004, Robledo *et al.*, 2008). Therefore, eS6 phosphorylation is largely dispensable, but still results in a phenotype that could be investigated in the future to establish its precise mechanisms. Perspectives to be explored are discussed in the four following sections.

4.3.1 Part-1: Through stress response, tolerance and recovery

One of the major avenues of investigation of the role of eS6-P is in stress tolerance and recovery because of its differential regulation under various stresses (Chapter 2). With the double mutant P-enabled and P-defective lines characterized, future work can use them to test for phenotypes under a variety of stress conditions. It is possible that the P-deficient plants might reveal specific stress tolerance and survival phenotypes under conditions that alter eS6-P, such as hypoxia, heat, or light and darkness. Chapter 3 has already explored hypoxia induced autophagy (MDC vesicles) showing an interesting behavior for *rps6a*. Therefore, hypoxia might be a prime candidate to start exploring the basis of eS6-P mechanisms under stress. A phenotype under stress conditions is also likely because other translational mutants such as GCN2 kinase mutants also display few mild phenotypes, grow normally under regular conditions and show a near-normal transcriptome. However, under prolonged continuous or high light, cold and salt stress, they show growth defects indicating a role for GCN2 kinase in adaptation to excess light (Lokdarshi *et al.*, 2020a,

Lokdarshi *et al.*, 2020b). Hence, stress phenotype screening will be a major line of future investigation with the promise of potential opportunities in investigating role of eS6-P in stress induced regulation using omics data analyses.

4.3.2 Part 2: Through defects in ribosome biogenesis

One of the major effects that we observed in the P-deficient proteome is the incomplete complementation of the ribosome biogenesis defects, but we did not yet characterize its translatome. This gap in the current work emphasizes the need to further characterize both *rps6* mutants and the transgenic plants through ribosome profiling, providing the translatome resolution to tease apart subtle defects. Additionally, P-deficient eS6 double mutant could be re-analyzed at embryonic stages and earlier developmental stages (day 6 or 7 seedling) because the asymmetry in cotyledons observed in the P-deficient plants indicate a defect either in cotyledon development during embryogenesis or early leaf expansion post-germination, while the shorter roots could be a consequence of a reduced number of functional ribosomes in the root meristem. *rps6* mutants and the transgenic plants could also benefit from a thorough analysis of the status of pre-rRNA processing which could aid in the interpretation of the above experiments.

4.3.3 Part 3: Biochemical characterization of eS6

Despite eS6-P being studied extensively, the subcellular compartmentalization of eS6 and eS6-P is not known. Determination of cytosolic vs nuclear eS6 for their respective phosphorylation status could be useful to understand the differential regulation of eS6-P

under normal and stress conditions. Moreover, insights from the nature of subcellular partitioning of eS6/eS6-P combined with our current understanding of eS6-P can rationalize efforts towards identifying the phosphatase responsible for eS6 dephosphorylation using phosphatase inhibitors. Additionally, the research community could also profit from characterization of specific eS6 and eS6-P interacting partners in plants using our eS6 and phospho-specific antibodies in a co-immunoprecipitation experiment, to advance towards a mechanistic understanding of the wide range of eS6-P behavior. The only evidence of eS6/eS6-P interacting partners is from HEK293 cells where P-null eS6 interacted with three nuclear proteins involved in the DNA damage response, Serine/arginine-rich splicing factor (SRSF1), Psip1 (transcriptional coactivator, PC4 and SFRS1-interacting protein 1), TOP2B (topoisomerase IIβ), one cytosolic protein (glutaminyl-tRNA synthetase, SYQ) and one membrane protein, ATP-binding cassette sub-family D member 3 (ABCD3) (Wittenberg *et al.*, 2016).

4.3.4 Part 4: Mechanistic characterization

All of the physiological and biochemical aspects of eS6/eS6-P since its discovery have led to a fundamental question on its role in affecting translation mechanistically. Although the role of eS6-P in eukaryotes seems largely absent in global translation (Ruvinsky *et al.*, 2005, Yerlikaya *et al.*, 2016), there are reports of a higher rate of translation, protein accumulation, slight increase in elongation rate and increased translation fidelity in eS6-P-deficient MEFs (Ruvinsky *et al.*, 2005, Wittenberg *et al.*, 2016). Now that we have established the P-enabled and P-defective transgenic lines these results deserve to be

investigated in plants. The puromycin incorporation assay can be used to determine rate of global protein synthesis and perform ribosome profiling (Weinberg *et al.*, 2016) or luciferase reporter assays (Kisly *et al.*, 2021) to determine elongation rate and accumulation. However, testing translation fidelity in plants is tricky since no such assays have been optimized to detect low levels of fidelity defects. Initial steps were taken to establish a translation fidelity assay using the dual-luciferase reporters (unpublished data), widely used for fidelity assays in mammals (Conn & Qian, 2013, Wittenberg et al., 2016), which can be used to investigate the role of eS6-P in plant translation fidelity. Another aspect of ribosome biochemistry where eS6-P may play a role is rescue from ribosome stalling and collisions events. However, the conditions triggering such events or the global cellular response to ribosome stalling, and collisions remain largely unexplored in plants except two reports (Sotta *et al.*, 2021, Tanaka *et al.*, 2016). In addition to elongation rate, determining the role of eS6-P in collided/stalled ribosomes induced by stress or anisomycin in the P-enabled and P-deficient transgenic lines followed by di-some seq and/or ribosome profiling could be an intriguing area of future work. While ribosome profiling will show global behavior, peaks in the footprint data can be corroborated by the disome results. Furthermore, the potential role of eS6-P in translation re-initiation through its interaction with RISP (Mancera-Martínez *et al.*, 2021) (Chapter 1) makes a case for further investigations with transient expression assays of re-initiation dependent reporters in P-enabled and P-deficient plants.

In summary, the data presented in chapter 2 and 3 combined with decades of research on eS6-P add to our understanding about the functional roles of eS6-P, simultaneously revealing open questions for a precise understanding of eS6-P function.

REFERENCES

Ahmad, Z., Magyar, Z., Bögre, L. and Papdi, C. (2019) Cell cycle control by the target of rapamycin signalling pathway in plants. *J Exp Bot,* **70,** 2275-2284.

Anger, A. M., Armache, J. P., Berninghausen, O., Habeck, M., Subklewe, M., Wilson, D. N., *et al.* (2013) Structures of the human and Drosophila 80S ribosome. *Nature,* **497,** 80-85.

Armache, J. P., Jarasch, A., Anger, A. M., Villa, E., Becker, T., Bhushan, S., *et al.* (2010) Cryo-EM structure and rRNA model of a translating eukaryotic 80S ribosome at 5.5-A resolution. *Proc Natl Acad Sci U S A,* **107,** 19748-19753.

Azad, M. B., Chen, Y., Henson, E. S., Cizeau, J., McMillan-Ward, E., Israels, S. J., *et al.* (2008) Hypoxia induces autophagic cell death in apoptosis-competent cells through a mechanism involving BNIP3. *Autophagy,* **4,** 195-204.

Baena-González, E. and Hanson, J. (2017) Shaping plant development through the SnRK1-TOR metabolic regulators. *Curr Opin Plant Biol,* **35,** 152-157.

Baena-González, E., Rolland, F., Thevelein, J. M. and Sheen, J. (2007) A central integrator of transcription networks in plant stress and energy signalling. *Nature,* **448,** 938-942.

Bailey-Serres, J. and Freeling, M. (1990) Hypoxic stress-induced changes in ribosomes of maize seedling roots. *Plant Physiol,* **94,** 1237-1243.

Bailey-Serres, J., Fukao, T., Gibbs, D. J., Holdsworth, M. J., Lee, S. C., Licausi, F., *et al.* (2012) Making sense of low oxygen sensing. *Trends Plant Sci,* **17,** 129-138.

Ban, N., Freeborn, B., Nissen, P., Penczek, P., Grassucci, R. A., Sweet, R., *et al.* (1998) A 9 A resolution X-ray crystallographic map of the large ribosomal subunit. *Cell,* **93,** 1105-1115.

Ban, N., Nissen, P., Hansen, J., Capel, M., Moore, P. B. and Steitz, T. A. (1999) Placement of protein and RNA structures into a 5 A-resolution map of the 50S ribosomal subunit. *Nature,* **400,** 841-847.

Ban, N., Nissen, P., Hansen, J., Moore, P. B. and Steitz, T. A. (2000) The complete atomic structure of the large ribosomal subunit at 2.4 A resolution. *Science,* **289,** 905-920.

Bandi, H. R., Ferrari, S., Krieg, J., Meyer, H. E. and Thomas, G. (1993) Identification of 40 S ribosomal protein S6 phosphorylation sites in Swiss mouse 3T3 fibroblasts stimulated with serum. *J Biol Chem,* **268,** 4530-4533.

Bassham, D. C. (2015) Methods for analysis of autophagy in plants. *Methods,* **75,** 181-188.

Beaud, G., Masse, T., Madjar, J. J. and Leader, D. P. (1989) Identification of induced protein kinase activities specific for the ribosomal proteins uniquely phosphorylated during infection of HeLa cells with vaccinia virus. *FEBS Lett,* **259,** 10-14.

Bellemer, C., Chabosseau, P., Gallardo, F., Gleizes, P.-E. and Stahl, G. (2010) Genetic interactions show the importance of rRNA modification machinery for the role of Rps15p during ribosome biogenesis in S. cerevisiae. *PloS one,* **5,** e10472.

Beltrán-Peña, E., Aguilar, R., Ortíz-López, A., Dinkova, T. D. and De Jiménez, E. S. (2002) Auxin stimulates S6 ribosomal protein phosphorylation in maize thereby affecting protein synthesis regulation. *Physiol Plant,* **115,** 291-297.

Ben-Sahra, I., Howell, J. J., Asara, J. M. and Manning, B. D. (2013) Stimulation of de novo pyrimidine synthesis by growth signaling through mTOR and S6K1. *Science,* **339,** 1323-1328.

Ben-Shem, A., Garreau de Loubresse, N., Melnikov, S., Jenner, L., Yusupova, G. and Yusupov, M. (2011) The structure of the eukaryotic ribosome at 3.0 A resolution. *Science,* **334,** 1524-1529.

Ben-Shem, A., Jenner, L., Yusupova, G. and Yusupov, M. (2010) Crystal structure of the eukaryotic ribosome. *Science,* **330,** 1203-1209.

Bernstein, K. A. and Baserga, S. J. (2004) The small subunit processome is required for cell cycle progression at G1. *Mol Biol Cell,* **15,** 5038-5046.

Biederbick, A., Kern, H. F. and Elsässer, H. P. (1995) Monodansylcadaverine (MDC) is a specific in vivo marker for autophagic vacuoles. *Eur J Cell Biol,* **66,** 3-14.

Biever, A., Valjent, E. and Puighermanal, E. (2015) Ribosomal Protein S6 Phosphorylation in the Nervous System: From Regulation to Function. *Front Mol Neurosci,* **8,** 75.

Blenis, J. (2017) TOR, the Gateway to Cellular Metabolism, Cell Growth, and Disease. *Cell,* **171,** 10-13.

Blenis, J. and Erikson, R. L. (1984) Phosphorylation of the ribosomal protein S6 is elevated in cells transformed by a variety of tumor viruses. *J Virol,* **50,** 966-969.

Boex-Fontvieille, E., Daventure, M., Jossier, M., Zivy, M., Hodges, M. and Tcherkez, G. (2013) Photosynthetic control of Arabidopsis leaf cytoplasmic translation initiation by protein phosphorylation. *PLoS One,* **8,** e70692.

Bohlen, J., Roiuk, M. and Teleman, A. A. (2021) Phosphorylation of ribosomal protein S6 differentially affects mRNA translation based on ORF length. *Nucleic Acids Res,* **49,** 13062-13074.

Branco-Price, C., Kaiser, K. A., Jang, C. J., Larive, C. K. and Bailey-Serres, J. (2008) Selective mRNA translation coordinates energetic and metabolic adjustments to cellular oxygen deprivation and reoxygenation in Arabidopsis thaliana. *Plant J,* **56,** 743-755.

Branco-Price, C., Kawaguchi, R., Ferreira, R. B. and Bailey-Serres, J. (2005) Genome-wide analysis of transcript abundance and translation in Arabidopsis seedlings subjected to oxygen deprivation. *Ann Bot,* **96,** 647-660.

Browning, K. S. and Bailey-Serres, J. (2015) Mechanism of cytoplasmic mRNA translation. *Arabidopsis Book,* **13,** e0176.

Brunkard, J. O. (2020) Exaptive Evolution of Target of Rapamycin Signaling in Multicellular Eukaryotes. *Dev Cell,* **54,** 142-155.

Bu, F., Yang, M., Guo, X., Huang, W. and Chen, L. (2020) Multiple Functions of ATG8 Family Proteins in Plant Autophagy. *Front Cell Dev Biol,* **8,** 466.

Bureau, M., Leh, V., Haas, M., Geldreich, A., Ryabova, L., Yot, P., *et al.* (2004) P6 protein of Cauliflower mosaic virus, a translation reinitiator, interacts with ribosomal protein L13 from Arabidopsis thaliana. *J Gen Virol,* **85,** 3765-3775.

Burkart, G. M. and Brandizzi, F. (2021) A Tour of TOR Complex Signaling in Plants. *Trends Biochem Sci,* **46,** 417-428.

Busche, M., Scarpin, M. R., Hnasko, R. and Brunkard, J. O. (2021) TOR coordinates nucleotide availability with ribosome biogenesis in plants. *Plant Cell,* **33,** 1615-1632.

Cardinali, B., Fiore, L., Campioni, N., De Dominicis, A. and Pierandrei-Amaldi, P. (1999) Resistance of ribosomal protein mRNA translation to protein synthesis shutoff induced by poliovirus. *J Virol,* **73,** 7070-7076.

Carroll, A. J. (2013) The Arabidopsis Cytosolic Ribosomal Proteome: From form to Function. *Front Plant Sci,* **4,** 32.

Cate, J. H., Yusupov, M. M., Yusupova, G. Z., Earnest, T. N. and Noller, H. F. (1999) X-ray crystal structures of 70S ribosome functional complexes. *Science,* **285,** 2095-2104.

Chang, R., Jang, C. J., Branco-Price, C., Nghiem, P. and Bailey-Serres, J. (2012) Transient MPK6 activation in response to oxygen deprivation and reoxygenation is mediated by mitochondria and aids seedling survival in Arabidopsis. *Plant Mol Biol,* **78,** 109-122.

Chantranupong, L., Wolfson, R. L. and Sabatini, D. M. (2015) Nutrient-sensing mechanisms across evolution. *Cell,* **161,** 67-83.

Chauvin, C., Koka, V., Nouschi, A., Mieulet, V., Hoareau-Aveilla, C., Dreazen, A., *et al.* (2014) Ribosomal protein S6 kinase activity controls the ribosome biogenesis transcriptional program. *Oncogene,* **33,** 474-483.

Chen, G. H., Liu, M. J., Xiong, Y., Sheen, J. and Wu, S. H. (2018) TOR and RPS6 transmit light signals to enhance protein translation in deetiolating Arabidopsis seedlings. *Proc Natl Acad Sci U S A,* **115,** 12823-12828.

Chen, H., Dong, J. and Wang, T. (2021) Autophagy in Plant Abiotic Stress Management. *Int J Mol Sci,* **22**.

Chen, L., Liao, B., Qi, H., Xie, L. J., Huang, L., Tan, W. J., *et al.* (2015) Autophagy contributes to regulation of the hypoxia response during submergence in Arabidopsis thaliana. *Autophagy,* **11,** 2233-2246.

Chen, L., Su, Z. Z., Huang, L., Xia, F. N., Qi, H., Xie, L. J., *et al.* (2017) The AMP-Activated Protein Kinase KIN10 Is Involved in the Regulation of Autophagy in Arabidopsis. *Front Plant Sci,* **8,** 1201.

Cho, H. Y., Loreti, E., Shih, M. C. and Perata, P. (2021) Energy and sugar signaling during hypoxia. *New Phytol,* **229,** 57-63.

Cho, H. Y., Wen, T. N., Wang, Y. T. and Shih, M. C. (2016) Quantitative phosphoproteomics of protein kinase SnRK1 regulated protein phosphorylation in Arabidopsis under submergence. *J Exp Bot,* **67,** 2745-2760.

Choudhary, M. K., Nomura, Y., Wang, L., Nakagami, H. and Somers, D. E. (2015) Quantitative Circadian Phosphoproteomic Analysis of Arabidopsis Reveals Extensive Clock Control of Key Components in Physiological, Metabolic, and Signaling Pathways. *Mol Cell Proteomics,* **14,** 2243-2260.

Clemons, W. M., Jr., May, J. L., Wimberly, B. T., McCutcheon, J. P., Capel, M. S. and Ramakrishnan, V. (1999) Structure of a bacterial 30S ribosomal subunit at 5.5 A resolution. *Nature,* **400,** 833-840.

Conn, C. S. and Qian, S. B. (2013) Nutrient signaling in protein homeostasis: an increase in quantity at the expense of quality. *Sci Signal,* **6,** ra24.

Contento, A. L., Xiong, Y. and Bassham, D. C. (2005) Visualization of autophagy in Arabidopsis using the fluorescent dye monodansylcadaverine and a GFP-AtATG8e fusion protein. *Plant J,* **42,** 598-608.

Cottilli, P., Itoh, Y., Nobe, Y., Petrov, A. S., Lisón, P., Taoka, M., *et al.* (2022) Cryo-EM structure and rRNA modification sites of a plant ribosome. *Plant Commun,* **3,** 100342.

Creff, A., Sormani, R. and Desnos, T. (2010) The two Arabidopsis RPS6 genes, encoding for cytoplasmic ribosomal proteins S6, are functionally equivalent. *Plant Mol Biol,* **73,** 533-546.

Crepin, N. and Rolland, F. (2019) SnRK1 activation, signaling, and networking for energy homeostasis. *Current Opinion in Plant Biology,* **51,** 29-36.

Dasgupta, A., Camacho, R. A. U., Enganti, R., Cho, S. K., Tucker, L. L., Torreverde, J. S., *et al.* (2023) A phosphorylation-deficient ribosomal protein eS6 is largely functional in Arabidopsis thaliana, rescuing mutant defects from global translation and gene expression to photosynthesis and growth. *bioRxiv,* 2023.2005.2030.542942.

Decker, S. (1981) Phosphorylation of ribosomal protein S6 in avian sarcoma virus-transformed chicken embryo fibroblasts. *Proc Natl Acad Sci U S A,* **78,** 4112-4115.

Degenhardt, R. F. and Bonham-Smith, P. C. (2008) Arabidopsis ribosomal proteins RPL23aA and RPL23aB are differentially targeted to the nucleolus and are disparately required for normal development. *Plant Physiol,* **147,** 128-142.

Delarue, M., Brittingham, G. P., Pfeffer, S., Surovtsev, I. V., Pinglay, S., Kennedy, K. J., *et al.* (2018) mTORC1 Controls Phase Separation and the Biophysical Properties of the Cytoplasm by Tuning Crowding. *Cell,* **174,** 338-349.e320.

Deprost, D., Yao, L., Sormani, R., Moreau, M., Leterreux, G., Nicolai, M., *et al.* (2007) The Arabidopsis TOR kinase links plant growth, yield, stress resistance and mRNA translation. *EMBO Rep,* **8,** 864-870.

Dobrenel, T., Caldana, C., Hanson, J., Robaglia, C., Vincentz, M., Veit, B., *et al.* (2016a) TOR Signaling and Nutrient Sensing. *Annu Rev Plant Biol,* **67,** 261-285.

Dobrenel, T., Mancera-Martinez, E., Forzani, C., Azzopardi, M., Davanture, M., Moreau, M., *et al.* (2016b) The Arabidopsis TOR Kinase Specifically Regulates the Expression of Nuclear Genes Coding for Plastidic Ribosomal Proteins and the Phosphorylation of the Cytosolic Ribosomal Protein S6. *Front Plant Sci,* **7,** 1611.

Duncan, R. and McConkey, E. H. (1982) Preferential utilization of phosphorylated 40-S ribosomal subunits during initiation complex formation. *Eur J Biochem,* **123,** 535-538.

Emmanuel, N., Ragunathan, S., Shan, Q., Wang, F., Giannakou, A., Huser, N., *et al.* (2017) Purine Nucleotide Availability Regulates mTORC1 Activity through the Rheb GTPase. *Cell Rep,* **19,** 2665-2680.

Enganti, R. (2018) Characterizing the regulation and the role of ribosomal protein S6 phosphorylation in Arabidopsis thaliana. University of Tennesee.

Enganti, R., Cho, S. K., Toperzer, J. D., Urquidi-Camacho, R. A., Cakir, O. S., Ray, A. P., *et al.* (2018) Phosphorylation of Ribosomal Protein RPS6 Integrates Light Signals and Circadian Clock Signals. *Frontiers in Plant Science,* **8**.

Field, S., Conner, W. C. and Roberts, D. M. (2021) Arabidopsis CALMODULIN-LIKE 38 Regulates Hypoxia-Induced Autophagy of SUPPRESSOR OF GENE SILENCING 3 Bodies. *Front Plant Sci,* **12,** 722940.

Fingar, D. C., Salama, S., Tsou, C., Harlow, E. and Blenis, J. (2002) Mammalian cell size is controlled by mTOR and its downstream targets S6K1 and 4EBP1/eIF4E. *Genes Dev,* **16,** 1472-1487.

Fütterer, J. and Hohn, T. (1992) Role of an upstream open reading frame in the translation of polycistronic mRNAs in plant cells. *Nucleic Acids Res,* **20,** 3851-3857.

García, I., Arenas-Alfonseca, L., Moreno, I., Gotor, C. and Romero, L. C. (2019) HCN Regulates Cellular Processes through Posttranslational Modification of Proteins by S-cyanylation. *Plant Physiol,* **179,** 107-123.

Gibbs, D. J. and Holdsworth, M. J. (2020) Every Breath You Take: New Insights into Plant and Animal Oxygen Sensing. *Cell,* **180,** 22-24.

Giuntoli, B., Lee, S. C., Licausi, F., Kosmacz, M., Oosumi, T., van Dongen, J. T., *et al.* (2014) A trihelix DNA binding protein counterbalances hypoxia-responsive transcriptional activation in Arabidopsis. *PLoS biology,* **12,** e1001950.

Gonzalez, A., Shimobayashi, M., Eisenberg, T., Merle, D. A., Pendl, T., Hall, M. N., *et al.* (2015) TORC1 promotes phosphorylation of ribosomal protein S6 via the AGC kinase Ypk3 in Saccharomyces cerevisiae. *PLoS One,* **10,** e0120250.

Greco, A., Laurent, A. M. and Madjar, J. J. (1997) Repression of beta-actin synthesis and persistence of ribosomal protein synthesis after infection of HeLa cells by herpes simplex virus type 1 infection are under translational control. *Mol Gen Genet,* **256,** 320-327.

Gressner, A. M. and Wool, I. G. (1974a) The phosphorylation of liver ribosomal proteins in vivo. Evidence that only a single small subunit protein (S6) is phosphorylated. *J Biol Chem,* **249,** 6917-6925.

Gressner, A. M. and Wool, I. G. (1974b) The stimulation of the phosphorylation of ribosomal protein S6 by cycloheximide and puromycin. *Biochem Biophys Res Commun,* **60,** 1482-1490.

Guan, B., Lin, Z., Liu, D., Li, C., Zhou, Z., Mei, F., *et al.* (2019) Effect of Waterlogging-Induced Autophagy on Programmed Cell Death in Arabidopsis Roots. *Front Plant Sci,* **10,** 468.

Guglielminetti, L., Yamaguchi, J., Perata, P. and Alpi, A. (1995) Amylolytic Activities in Cereal Seeds under Aerobic and Anaerobic Conditions. *Plant Physiol,* **109,** 1069-1076.

Guzy, R. D., Mack, M. M. and Schumacker, P. T. (2007) Mitochondrial complex III is required for hypoxia-induced ROS production and gene transcription in yeast. *Antioxid Redox Signal,* **9,** 1317-1328.

Gwinn, D. M., Shackelford, D. B., Egan, D. F., Mihaylova, M. M., Mery, A., Vasquez, D. S., *et al.* (2008) AMPK phosphorylation of raptor mediates a metabolic checkpoint. *Mol Cell,* **30,** 214-226.

Hamanaka, R. B., Weinberg, S. E., Reczek, C. R. and Chandel, N. S. (2016) The Mitochondrial Respiratory Chain Is Required for Organismal Adaptation to Hypoxia. *Cell Rep,* **15,** 451-459.

Hannan, K. M., Brandenburger, Y., Jenkins, A., Sharkey, K., Cavanaugh, A., Rothblum, L., *et al.* (2003) mTOR-dependent regulation of ribosomal gene transcription requires S6K1 and is mediated by phosphorylation of the carboxy-terminal activation domain of the nucleolar transcription factor UBF. *Mol Cell Biol,* **23,** 8862-8877.

Hatsugai, N., Yamada, K., Goto-Yamada, S. and Hara-Nishimura, I. (2015) Vacuolar processing enzyme in plant programmed cell death. *Front Plant Sci,* **6,** 234.

Hauge, C. and Frodin, M. (2006) RSK and MSK in MAP kinase signalling. *J Cell Sci,* **119,** 3021-3023.

Henriques, R., Magyar, Z., Monardes, A., Khan, S., Zalejski, C., Orellana, J., *et al.* (2010) Arabidopsis S6 kinase mutants display chromosome instability and altered RBR1-E2F pathway activity. *EMBO J,* **29,** 2979-2993.

Hoxhaj, G., Hughes-Hallett, J., Timson, R. C., Ilagan, E., Yuan, M., Asara, J. M., *et al.* (2017) The mTORC1 Signaling Network Senses Changes in Cellular Purine Nucleotide Levels. *Cell Rep,* **21,** 1331-1346.

Hutchinson, J. A., Shanware, N. P., Chang, H. and Tibbetts, R. S. (2011) Regulation of ribosomal protein S6 phosphorylation by casein kinase 1 and protein phosphatase 1. *J Biol Chem,* **286,** 8688-8696.

Ingargiola, C., Jéhanno, I., Forzani, C., Marmagne, A., Broutin, J., Clément, G., *et al.* (2023) The Arabidopsis Target of Rapamycin (TOR) kinase regulates ammonium assimilation and glutamine metabolism. *Plant Physiol*.

Jakubowicz, T. and Leader, D. P. (1987) Activation of a ribosomal protein S6 kinase in mouse fibroblasts during infection with herpesvirus. *Eur J Biochem,* **168,** 371-376.

Jamsheer, K. M., Jindal, S., Sharma, M., Awasthi, P., S, S., Sharma, M., *et al.* (2022) A negative feedback loop of TOR signaling balances growth and stress-response trade-offs in plants. *Cell Rep,* **39,** 110631.

Jia, C. H., Li, M., Liu, J., Zhao, L., Lin, J., Lai, P. L., *et al.* (2013) IKK-β mediates hydrogen peroxide induced cell death through p85 S6K1. *Cell Death Differ,* **20,** 248-258.
Johansen, T. and Lamark, T. (2011) Selective autophagy mediated by autophagic adapter proteins. *Autophagy,* **7,** 279-296.
Juntawong, P., Girke, T., Bazin, J. and Bailey-Serres, J. (2014) Translational dynamics revealed by genome-wide profiling of ribosome footprints in Arabidopsis. *Proc Natl Acad Sci U S A,* **111,** E203-212.
Kabat, D. (1970) Phosphorylation of ribosomal proteins in rabbit reticulocytes. Characterization and regulatory aspects. *Biochemistry,* **9,** 4160-4175.
Kaerlein, M. and Horak, I. (1976) Phosphorylation of ribosomal proteins in HeLa cells infected with vaccinia virus. *Nature,* **259,** 150-151.
Katan, M., McGarvey, M. J., Stevely, W. S. and Leader, D. P. (1986) The phosphorylation of ribosomal protein S6 by protein kinases from cells infected with pseudorabies virus. *Biochem J,* **239,** 205-211.
Kellner, R., De la Concepcion, J. C., Maqbool, A., Kamoun, S. and Dagdas, Y. F. (2017) ATG8 Expansion: A Driver of Selective Autophagy Diversification? *Trends Plant Sci,* **22,** 204-214.
Kennedy, I. M. and Leader, D. P. (1981) Increased phosphorylation of ribosomal protein S6 in hamster fibroblasts transformed by polyoma virus and simian virus 40. *Biochem J,* **198,** 235-237.
Kennedy, I. M., Leader, D. P. and Stevely, W. S. (1984) The phosphorylation of ribosomal protein S6 in hamster fibroblasts infected with pseudorabies virus inactivated by ultraviolet radiation. *J Gen Virol,* **65 (Pt 9),** 1621-1624.
Khalaileh, A., Savetsky, I., Adileh, M., Elazary, R., Abu-Gazala, M., Abu Gazala, S., *et al.* (2013) Robotic-assisted enucleation of a large lower esophageal leiomyoma and review of literature. *Int J Med Robot,* **9,** 253-257.
Khatter, H., Myasnikov, A. G., Natchiar, S. K. and Klaholz, B. P. (2015) Structure of the human 80S ribosome. *Nature,* **520,** 640.
Kim, Y. K., Kim, S., Shin, Y. J., Hur, Y. S., Kim, W. Y., Lee, M. S., *et al.* (2014) Ribosomal protein S6, a target of rapamycin, is involved in the regulation of rRNA genes by possible epigenetic changes in Arabidopsis. *J Biol Chem,* **289,** 3901-3912.
Kirschner, L. S., Yin, Z., Jones, G. N. and Mahoney, E. (2009) Mouse models of altered protein kinase A signaling. *Endocr Relat Cancer,* **16,** 773-793.
Kisly, I., Kattel, C., Remme, J. and Tamm, T. (2021) Luciferase-based reporter system for in vitro evaluation of elongation rate and processivity of ribosomes. *Nucleic Acids Research,* **49,** e59-e59.
Kleinboelting, N., Huep, G., Kloetgen, A., Viehoever, P. and Weisshaar, B. (2012) GABI-Kat SimpleSearch: new features of the Arabidopsis thaliana T-DNA mutant database. *Nucleic Acids Res,* **40,** D1211-1215.
Kosmacz, M., Parlanti, S., Schwarzländer, M., Kragler, F., Licausi, F. and Van Dongen, J. T. (2015) The stability and nuclear localization of the transcription factor RAP2.12

are dynamically regulated by oxygen concentration. *Plant Cell Environ,* **38,** 1094-1103.

Krieg, J., Hofsteenge, J. and Thomas, G. (1988) Identification of the 40 S ribosomal protein S6 phosphorylation sites induced by cycloheximide. *J Biol Chem,* **263,** 11473-11477.

Kroemer, G., Mariño, G. and Levine, B. (2010) Autophagy and the integrated stress response. *Mol Cell,* **40,** 280-293.

Kunkowska, A. B., Fontana, F., Betti, F., Soeur, R., Beckers, G. J. M., Meyer, C., *et al.* (2023) Target of rapamycin signaling couples energy to oxygen sensing to modulate hypoxic gene expression in Arabidopsis. *Proc Natl Acad Sci U S A,* **120,** e2212474120.

Lai, L. T. F., Ye, H., Zhang, W., Jiang, L. and Lau, W. C. Y. (2019) Structural Biology and Electron Microscopy of the Autophagy Molecular Machinery. *Cells,* **8**.

Lan, T., Xiong, W., Chen, X., Mo, B. and Tang, G. (2022) Plant cytoplasmic ribosomal proteins: an update on classification, nomenclature, evolution and resources. *Plant J,* **110,** 292-318.

Laplante, M. and Sabatini, D. M. (2012) mTOR signaling in growth control and disease. *Cell,* **149,** 274-293.

Lara, R., Seckl, M. J. and Pardo, O. E. (2013) The p90 RSK family members: common functions and isoform specificity. *Cancer Res,* **73,** 5301-5308.

Lastdrager, J., Hanson, J. and Smeekens, S. (2014) Sugar signals and the control of plant growth and development. *J Exp Bot,* **65,** 799-807.

Le Bars, R., Marion, J., Le Borgne, R., Satiat-Jeunemaitre, B. and Bianchi, M. W. (2014) ATG5 defines a phagophore domain connected to the endoplasmic reticulum during autophagosome formation in plants. *Nat Commun,* **5,** 4121.

Li, S. (2019) Regulation of Ribosomal Proteins on Viral Infection. *Cells,* **8**.

Li, Y., Mitsuhashi, S., Ikejo, M., Miura, N., Kawamura, T., Hamakubo, T., *et al.* (2012) Relationship between ATM and ribosomal protein S6 revealed by the chemical inhibition of Ser/Thr protein phosphatase type 1. *Biosci Biotechnol Biochem,* **76,** 486-494.

Licausi, F., Kosmacz, M., Weits, D. A., Giuntoli, B., Giorgi, F. M., Voesenek, L. A., *et al.* (2011) Oxygen sensing in plants is mediated by an N-end rule pathway for protein destabilization. *Nature,* **479,** 419-422.

Lin, I. S., Wu, Y.-S., Chen, C.-T., Chen, G.-H., Hwang, S.-G., Jauh, G.-Y., *et al.* (2017) AtRBOH I confers submergence tolerance and is involved in auxin-mediated signaling pathways under hypoxic stress. *Plant Growth Regulation,* **83,** 277-285.

Liu, B., Sun, L., Ma, L. and Hao, F. S. (2017) Both AtrbohD and AtrbohF are essential for mediating responses to oxygen deficiency in Arabidopsis. *Plant Cell Rep,* **36,** 947-957.

Liu, M. J., Wu, S. H., Chen, H. M. and Wu, S. H. (2012) Widespread translational control contributes to the regulation of Arabidopsis photomorphogenesis. *Mol Syst Biol,* **8,** 566.

Liu, Y. and Bassham, D. C. (2012) Autophagy: pathways for self-eating in plant cells. *Annu Rev Plant Biol,* **63,** 215-237.

Liu, Y., Xiong, Y. and Bassham, D. C. (2009) Autophagy is required for tolerance of drought and salt stress in plants. *Autophagy,* **5,** 954-963.

Lokdarshi, A., Conner, W. C., McClintock, C., Li, T. and Roberts, D. M. (2016) Arabidopsis CML38, a Calcium Sensor That Localizes to Ribonucleoprotein Complexes under Hypoxia Stress. *Plant Physiol,* **170,** 1046-1059.

Lokdarshi, A., Guan, J., Urquidi Camacho, R. A., Cho, S. K., Morgan, P. W., Leonard, M., *et al.* (2020a) Light Activates the Translational Regulatory Kinase GCN2 via Reactive Oxygen Species Emanating from the Chloroplast. *Plant Cell,* **32,** 1161-1178.

Lokdarshi, A., Morgan, P. W., Franks, M., Emert, Z., Emanuel, C. and von Arnim, A. G. (2020b) Light-Dependent Activation of the GCN2 Kinase Under Cold and Salt Stress Is Mediated by the Photosynthetic Status of the Chloroplast. *Front Plant Sci,* **11,** 431.

Loreti, E., Poggi, A., Novi, G., Alpi, A. and Perata, P. (2005) A genome-wide analysis of the effects of sucrose on gene expression in Arabidopsis seedlings under anoxia. *Plant Physiol,* **137,** 1130-1138.

Loreti, E., Valeri, M. C., Novi, G. and Perata, P. (2018) Gene Regulation and Survival under Hypoxia Requires Starch Availability and Metabolism. *Plant Physiol,* **176,** 1286-1298.

Loreti, E., van Veen, H. and Perata, P. (2016) Plant responses to flooding stress. *Curr Opin Plant Biol,* **33,** 64-71.

Ma, J., Hanssen, M., Lundgren, K., Hernández, L., Delatte, T., Ehlert, A., *et al.* (2011) The sucrose-regulated Arabidopsis transcription factor bZIP11 reprograms metabolism and regulates trehalose metabolism. *New Phytol,* **191,** 733-745.

Mahfouz, M. M., Kim, S., Delauney, A. J. and Verma, D. P. S. (2006) Arabidopsis TARGET OF RAPAMYCIN Interacts with RAPTOR, Which Regulates the Activity of S6 Kinase in Response to Osmotic Stress Signals. *The Plant Cell,* **18,** 477-490.

Maller, J. L., Foulkes, J. G., Erikson, E. and Baltimore, D. (1985) Phosphorylation of ribosomal protein S6 on serine after microinjection of the Abelson murine leukemia virus tyrosine-specific protein kinase into Xenopus oocytes. *Proc Natl Acad Sci U S A,* **82,** 272-276.

Mancera-Martínez, E., Dong, Y., Makarian, J., Srour, O., Thiébeauld, O., Jamsheer, M., *et al.* (2021) Phosphorylation of a reinitiation supporting protein, RISP, determines its function in translation reinitiation. *Nucleic Acids Res,* **49,** 6908-6924.

Margalha, L., Confraria, A. and Baena-González, E. (2019) SnRK1 and TOR: modulating growth-defense trade-offs in plant stress responses. *J Exp Bot,* **70,** 2261-2274.

Marshall, R. S. and Vierstra, R. D. (2018) Autophagy: The Master of Bulk and Selective Recycling. *Annu Rev Plant Biol,* **69,** 173-208.

Martínez-Barajas, E. and Coello, P. (2020) Review: How do SnRK1 protein kinases truly work? *Plant Sci,* **291,** 110330.

Martinez-Seidel, F., Beine-Golovchuk, O., Hsieh, Y. C. and Kopka, J. (2020) Systematic Review of Plant Ribosome Heterogeneity and Specialization. *Front Plant Sci,* **11,** 948.

Mazure, N. M. and Pouysségur, J. (2010) Hypoxia-induced autophagy: cell death or cell survival? *Curr Opin Cell Biol,* **22,** 177-180.

Melnikov, S., Ben-Shem, A., Garreau de Loubresse, N., Jenner, L., Yusupova, G. and Yusupov, M. (2012) One core, two shells: bacterial and eukaryotic ribosomes. *Nat Struct Mol Biol,* **19,** 560-567.

Meyuhas, O. (2008) Physiological roles of ribosomal protein S6: one of its kind. *Int Rev Cell Mol Biol,* **268,** 1-37.

Meyuhas, O. (2015) Ribosomal Protein S6 Phosphorylation: Four Decades of Research. *Int Rev Cell Mol Biol,* **320,** 41-73.

Meyuhas, O. and Dreazen, A. (2009) Ribosomal protein S6 kinase from TOP mRNAs to cell size. *Prog Mol Biol Transl Sci,* **90,** 109-153.

Minibayeva, F., Dmitrieva, S., Ponomareva, A. and Ryabovol, V. (2012) Oxidative stress-induced autophagy in plants: the role of mitochondria. *Plant Physiol Biochem,* **59,** 11-19.

Montgomery, S. A., Berglund, P., Beard, C. W. and Johnston, R. E. (2006) Ribosomal protein S6 associates with alphavirus nonstructural protein 2 and mediates expression from alphavirus messages. *J Virol,* **80,** 7729-7739.

Moore, C. E., Xie, J., Gomez, E. and Herbert, T. P. (2009) Identification of cAMP-dependent kinase as a third in vivo ribosomal protein S6 kinase in pancreatic beta-cells. *J Mol Biol,* **389,** 480-494.

Munafó, D. B. and Colombo, M. I. (2001) A novel assay to study autophagy: regulation of autophagosome vacuole size by amino acid deprivation. *J Cell Sci,* **114,** 3619-3629.

Murchie, E. H. and Lawson, T. (2013) Chlorophyll fluorescence analysis: a guide to good practice and understanding some new applications. *Journal of Experimental Botany,* **64,** 3983-3998.

Nakatogawa, H. (2020) Mechanisms governing autophagosome biogenesis. *Nature reviews. Molecular cell biology,* **21,** 439-458.

Noda, N. N., Ohsumi, Y. and Inagaki, F. (2010) Atg8-family interacting motif crucial for selective autophagy. *FEBS Lett,* **584,** 1379-1385.

Nukarinen, E., Nagele, T., Pedrotti, L., Wurzinger, B., Mair, A., Landgraf, R., *et al.* (2016) Quantitative phosphoproteomics reveals the role of the AMPK plant ortholog SnRK1 as a metabolic master regulator under energy deprivation. *Sci Rep,* **6,** 31697.

Pachler, K., Karl, T., Kolmann, K., Mehlmer, N., Eder, M., Loeffler, M., *et al.* (2004) Functional interaction in establishment of ribosomal integrity between small subunit protein rpS6 and translational regulator rpL10/Grc5p. *FEMS Yeast Res,* **5,** 271-280.

Panchy, N., von Arnim, A. G. and Hong, T. (2020) Early Detection of Daylengths with a Feedforward Circuit Coregulated by Circadian and Diurnal Cycles. *Biophys J,* **119,** 1878-1895.

Park, H. S., Himmelbach, A., Browning, K. S., Hohn, T. and Ryabova, L. A. (2001) A plant viral "reinitiation" factor interacts with the host translational machinery. *Cell,* **106,** 723-733.

Pelletier, J., Thomas, G. and Volarevic, S. (2018) Ribosome biogenesis in cancer: new players and therapeutic avenues. *Nat Rev Cancer,* **18,** 51-63.

Pende, M., Um, S. H., Mieulet, V., Sticker, M., Goss, V. L., Mestan, J., *et al.* (2004) S6K1(-/-)/S6K2(-/-) mice exhibit perinatal lethality and rapamycin-sensitive 5'-terminal oligopyrimidine mRNA translation and reveal a mitogen-activated protein kinase-dependent S6 kinase pathway. *Mol Cell Biol,* **24,** 3112-3124.

Perata, P., Guglielminetti, L. and Alpi, A. (1997) Mobilization of Endosperm Reserves in Cereal Seeds under Anoxia. *Annals of Botany,* **79,** 49-56.

Pfeiffer, A., Janocha, D., Dong, Y., Medzihradszky, A., Schone, S., Daum, G., *et al.* (2016) Integration of light and metabolic signals for stem cell activation at the shoot apical meristem. *Elife,* **5**.

Pooggin, M. M. and Ryabova, L. A. (2018) Ribosome Shunting, Polycistronic Translation, and Evasion of Antiviral Defenses in Plant Pararetroviruses and Beyond. *Front Microbiol,* **9,** 644.

Pu, Y. and Bassham, D. C. (2023) Detection of Autophagy in Plants by Fluorescence Microscopy. *Methods in molecular biology (Clifton, N.J.),* **2581,** 135-147.

Pu, Y., Luo, X. and Bassham, D. C. (2017) TOR-Dependent and -Independent Pathways Regulate Autophagy in Arabidopsis thaliana. *Front Plant Sci,* **8,** 1204.

Puighermanal, E., Biever, A., Pascoli, V., Melser, S., Pratlong, M., Cutando, L., *et al.* (2017) Ribosomal Protein S6 Phosphorylation Is Involved in Novelty-Induced Locomotion, Synaptic Plasticity and mRNA Translation. *Front Mol Neurosci,* **10,** 419.

Qi, H., Xia, F. N. and Xiao, S. (2021) Autophagy in plants: Physiological roles and post-translational regulation. *J Integr Plant Biol,* **63,** 161-179.

Rajamäki, M. L., Xi, D., Sikorskaite-Gudziuniene, S., Valkonen, J. P. T. and Whitham, S. A. (2017) Differential Requirement of the Ribosomal Protein S6 and Ribosomal Protein S6 Kinase for Plant-Virus Accumulation and Interaction of S6 Kinase with Potyviral VPg. *Mol Plant Microbe Interact,* **30,** 374-384.

Reiter, A. K., Bolster, D. R., Crozier, S. J., Kimball, S. R. and Jefferson, L. S. (2005) Repression of protein synthesis and mTOR signaling in rat liver mediated by the AMPK activator aminoimidazole carboxamide ribonucleoside. *American Journal of Physiology-Endocrinology and Metabolism,* **288,** E980-E988.

Ren, M., Qiu, S., Venglat, P., Xiang, D., Feng, L., Selvaraj, G., *et al.* (2011) Target of rapamycin regulates development and ribosomal RNA expression through kinase domain in Arabidopsis. *Plant Physiol,* **155,** 1367-1382.

Ren, M., Venglat, P., Qiu, S., Feng, L., Cao, Y., Wang, E., *et al.* (2012) Target of rapamycin signaling regulates metabolism, growth, and life span in Arabidopsis. *Plant Cell,* **24,** 4850-4874.

Robitaille, A. M., Christen, S., Shimobayashi, M., Cornu, M., Fava, L. L., Moes, S., *et al.* (2013) Quantitative phosphoproteomics reveal mTORC1 activates de novo pyrimidine synthesis. *Science,* **339,** 1320-1323.

Robledo, S., Idol, R. A., Crimmins, D. L., Ladenson, J. H., Mason, P. J. and Bessler, M. (2008) The role of human ribosomal proteins in the maturation of rRNA and ribosome production. *RNA,* **14,** 1918-1929.

Roux, P. P., Shahbazian, D., Vu, H., Holz, M. K., Cohen, M. S., Taunton, J., *et al.* (2007) RAS/ERK signaling promotes site-specific ribosomal protein S6 phosphorylation via RSK and stimulates cap-dependent translation. *J Biol Chem,* **282,** 14056-14064.

Ruiz-Gayosso, A., Rodríguez-Sotres, R., Martínez-Barajas, E. and Coello, P. (2018) A role for the carbohydrate-binding module (CBM) in regulatory SnRK1 subunits: the effect of maltose on SnRK1 activity. *Plant J,* **96,** 163-175.

Ruvinsky, I., Katz, M., Dreazen, A., Gielchinsky, Y., Saada, A., Freedman, N., *et al.* (2009) Mice deficient in ribosomal protein S6 phosphorylation suffer from muscle weakness that reflects a growth defect and energy deficit. *PLoS One,* **4,** e5618.

Ruvinsky, I. and Meyuhas, O. (2006) Ribosomal protein S6 phosphorylation: from protein synthesis to cell size. *Trends Biochem Sci,* **31,** 342-348.

Ruvinsky, I., Sharon, N., Lerer, T., Cohen, H., Stolovich-Rain, M., Nir, T., *et al.* (2005) Ribosomal protein S6 phosphorylation is a determinant of cell size and glucose homeostasis. *Genes Dev,* **19,** 2199-2211.

Sasidharan, R., Bailey-Serres, J., Ashikari, M., Atwell, B. J., Colmer, T. D., Fagerstedt, K., *et al.* (2017) Community recommendations on terminology and procedures used in flooding and low oxygen stress research. *New Phytol,* **214,** 1403-1407.

Saxton, R. A. and Sabatini, D. M. (2017) mTOR signaling in growth, metabolism, and disease. *Cell,* **168,** 960-976.

Scarpin, M. R., Leiboff, S. and Brunkard, J. O. (2020) Parallel global profiling of plant TOR dynamics reveals a conserved role for LARP1 in translation. *Elife,* **9**.

Scarpin, M. R., Simmons, C. H. and Brunkard, J. O. (2022) Translating across kingdoms: target of rapamycin promotes protein synthesis through conserved and divergent pathways in plants. *J Exp Bot,* **73,** 7016-7025.

Scharf, K. D. and Nover, L. (1982) Heat-shock-induced alterations of ribosomal protein phosphorylation in plant cell cultures. *Cell,* **30,** 427-437.

Schepetilnikov, M., Dimitrova, M., Mancera-Martinez, E., Geldreich, A., Keller, M. and Ryabova, L. A. (2013) TOR and S6K1 promote translation reinitiation of uORF-containing mRNAs via phosphorylation of eIF3h. *EMBO J,* **32,** 1087-1102.

Schepetilnikov, M., Kobayashi, K., Geldreich, A., Caranta, C., Robaglia, C., Keller, M., *et al.* (2011) Viral factor TAV recruits TOR/S6K1 signalling to activate reinitiation after long ORF translation. *Embo j,* **30,** 1343-1356.

Schmidt, R. R., Fulda, M., Paul, M. V., Anders, M., Plum, F., Weits, D. A., *et al.* (2018a) Low-oxygen response is triggered by an ATP-dependent shift in oleoyl-CoA in Arabidopsis. *Proc Natl Acad Sci U S A,* **115,** E12101-e12110.

Schmidt, R. R., Weits, D. A., Feulner, C. F. J. and van Dongen, J. T. (2018b) Oxygen Sensing and Integrative Stress Signaling in Plants. *Plant Physiol,* **176,** 1131-1142.

Schneider, C. A., Rasband, W. S. and Eliceiri, K. W. (2012) NIH Image to ImageJ: 25 years of image analysis. *Nat Methods,* **9,** 671-675.

Seo, E., Woo, J., Park, E., Bertolani, S. J., Siegel, J. B., Choi, D., *et al.* (2016) Comparative analyses of ubiquitin-like ATG8 and cysteine protease ATG4 autophagy genes in the plant lineage and cross-kingdom processing of ATG8 by ATG4. *Autophagy,* **12,** 2054-2068.

Shi, L., Wu, Y. and Sheen, J. (2018) TOR signaling in plants: conservation and innovation. *Development,* **145**.

Sieńko, K., Poormassalehgoo, A., Yamada, K. and Goto-Yamada, S. (2020) Microautophagy in Plants: Consideration of Its Molecular Mechanism. *Cells,* **9**.

Signorelli, S., Tarkowski Ł, P., Van den Ende, W. and Bassham, D. C. (2019) Linking Autophagy to Abiotic and Biotic Stress Responses. *Trends Plant Sci,* **24,** 413-430.

Simsek, D. and Barna, M. (2017) An emerging role for the ribosome as a nexus for post-translational modifications. *Curr Opin Cell Biol,* **45,** 92-101.

Sirko, A. and Masclaux-Daubresse, C. (2021) Advances in Plant Autophagy. *Cells,* **10**.

Smeekens, S., Ma, J., Hanson, J. and Rolland, F. (2010) Sugar signals and molecular networks controlling plant growth. *Curr Opin Plant Biol,* **13,** 274-279.

Smirnova, J., Loerke, J., Kleinau, G., Schmidt, A., Bürger, J., Meyer, E. H., *et al.* (2023) Structure of the actively translating plant 80S ribosome at 2.2 Å resolution. *Nat Plants,* **9,** 987-1000.

Soto-Burgos, J., Zhuang, X., Jiang, L. and Bassham, D. C. (2018) Dynamics of Autophagosome Formation. *Plant Physiol,* **176,** 219-229.

Sotta, N., Chiba, Y., Miwa, K., Takamatsu, S., Tanaka, M., Yamashita, Y., *et al.* (2021) Global analysis of boron-induced ribosome stalling reveals its effects on translation termination and unique regulation by AUG-stops in Arabidopsis shoots. *Plant J,* **106,** 1455-1467.

Stephani, M. and Dagdas, Y. (2020) Plant Selective Autophagy-Still an Uncharted Territory With a Lot of Hidden Gems. *J Mol Biol,* **432,** 63-79.

Su, T., Li, X., Yang, M., Shao, Q., Zhao, Y., Ma, C., *et al.* (2020a) Autophagy: An Intracellular Degradation Pathway Regulating Plant Survival and Stress Response. *Front Plant Sci,* **11,** 164.

Su, W., Bao, Y., Yu, X., Xia, X., Liu, C. and Yin, W. (2020b) Autophagy and Its Regulators in Response to Stress in Plants. *Int J Mol Sci,* **21**.

Sulic, S., Panic, L., Barkic, M., Mercep, M., Uzelac, M. and Volarevic, S. (2005) Inactivation of S6 ribosomal protein gene in T lymphocytes activates a p53-dependent checkpoint response. *Genes Dev,* **19,** 3070-3082.

Sun, L., Yu, Y., Hu, W., Min, Q., Kang, H., Li, Y., *et al.* (2016) Ribosomal protein S6 kinase1 coordinates with TOR-Raptor2 to regulate thylakoid membrane biosynthesis in rice. *Biochim Biophys Acta,* **1861,** 639-649.

Tanaka, M., Sotta, N., Yamazumi, Y., Yamashita, Y., Miwa, K., Murota, K., *et al.* (2016) The Minimum Open Reading Frame, AUG-Stop, Induces Boron-Dependent Ribosome Stalling and mRNA Degradation. *Plant Cell,* **28,** 2830-2849.

Tatebe, H. and Shiozaki, K. (2017) Evolutionary Conservation of the Components in the TOR Signaling Pathways. *Biomolecules,* **7**.

Turck, F., Kozma, S. C., Thomas, G. and Nagy, F. (1998) A heat-sensitive Arabidopsis thaliana kinase substitutes for human p70s6k function in vivo. *Mol Cell Biol,* **18,** 2038-2044.

Turck, F., Zilbermann, F., Kozma, S. C., Thomas, G. and Nagy, F. (2004) Phytohormones participate in an S6 kinase signal transduction pathway in Arabidopsis. *Plant Physiol,* **134,** 1527-1535.

Turkina, M. V., Klang Arstrand, H. and Vener, A. V. (2011) Differential phosphorylation of ribosomal proteins in Arabidopsis thaliana plants during day and night. *PLoS One,* **6,** e29307.

Tyutereva, E. V., Murtuzova, A. V. and Voitsekhovskaja, O. V. (2022) Autophagy and the Energy Status of Plant Cells. *Russian Journal of Plant Physiology,* **69,** 19.

Urban, J., Soulard, A., Huber, A., Lippman, S., Mukhopadhyay, D., Deloche, O., *et al.* (2007) Sch9 is a major target of TORC1 in Saccharomyces cerevisiae. *Mol Cell,* **26,** 663-674.

Urquidi Camacho, R. A. (2023) Studying Translational Regulation in Arabidopsis Thaliana through a Bioinformatic and Mathematical Lens. University of Tennessee.

Valjent, E., Bertran-Gonzalez, J., Bowling, H., Lopez, S., Santini, E., Matamales, M., *et al.* (2011) Haloperidol regulates the state of phosphorylation of ribosomal protein S6 via activation of PKA and phosphorylation of DARPP-32. *Neuropsychopharmacology,* **36,** 2561-2570.

Valvezan, A. J., Turner, M., Belaid, A., Lam, H. C., Miller, S. K., McNamara, M. C., *et al.* (2017) mTORC1 Couples Nucleotide Synthesis to Nucleotide Demand Resulting in a Targetable Metabolic Vulnerability. *Cancer Cell,* **32,** 624-638.e625.

van Doorn, W. G. and Papini, A. (2013) Ultrastructure of autophagy in plant cells: a review. *Autophagy,* **9,** 1922-1936.

Van Leene, J., Han, C., Gadeyne, A., Eeckhout, D., Matthijs, C., Cannoot, B., *et al.* (2019) Capturing the phosphorylation and protein interaction landscape of the plant TOR kinase. *Nat Plants,* **5,** 316-327.

Van Lijsebettens, M., Vanderhaeghen, R., De Block, M., Bauw, G., Villarroel, R. and Van Montagu, M. (1994) An S18 ribosomal protein gene copy at the Arabidopsis PFL locus affects plant development by its specific expression in meristems. *Embo j,* **13,** 3378-3388.

Vasiliev, V. D. (1974) Morphology of the ribosomal 30S subparticle according to electron microscopic data. *Acta Biol Med Ger,* **33,** 779-793.

Wang, L., Li, H., Zhao, C., Li, S., Kong, L., Wu, W., *et al.* (2017) The inhibition of protein translation mediated by AtGCN1 is essential for cold tolerance in Arabidopsis thaliana. *Plant Cell Environ,* **40,** 56-68.

Watson, K. L., Chou, M. M., Blenis, J., Gelbart, W. M. and Erikson, R. L. (1996) A Drosophila gene structurally and functionally homologous to the mammalian 70-kDa s6 kinase gene. *Proc Natl Acad Sci U S A,* **93,** 13694-13698.

Weinberg, D. E., Shah, P., Eichhorn, S. W., Hussmann, J. A., Plotkin, J. B. and Bartel, D. P. (2016) Improved Ribosome-Footprint and mRNA Measurements Provide Insights into Dynamics and Regulation of Yeast Translation. *Cell Rep,* **14,** 1787-1799.

Wiese, A., Elzinga, N., Wobbes, B. and Smeekens, S. (2004) A conserved upstream open reading frame mediates sucrose-induced repression of translation. *Plant Cell,* **16,** 1717-1729.

Willems, P., Horne, A., Van Parys, T., Goormachtig, S., De Smet, I., Botzki, A., *et al.* (2019) The Plant PTM Viewer, a central resource for exploring plant protein modifications. *Plant J,* **99,** 752-762.

Williams, A. J., Werner-Fraczek, J., Chang, I. F. and Bailey-Serres, J. (2003) Regulated phosphorylation of 40S ribosomal protein S6 in root tips of maize. *Plant Physiol,* **132,** 2086-2097.

Wittenberg, A. D., Azar, S., Klochendler, A., Stolovich-Rain, M., Avraham, S., Birnbaum, L., *et al.* (2016) Phosphorylated Ribosomal Protein S6 Is Required for Akt-Driven Hyperplasia and Malignant Transformation, but Not for Hypertrophy, Aneuploidy and Hyperfunction of Pancreatic beta-Cells. *PLoS One,* **11,** e0149995.

Wu, Y., Shi, L., Li, L., Fu, L., Liu, Y., Xiong, Y., *et al.* (2019) Integration of nutrient, energy, light, and hormone signalling via TOR in plants. *J Exp Bot,* **70,** 2227-2238.

Xiong, Y., McCormack, M., Li, L., Hall, Q., Xiang, C. and Sheen, J. (2013) Glucose-TOR signalling reprograms the transcriptome and activates meristems. *Nature,* **496,** 181-186.

Xiong, Y. and Sheen, J. (2012) Rapamycin and glucose-target of rapamycin (TOR) protein signaling in plants. *J Biol Chem,* **287,** 2836-2842.

Xiong, Y. and Sheen, J. (2014) The role of target of rapamycin signaling networks in plant growth and metabolism. *Plant Physiol,* **164,** 499-512.

Xue, H., Zhang, Q., Wang, P., Cao, B., Jia, C., Cheng, B., *et al.* (2022) qPTMplants: an integrative database of quantitative post-translational modifications in plants. *Nucleic Acids Res,* **50,** D1491-d1499.

Yakovleva, L. A. and Kulaeva, O. N. (1987) The Effect of Phytohormones on Phosphorylation of Ribosomal Proteins in Detached Pumpkin Cotyledons. *Biochemie und Physiologie der Pflanzen,* **182,** 359-365.

Yang, C., Zhang, C., Dittman, J. D. and Whitham, S. A. (2009) Differential requirement of ribosomal protein S6 by plant RNA viruses with different translation initiation strategies. *Virology,* **390,** 163-173.

Yerlikaya, S., Meusburger, M., Kumari, R., Huber, A., Anrather, D., Costanzo, M., *et al.* (2016) TORC1 and TORC2 work together to regulate ribosomal protein S6 phosphorylation in Saccharomyces cerevisiae. *Mol Biol Cell,* **27,** 397-409.

Yi, Y. W., You, K. S., Park, J. S., Lee, S. G. and Seong, Y. S. (2021) Ribosomal Protein S6: A Potential Therapeutic Target against Cancer? *Int J Mol Sci,* **23**.

Yoon, S. H. and Chung, T. (2019) Protein and RNA Quality Control by Autophagy in Plant Cells. *Mol Cells,* **42,** 285-291.

Yu, S. M., Lee, H. T., Lo, S. F. and Ho, T. D. (2021) How does rice cope with too little oxygen during its early life? *New Phytol,* **229,** 36-41.

Yusupova, G. and Yusupov, M. (2014) High-resolution structure of the eukaryotic 80S ribosome. *Annu Rev Biochem,* **83,** 467-486.

Zhan, N., Wang, C., Chen, L., Yang, H., Feng, J., Gong, X., *et al.* (2018) S-Nitrosylation Targets GSNO Reductase for Selective Autophagy during Hypoxia Responses in Plants. *Mol Cell,* **71,** 142-154.e146.

Zhang, Y., Wang, Y., Kanyuka, K., Parry, M. A., Powers, S. J. and Halford, N. G. (2008) GCN2-dependent phosphorylation of eukaryotic translation initiation factor-2alpha in Arabidopsis. *J Exp Bot,* **59,** 3131-3141.

Zhang, Z., Boonen, K., Ferrari, P., Schoofs, L., Janssens, E., van Noort, V., *et al.* (2016) UV crosslinked mRNA-binding proteins captured from leaf mesophyll protoplasts. *Plant Methods,* **12,** 42.

VITA

Originating from Agartala, India, Anwesha Dasgupta spent her formative years in her hometown, where her passion for Biology first took root. Following her high school education, she enrolled at the esteemed University of Hyderabad, India, where she pursued a 5-year Integrated Bachelors and Masters of Science degree with a major in Systems Biology. After successfully completing her degree, she ventured into the realm of research, working as a Research Assistant in the laboratory of Dr. Nagaraj Balasubramanian at the Indian Institute of Science Education and Research, Pune, India. During her time in Hyderabad and Pune, the allure of advanced research and academia captivated her, propelling her to embark on a new academic journey. In 2016, she made her way to the distinguished University of Tennessee, Knoxville, to pursue a Doctor of Philosophy degree. In Spring 2017, she joined Dr. Albrecht von Arnim's lab, dedicating her efforts to investigating the biochemical significance of ribosomal protein S6 phosphorylation. Anwesha expresses deep gratitude for the unwavering support of her family and friends throughout her academic and research pursuits. As she approaches graduation, she eagerly anticipates commencing her role as a Postdoctoral Research Fellow at the University of Michigan, where she is determined to make impactful contributions to her field.